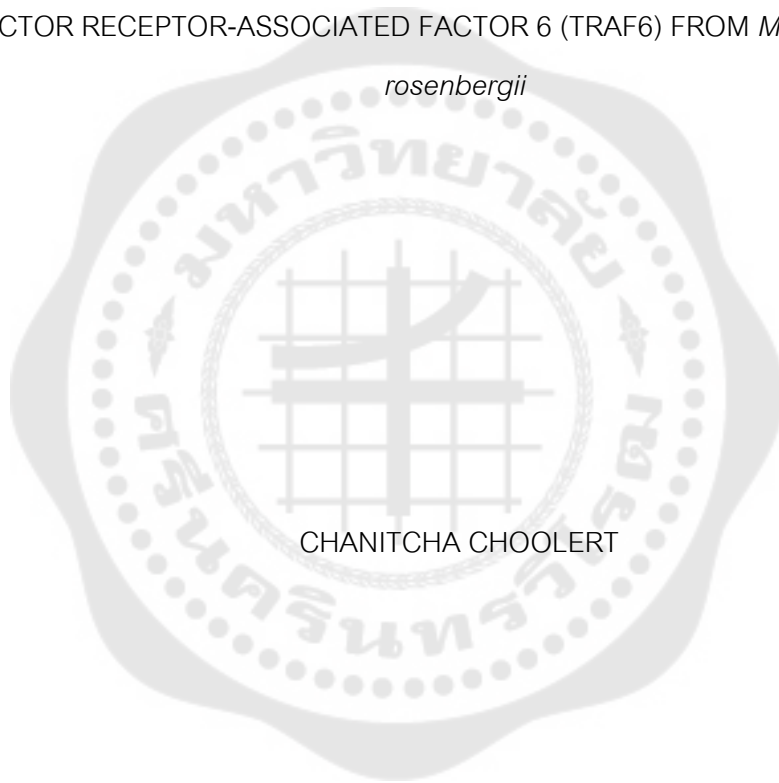MOLECULAR ISOLATION AND CHARACTERIZATION OF THE TUMOR NECROSIS

FACTOR RECEPTOR-ASSOCIATED FACTOR 6 (TRAF6) FROM *Macrobrachium*

rosenbergii

CHANITCHA CHOOLERT

Graduate School Srinakharinwirot University

2022

การแยกและศึกษาคุณลักษณะของยีน Tumor Necrosis Factor Receptor-associated

Factor 6 (TRAF6) จากกุ้งก้ามกราม (*Macrobrachium rosenbergii*)

จนิสชา ชูเลิศ

ปริญญานิพนธ์นี้เป็นส่วนหนึ่งของการศึกษาตามหลักสูตร
ปรัชญาดุษฎีบัณฑิต สาขาวิชาเทคโนโลยีชีวภาพ
คณะวิทยาศาสตร์ มหาวิทยาลัยศรีนครินทรวิโรฒ
ปีการศึกษา 2565

MOLECULAR ISOLATION AND CHARACTERIZATION OF THE TUMOR NECROSIS

FACTOR RECEPTOR-ASSOCIATED FACTOR 6 (TRAF6) FROM *Macrobrachium*

rosenbergii

CHANITCHA CHOOLERT

A Dissertation Submitted in Partial Fulfillment of the Requirements

for the Degree of DOCTOR OF PHILOSOPHY

(Biotechnology)

Faculty of Science, Srinakharinwirot University

2022

THE DISSERTATION TITLED

MOLECULAR ISOLATION AND CHARACTERIZATION OF THE TUMOR NECROSIS FACTOR

RECEPTOR-ASSOCIATED FACTOR 6 (TRAF6) FROM *MACROBRACHIUM ROSENBERGII*

BY

CHANITCHA CHOOLERT

HAS BEEN APPROVED BY THE GRADUATE SCHOOL IN PARTIAL FULFILLMENT

OF THE REQUIREMENTS FOR THE DOCTOR OF PHILOSOPHY

IN BIOTECHNOLOGY AT SRINAKHARINWIROT UNIVERSITY

....

(Assoc. Prof. Dr. Chatchai Ekpanyaskul, MD.)

Dean of Graduate School

....

ORAL DEFENSE COMMITTEE

.... Major-advisor

(Prof. Dr.Parin Chaivisuthangkura)

.... Chair

(Dr.Saengchan Senapin)

.... Co-advisor

(Assoc. Prof. Dr.Siwaporn Longyant)

.... Committee

(Assoc. Prof. Dr.Achariya Rangsiruji)

.... Committee

(Assoc. Prof. Dr.Thapana Chontananarth)

Title	MOLECULAR ISOLATION AND CHARACTERIZATION OF THE TUMOR NECROSIS FACTOR RECEPTOR-ASSOCIATED FACTOR 6 (TRAF6) FROM *Macrobrachium rosenbergii*
Author	CHANITCHA CHOOLERT
Degree	DOCTOR OF PHILOSOPHY
Academic Year	2022
Thesis Advisor	Professor Dr. Parin Chaivisuthangkura
Co Advisor	Associate Professor Dr. Siwaporn Longyant

Tumor necrosis factor receptor-associated factor 6 (TRAF6) is an adapter protein that can be participated in both tumor necrosis factor receptor (TNFR) and interleukin-1 receptor/Toll-like receptor (IL1/TLR) superfamily. TRAF6 is involved in various biological processes such as development of T-cells, cell proliferation, apoptosis, as well as innate and adaptive immunity. In this study, a novel TRAF6 gene was identified and characterized from *Macrobrachium rosenbergii,* designated as *MrTRAF6*. The full-length cDNA of *MrTRAF6* was 2,114 nucleotides long with an open reading frame (ORF) of 1,695 nucleotides that encoded a protein of 564 amino acid residues. The *Mr*TRAF6 protein consisted of two RING type Zinc fingers, and a C-terminal meprin and TRAF homology (MATH) domain. The amino acid sequence of *Mr*TRAF6 shared 46.1-87.6% identity with TRAF6s from other crustacean species with the highest identity to TRAF6 of *Macrobrachium nipponense*. Phylogenetic analysis indicated that *Mr*TRAF6 showed a close relationship with TRAF6 proteins of invertebrates and formed a cluster with other crustacean TRAF6 proteins. Tissue distribution and expression analysis demonstrated that *MrTRAF6* transcript was widely expressed in all tissues examined, with the highest expression level in the gills and the lowest in muscle tissue. After challenge with *Aeromonas hydrophila*, *MrTRAF6* was significantly upregulated in the muscle, hemocyte, gill, and hepatopancreas tissues. To investigate the specific role of *MrTRAF6* in immunity, RNA interference (RNAi) was performed. The results showed that silencing of *MrTRAF6* by dsRNA could reduce the expression of crustin, and mannose-binding lectin (MBL) but no significant change was observed in anti-lipopolysaccharide factor 5 (ALF5) level. Furthermore, the silencing of *MrTRAF6* led to a significant increase in cumulative mortality rate after exposure to *A. hydrophila*. These results suggest that *MrTRAF6* plays a crucial role in the innate immune response of *M. rosenbergii*, specifically in terms of antibacterial activity.

Keyword : Macrobrachium rosenbergii, Tumor necrosis factor receptor-associated factor 6 (TRAF6), Innate immune system, RNA interference,

ACKNOWLEDGEMENTS

TABLE OF CONTENTS

LIST OF TABLES

LIST OF FIGURES

CHAPTER 1

INTRODUCTION

1.1 Background

Giant freshwater prawn (*Macrobrachium rosenbergii*) culture is one of the economically important inland aquacultures especially in South and Southeast Asia, as well as in Northern Oceania and in the Western Pacific Islands. The major freshwater prawn producing countries are in Asia (e.g. China, Thailand, India, Taiwan, Bangladesh and Vietnam (Holthuis, 1980). In Thailand, the freshwater prawn farming is mostly spread in the central of Thailand and becomes a predominantly cooperative and profitable venture that supports rural economies (Schwantes, Diana, & Yi, 2007). Due to the marketing demand, prawn farming has rapidly expanded since 1980. The production of *M. rosenbergii* has been gradually rising and reaches to the peak of 9,530 tons in 2021 (FAO, 2023).

However, the success of prawn's production has been limited by the emergence of infectious diseases mainly caused by bacteria and viruses. For instances, bacterial diseases e.g. luminescent larval syndrome (caused by *Vibrio harveyi*), Black spot disease (caused by *Pseudomonas* sp., *Aeromonas* sp.); viral diseases e.g. White tail disease (WTD) (caused by *Mr*NV and XSV); and some others caused by fungi and protozoa (FAO, 2020; Pillai & Bonami, 2012).

Similar to crustaceans, shrimp solely rely on their effective cellular and humoral innate immune responses for the host defense against invading pathogens (Aguirre-Guzman, Sanchez-Martinez, Campa-Cordova, Luna-Gonzalez, & Ascencio, 2009) Shrimp cells identify pathogens through pattern recognition receptors (PRRs). The PRRs can bind to the pathogen-associated molecular patterns (PAMPs). The recognition of PAMPs by various PRRs leads to the activation of both cellular and humoral responses (Jensen & Thomsen Allan, 2012; F. Li & Xiang, 2013a; X.-W. Wang & Wang, 2013). The cellular immune response is mainly mediated by hemocytes that are capable to neutralize the pathogens in phagocytosis, encapsulation, and hemocyte nodulation

processes, whereas the humoral immune response involves the production of immune effectors molecules that are kept in the granules such as antimicrobial peptides (AMPs), Prophenol oxidase (ProPO) and clotting proteins and released to the hemolymph immediately after pathogens infection. These immune effectors genes are generally regulated via signal transduction pathways (Lemaitre & Hoffmann, 2007; Vazquez et al., 2009).

Toll pathway is one of the major signaling pathways that plays a crucial role in innate immune system, the first-line defense in invertebrates. The Toll pathway mainly involves in Gram-positive bacteria, Gram-negative bacteria, and also some viruses infection (F. Li & Xiang, 2013b). Although Toll receptors are functionally identified as PRRs, they cannot directly bind to the PAMPs. The Toll receptors require the cytokine-like molecule named Spätzle as an extracellular ligand(Hoffmann et al., 2008). The infectious pathogens can activate the inactive form of Spätzle (pro-Spätzle) which thereby cleaves into an active Spätzle by serine protease cascade. The active Spätzle then binds to the Toll receptor initiating the signal transduction to induce the production of AMPs and others immune proteins (Mulinari, Häcker, & Castillejo-López, 2006). The series of proteins participated in Toll signaling pathway of penaeid shrimp includes MyD88 which interacts with Toll receptor through their Toll/Interleukin-1 receptor (TIR) domains, Tube, Pelle (MyD88, Tube and Pelle form heterotrimeric complex through their dead domains), TRAF6, Cactus and transcriptional factor Dorsal, respectively (Y. Huang, Chen, Wang, Wang, & Ren, 2014; P.-H. Wang, Wan, et al., 2011; Wen, Li, Sun, Li, & Xiang, 2013; Y. Xu, Huang, & Cai, 2017; Zhang et al., 2012).

In *M. rosenbergii*, the several components of Toll pathway have been found and characterized including Spätzle (Vaniksampanna, Longyant, Charoensapsri, Sithigorngul, & Chaivisuthangkura, 2019), Toll receptor (Srisuk et al., 2016), Dorsal (Huang et al., 2016) that are all investigated to response to bacteria and virus infection by regulating expression of AMPs. This may suggest that Toll pathway in *M. rosenbergii* plays a crucial role in innate immune system like penaeid shrimp and other crustaceans.

Tumor necrosis factor receptor-associated factors 6 (TRAF6) has been identified as the major signal transducers for both TNF receptor superfamily and interleukin-1 receptor/Toll-like receptor (IL-1R/TLR). TRAF6 involves in a wide range of biological functions including innate immunity, adaptive immunity, development, apoptosis, and stress response (Arch et al., 2000; Magnusson & Vaux, 1999).

Similar to other TRAFs, TRAF6 contains all the unique characteristics of TRAFs proteins including a TRAF domain at the C-terminus (a coiled-coil domain followed by a highly conserved TRAF-C domain) and a RING finger (several putative zinc-finger motifs) at the N-terminus (Chung, Park, Ye, & Wu, 2002; Rothe, Wong, Henzel, & Goeddel, 1994; Wajant, Henkler, & Scheurich, 2001). The RING finger motif of TRAF6 possesses the ubiquitin (E3) ligase catalytic domain, which is important for activating the downstream signaling cascades (Budhidarmo, Nakatani, & Day, 2012). A coiled-coil domain is crucial for auto-ubiquitination process and activating NF-kB signaling pathway (Yang et al., 2004). The TRAF-C domain at the C-terminus can catalyze the oligomerization of TRAF6 and is used for receptor binding (Megas et al., 2010).

TRAF6 is well characterized in humans and other vertebrates. Besides mammalian TRAF6, there are several studies reported on the characterization of TRAF6 homologs in other invertebrates such as mollusks (He et al., 2013; D. Huang, Bai, Shen, Zhao, & Jiale, 2018; Mao et al., 2017; Qiu et al., 2009) and crustaceans including shrimp species (Cai, Huang, Wang, Jian, & Xu, 2017; Deepika, Sreedharan, Paria, Makesh, & Rajendran, 2014; B. Li et al., 2020; Sun et al., 2017; P.-H. Wang, Wan, et al., 2011; Zhou et al., 2015). The previous studies shaded same lights of the involvements of TRAF6 in innate immunity that could be induced by various stimulators and play a crucial role in innate immune system. In shrimp, *Litopenaeus vannamei* TRAF6 (*LvTRAF6*) could up-regulate in gills and hepatopancreas after white spot syndrome virus (WSSV) challenge, and down-regulate in intestine after *Vibrio alginolyticus* challenge (Wang, Wan, et al., 2011). For black tiger shrimp, *Penaeus monodon*, the expression of *PmTRAF6* was up-regulated after WSSV challenge but no significant change after inducing with viral-mimic molecule, poly I:C (Deepika et al., 2014). The expression of *TRAF6* from

Fenneropenaeus penicillatus (*FpTRAF6*) was dynamic after WSSV and *V. alginolyticus* injection and it was also reported that *FpTRAF6* could regulate the expression of peroxinectin gene. In red swamp crayfish (*Procambarus clarkii*), the significant up-regulation of *Pc-TRAF6* like transcript was detected after being challenged by *Staphylococcus aureus* and *Edwardsiella ictaluri*, and knockdown of *Pc-TRAF6* like gene could inhibit the expression of the downstream molecules such as Dorsal and some immune effector genes (B. Li et al., 2020). However, *TRAF6* from giant freshwater prawn, *M. rosenbergii* have not been functionally characterized to date.

In the present study, a novel TRAF6 homologue, termed *MrTRAF6*, was firstly identified in *M. rosenbergii*. The tissue distribution of *MrTRAF6* was analyzed by real-time RT-PCR. The temporal expression of *MrTRAF6* was examined in tissue selected after being challenged by Gram negative bacteria, *Aeromonas hydrophila*. To investigate the potential involvement of *MrTRAF6* in antibacterial activity, RNA interference (RNAi) was used to silence the expression of *MrTRAF6* and the mortality rate after *A. hydrophila* infection was analyzed. The present study provided further evidence for the existence of TLR signaling pathway in *M. rosenbergii* and it contributed to a better understanding of the innate immune system of freshwater prawns.

1.2 Objectives

1. To isolate and characterize the *TRAF6* from *M. rosenbergii* (*MrTRAF6*)

2. To analyze the expression patterns of *MrTRAF6* among various tissues using real-time RT-PCR

3. To examine the temporal expression of *MrTRAF6* in response to Gram-negative bacteria, *Aeromonas hydrophila*

4. To characterize the role of *MrTRAF6* in antibacterial response using RNA interference (RNAi)

1.3 Research hypotheses

1. The gene *MrTRAF6* can be successfully isolated and characterized from the *M. rosenbergii*.

2. The expression of *MrTRAF6* is upregulated in response to Gram-negative bacterial infection, *Aeromonas hydrophila*.

3. *MrTRAF6* plays a crucial role in the immune response against *Aeromonas hydrophila*, potentially through its involvement in downstream signaling pathways.

4. The characterization of *MrTRAF6* will reveal its structural and functional properties, providing insights into its role in immune signaling.

1.4 Scopes

1. Isolation of *MrTRAF6*: The research focused on isolating the *MrTRAF6* gene from *M. rosenbergii*. This includes identifying suitable tissue, designing degenerate primers for PCR amplification, and using RACEs technique.

2. Sequence analysis and structural characterization: The isolated *MrTRAF6* gene was subjected to sequence analysis to determine its nucleotide sequence as well as investigating the structural properties of *Mr*TRAF6, such as its protein structure and domains. This analysis involved using bioinformatics tools.

3. Expression analysis: The distribution of *MrTRAF6* among tissues was investigated by real-time RT-PCR.

4. Functional characterization: The functional aspects of *MrTRAF6* were explored, including its role in immune signaling pathways and response to *A. hydrophila*. This was involved in experiments to study its role using RNAi followed by cumulative mortality analysis.

CHAPTER 2

LITERATURE REVIEW

2.1 *Macrobrachium rosenbergii*

Macrobrachium rosenbergii, also known as giant freshwater prawn, is considered to be one of the major commercial crustacean species throughout the world. It is widely cultured in many countries especially in South and Southeast Asia, as well as in Northern Oceania and in the Western Pacific Islands (B. M. New, 2002). Moreover, *M. rosenbergii* has been introduced to many other tropical and subtropical areas of the world for aquaculture. The global production of *M. rosenbergii* has gradually increased from 2,816 tons in 1980 to 9,530 tons in 2021 (FAO, 2023).

2.1.1 Scientific classification

The name of "*Macrobrachium rosenbergii*" by De Man (1879) became universally accepted. *M. rosenbergii* belongs to the genus *Macrobrachium* which is the largest genus of the family Palaemonidae. The scientific classification of *M. rosenbergii*, the largest species of the genus, is reported below (CABI, 2019; WoRMS, 2007):

Domain: Eukaryota

Kingdom: Metazoa

Phylum: Arthropoda

Subphylum: Crustacea

Class: Malacostraca

Subclass: Eumalacostraca

Order: Decapoda

Suborder: Natantia

Superfamily: Palaeomonoidea

Family: Palaemonidae

Genus: *Macrobrachium*

Species: *Macrobrachium rosenbergii*

2.1.2 Biological features

2.1.2.1 Morphological characteristics

In general, mature males usually attain larger size than females. The total body length of adult males can reach 320 mm, whereas females' can reach 250 mm. The body color is greenish-grey. As a decapod crustacean, the typical body of *M. rosenbergii* (Figure 1) consists of two major segments - cephalothorax and abdomen (B. M. New, 2002).
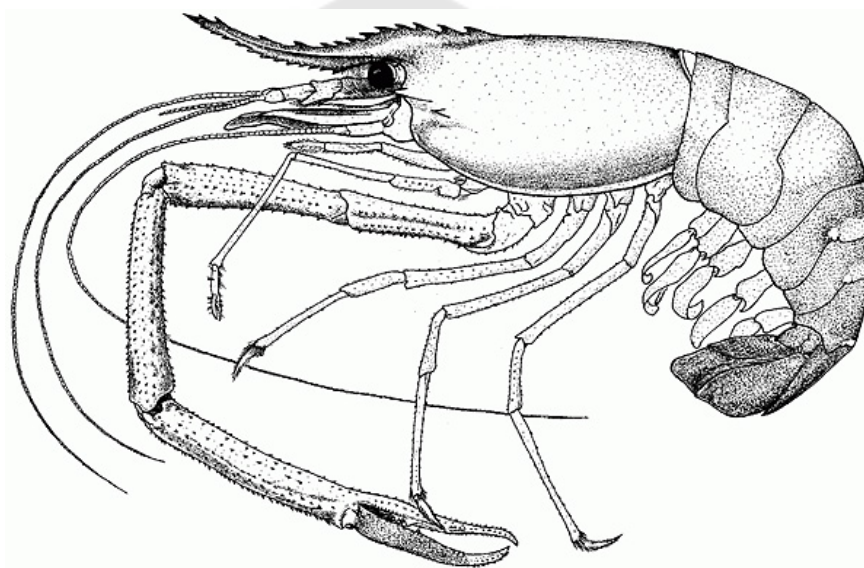
Figure 1 *Macrobrachium rosenbergii* (De Man, 1879).

Source: FAO. (2020). *Macrobrachium rosenbergii* (De Man, 1879). Retrieved from http://www.fao.org/fishery/culturedspecies/Macrobrachium_rosenbergii/en.

The cephalothorax where head and thorax fused together is covered with a smooth and hard dorsal and lateral shield called carapace. It normally has a very long rostrum at the front end which appears 11-14 dorsal teeth and 8-10 ventral teeth. The cephalon (front portion of cephalothorax) consists of six segments including the eye stalks and five pairs of appendages; the antennules (first antennae), the antennae (second antennae), the mandibles, the first maxillae (maxillules) and the second

maxillae. The thorax (rear portion) consists of eight fused segments. The first three pairs are in terms of maxillipeds, and the remaining five pairs are pereopods or walking legs. The first two pairs of walking leg carried chelae are normally called chelipeds. A second pair of chelipeds contains numerous spines and excessively larger and stronger than any others (sometimes called "great chela"). This pair of chelipeds are extremely longer and thicker in adult males. The males' genital pores are located at the fifth walking legs, whereas the females' are at the third walking legs (FAO, 2020; (B. M. New, 2002).

The abdomen (tail) consists of six obvious segments with a pair of appendages each called pleopods or swimmerets. The sixth pair of swimmerets are called uropod. In the last segment, there are a broad point central appendage with two spines, known as telson. The uropod and the telson form the tail fan, which can be used to move the prawn suddenly. In males, the abdomen seems narrower than females and the second pair of swimmerets is modified for use in copulation (FAO, 2020; B. M. New, 2002).

2.1.2.2 Habitat and life cycle

M. rosenbergii is often found in most inland freshwater areas including rivers, lakes, canals, and ponds, as well as in estuarine areas in extremely turbid conditions. They live in tropical freshwater environments adjacent to brackish water areas, because this species requires brackish water in the initial stages of their life cycle for survival. The giant freshwater prawns normally appear in four distinct stages in their life cycle, namely eggs, larvae, post larvae (PL) and adults (Figure 2) (FAO, 2020; New et al., 2010).

The ovigerous females migrate to the estuaries for hatching. The eggs hatch as a free-swimming larva which are planktonic. They mostly consume zooplankton, very small worms, and any other aquatic invertebrate larvae. The freshwater prawn larvae pass through eleven zoeal stages which takes sixteen days (depending on environmental factors, mainly temperature) before metamorphosis. Their larvae stages have been completed when freshwater prawns metamorphose into post larvae (PL). The PL can swim as adult prawns. After staying in brackish water for up to

two weeks, they become a more benthic lifestyle and begin to migrate to freshwater conditions. Becoming adults, males and females have different growth rates. Males have heterogenous individual growth (HIG) which exhibit three distinct morphotypes such as small male (SM), orange claw males (OC), and blue claw males (BC). The males generally develop in order from the SM to OC and to BC which extremely long second chelipeds are presented. Both of PL and adult freshwater prawns are omnivores which their natural diets are algae, aquatic plants, aquatic insects and their larvae, small mollusks, and other crustaceans (B. M. New, 2002; FAO, 2020).
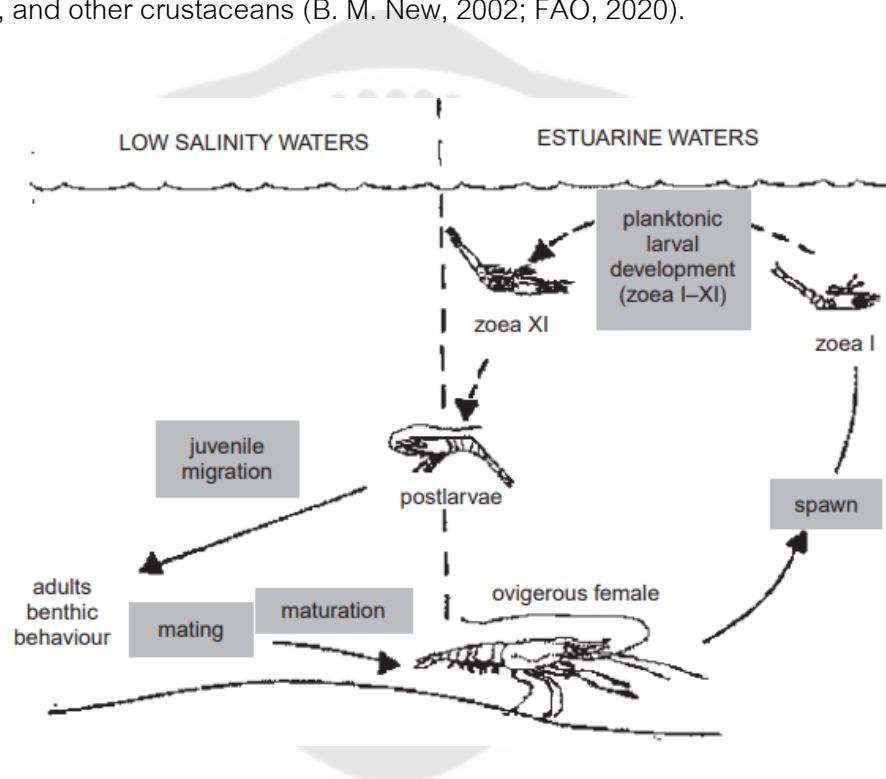
Figure 2 Life cycle of *M. rosenbergii.*

Source: New, M. B., Valenti, W. C., Tidwell, H. J., D'Abramo, L. R., & Kutty, M. N. (2010). *Freshwater Prawns Biology and Farming* (1st ed). United Kingdom: John Wiley & Sons, Ltd.,

2.2 Diseases of *M. rosenbergii*

Advances in molecular biology techniques have made it easier to detect both known and emerging pathogens. These techniques allow for the rapid identification of novel pathogens without relying on traditional methods of culturing. In the case of *M. rosenbergii,* the giant freshwater prawn, various disease-causing agents, including bacteria, viruses, fungi, and other eukaryotic pathogens, have been found to infect them. These pathogens can lead to significant losses in the aquaculture industry, either through mortality or by producing smaller or lower-quality animals that have reduced market value. Recent improvements in molecular detection methods have facilitated the identification of several newly discovered pathogenic agents in giant river prawn culture, as summarized in Table 1, and their life stage(s) affected were shown in Figure 3.

Table 1 Pathogens infecting *M. rosenbergii.*

Pathogens	Clinical sign of infection
Viruses	
Covert mortality nodavirus (CMNV)	- Slow growth, pale hepatopancreas, soft shell, muscle whitening and necrosis, mortality.
Crustacea hepe-like virus 1 (CHEV1)	- Slow growth (Iron Prawn Syndrome).
Decapod iridescent virus 1 (DIV1)	- White triangle under the carapace at the bottom of the rostrum, yellow gills, loss of swimming ability, migration to deep water, mortality.
Infectious hypodermal haematopoietic necrosis virus (IHHNV) AKA *Penaeus stylirostris penstyldensovirus* 1 (PstDV1)	- Slow growth, muscular atrophy, reddish discoloration, deformities to cuticle, opaque musculature, mortality.

Table 1 (Continued).

Pathogens	Clinical sign of infection
Infectious precocity virus (IPV)	- Slow growth (Iron Prawn Syndrome).
Macrobrachium rosenbergii Golda virus (*Mr*GV)	- Problems with swimming and feeding, slow growth, white discoloration, mortality.
Macrobrachium rosenbergii nodavirus (*Mr*NV)	- White opaque discoloration of abdomen that gradually progresses towards the head, abnormal exuviae, mortality.
Macrobrachium rosenbergii Taihu virus (*Mr*TV)	- Problems with feeding and molting, reddish exuviae, decreased response to stimuli, mortality.
White spot syndrome virus (WSSV)	- White spots on carapace, lethargy, increased cannibalism, mortality.
Bacteria	
Aeromonas hydrophila	- "Black spot disease"—dark necrotic lesions on exoskeleton and appendages, mortality.
Aeromonas veronii	- Shell lesions, opaque white musculature, hepatopancreatic erosion, mortality.
Aeromonas caviae	- Mortality.
Bacillus sp.	- "Black spot disease"—dark necrotic lesions on exoskeleton, mortality.
Citrobacter freundii	- "Water bubble disease (WDB)— Formation of a "water bubble" with a diameter of 7 mm under the carapace, loss of appetite, inactivity, weight loss.
Enterobacter cloacae	- Weakness, poor appetite, mortality in larvae. Slow growth (iron prawn) in juveniles.

Table 1 (Continued).

Pathogens	Clinical sign of infection
Enterococcus casseliflavus	- Mortality.
Exiguobacterium profundum	- Mortality.
Klebsiella pneumoniae	- Mortality.
Lactococcus garvieae	- Anorexia, poor growth, inactivity, opaque, white musculature in cephalothorax and abdominal segments, mortality.
Pseudomonas aeruginosa	- Opaque, white musculature in cephalothorax and abdominal segments, mortality.
Spiroplasma eriocheiris	- Weakness, aggregation at the side of ponds, mortality.
Vibrio alginolyticus	- Mortality in larvae and post larvae. Mortality, cloudy muscle appearance, loss of appendages and soft and dark-brown hepatopancreas in adults.
Vibrio anguillarum	- Mortality.
Vibrio campbelli	- Mortality.
Vibrio carchariae	- Mortality.
Vibrio cholerae	- Mortality in larvae and post larvae. Red discoloration, anorexia, swimming alone in juveniles/ adults.
Vibrio harveyi	- "Luminescent larvae syndrome"—glowing appearance of dead and moribund larvae. In juveniles—swelling and deformation of the hepatopancreas with appearance of white spots. Mortality.

Table 1 (Continued).

Pathogens	Clinical sign of infection
Vibrio mimicus	- Mortality.
Vibrio neocaledonicus	- Mortality.
Vibrio parahaemolyticus (non-AHPND strains)	- Red discoloration with black spots on carapace, loss of appendages and telson, brittle shells and mortality in juveniles/adults. Mortality in larvae.
Vibrio parahaemolyticus (AHPND strains)	- Mortality in larvae and adults.
Vibrio vulnificus	- Dark brown focal lesions and necrosis on appendages of juveniles/adults. Infected larvae are weak, have poor appetite and slowed growth prior to mortality.
Fungi and microsporidia	
Batrachochytrium dendrobatidis	- Greyish-white body coloration, spongy appearance, lethargy, anorexia, abnormal swimming, fading of eye color, dark spots and melanization on cephalothorax and muscles, greyish-white filaments on claws and mortality.
Candida sake *Candida mogii*	- Yellowish-brown discoloration, white opaque eyes, swelling between cephalothorax and abdomen, cloudy white hemolymph, light yellow hepatopancreas, slow swimming, lethargic, anorexia, mortality.

Table 1 (Continued).

Pathogens	Clinical sign of infection
Debaryomyces hansenii	- Yellowish-brown discoloration, swollen hepatopancreas, cloudy hemolymph, whitish opaque musculature, mortality
Fusarium sp.	- Dark lesions on exoskeleton following injury, mortality
Metschnikowia bicuspidata	- Poor growth, anorexia, yellowish-brown discoloration of body, swelling between cephalothorax and abdomen, swollen hepatopancreas, milky hemolymph, whitish, opaque musculature with whitish-yellow spots, mortality.
Enterocytozoon hepatopenaei (EHP)	- Not described—PCR positive only.

Modified from: Hooper et al., 2023.
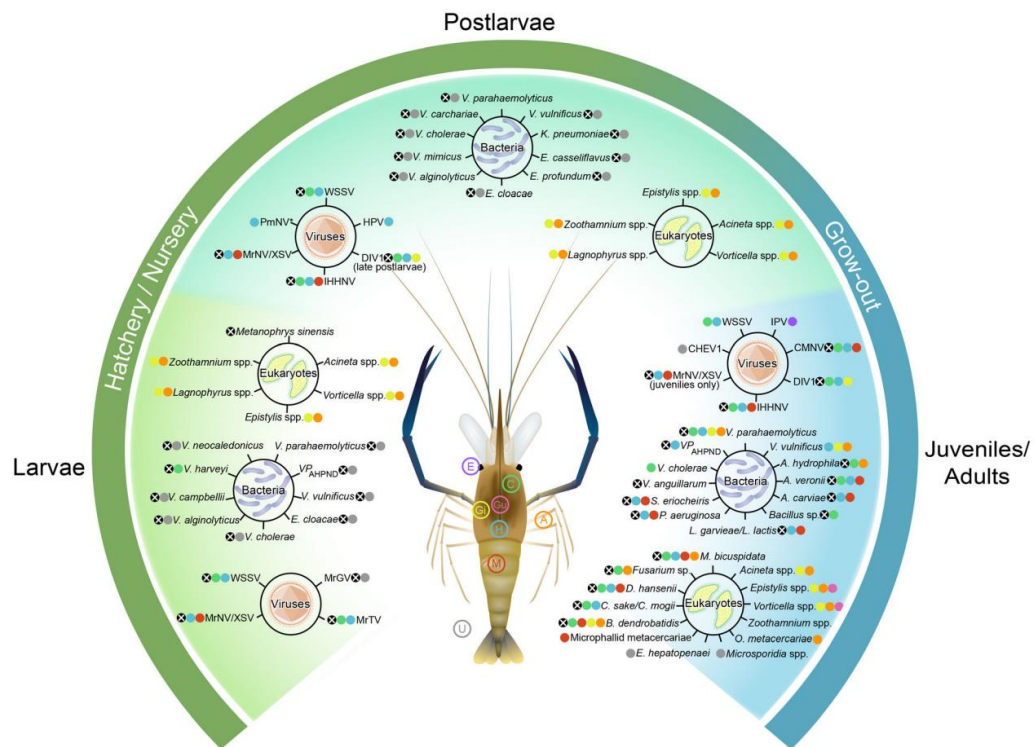
Figure 3 Impact of diseases on different life stages of *Macrobrachium rosenbergii*.

Source: Hooper, C., et al. (2023). "Diseases of the giant river prawn *Macrobrachium rosenbergii*: A review for a growing industry." Reviews in Aquaculture 15(2): 738-758.

2.3 The immune system in shrimp

Recently, the basic knowledge of shrimp immune system has been reported for development of efficient strategies to prevent disease outbreaks. Similar to other crustaceans, shrimp mainly relies on the non-specific immune system or innate immune system acted as a defense mechanism against invading pathogens. The shrimps protect themselves from infectious microbes by recognizing and eliminating through different two ways of responses - cellular and humoral immunity (F. Li & Xiang, 2013a; Tassanakajon et al., 2018).

Shrimp cells are able to response generally to the generic pathogen-associated molecular patterns (PAMPs) located on the surface of microorganisms that can be recognized by host pattern recognition receptors (PRRs). The engagement between PAMPs and PRRs can rapidly initiate a series of immune cells in both cellular and humoral immune responses through intracellular signaling cascades. The defense mechanism normally takes place in the hemolymph in which hemocytes, the cells involved in immune response, are circulated. Shrimp possesses three types of hemocytes which are defined as hyaline (agranular), semigranular, and granular hemocytes (Tassanakajon, Somboonwiwat, Supungul, & Tang, 2013). The cellular immune response, mediated directly by hemocytes, is involved in phagocytosis, apoptosis, nodule formation, and encapsulation (Lemaitre & Hoffmann, 2007). The humoral immune response, on the other hands, is intensively involved in activation and secretion of molecules within hemocytes such as prophenol oxidase system (ProPO), clotting proteins, melanization and antimicrobial peptides (AMPs) (Vazquez et al., 2009).

2.3.1 Pattern recognition receptors (PRRs)

The innate immune system plays a crucial role in recognizing pathogens, and this recognition is facilitated by pattern recognition receptors (PRRs) (Aguirre et al., 2009). PRRs detect pathogens by binding to specific molecular patterns known as pathogen-associated molecular patterns (PAMPs). These PAMPs are shared among groups of microbes and are essential for their survival and infectivity (Li & Xiang, 2013b; Wang & Wang, 2013). PAMPs can include various components found on the surface of microbes, such as polysaccharides and glycoproteins like peptidoglycans and lipoteichoic acid (LTA) from Gram-positive bacteria, lipopolysaccharide (LPS) from Gram-negative bacteria, and glucans from fungal cells. In addition, PAMPs can also consist of nucleic acid motifs, such as unmethylated CpG DNA from bacteria and viruses, as well as single-stranded RNA (ssRNA) and double-stranded RNA (dsRNA) from viruses. (Jensen & Thomsen, 2012; F. Li & Xiang, 2013b).

There are several types of identified PRRs that have been reported in shrimp as well as other crustaceans which are responsible for recognizing all existed

PAMPs of invasive pathogens e.g. β-1,3-glucanase-related proteins (BGRP), also known as, LGBP, β-1,3-glucan binding proteins (BGBPs), and Gram-negative bacteria-binding protein (GNBP) (Sritunyalucksana et al., 2002; Wang & Wang, 2013), Peptidoglycan recognition proteins (PGRPs) which strongly bind to Gram-negative bacteria (Du, Zhao, & Wang, 2007), C-type lectins (CTLs) significantly involved in sensing, eradicating any potential pathogens in invertebrates species and participating in the phagocytosis (Liu et al., 2020; Xu et a., 2014), Scavenger receptors (SRs) that can bind modified low-density lipoproteins (LDLs) as well as LTA, LPS, and yeast zymosan/B-glucan, and can mediate phagocytosis after WSSV infection (Areschoug & Gordon, 2009; Liu et al., 2020; Wang & Wang, 2013), Fibrinogen-related proteins (FREPs) that can recognize many different pathogens such as peptidoglycans, LPS, and VP28 of WSSV (Chai et al., 2012), DSCAM (Down syndrome cell adhesion molecule), a member of the immunoglobulin superfamily (IgSF). It plays a role in both the pathogen-specific immune response and phagocytosis. Additionally, DSCAM has the potential to function as an analog of antibodies. (Huang & Ren, 2020; Liu et al., 2020; Xu et al., 2014).

2.3.2 Immune signaling pathways in shrimp

The PRRs specifically detect the molecular patterns after the pathogens immediately infecting cells leading to initiate the signaling cascades via two major signaling pathways, Toll and Immune deficiency (IMD) (Figure 3). The signaling cascades are activated as a series. Eventually, the immune effectors are activated to destroy pathogens (Tassanakajon et al., 2018).

2.3.2.1 Toll signaling pathway

The Toll pathway plays a crucial role in the response to Gram-positive bacteria, fungi, and some viruses by regulating a large set of genes. This cascade finally activates the NF-kB transcription factors leading to synthesis of antibacterial peptides (AMPs) to eliminate the invasive pathogens (Belvin & Anderson, 1996; Lemaitre & Hoffmann, 2007; Tassanakajon et al., 2018). The Toll pathway reported in penaeid shrimp initiates with the binding of microbial pattern molecule to the PRR of shrimp cells leading to activation of a proteolytic cascade and eventually cleaves a pro-

Spätzle into an active Spätzle, extracellular ligand of Toll receptor (Hoffmann et al., 2008). The active Spätzle will then bind to the Toll receptor which are in the cell membrane. Activation of Toll leads to the activation of three cytoplasmic proteins, which are Myeloid differentiation primary response 88 (MyD88), Tube and Pelle forming the heterotrimeric complex through their death domains downstream of the activated Toll receptor (Huang et al., 2014; Moncrieffe et al., 2008; Tassanakajon et al., 2018). Pelle can associate with the Tumor necrosis factor receptor-associated factor 6 (TRAF6), an adaptor protein that identified as a downstream of Pelle during Toll signal transduction (Wang et al., 2011) leading to form Dorsal-Cactus complex. Cactus is normally phosphorylated and degraded, whereas, the Dorsal (NF-kB transcription factor) can translocate into the nucleus to regulate the transcription of AMP genes such as penaeidin3a and antilipopolysaccharide factors (ALFs), crustin, and lysozyme (Hou et al., 2014; Tassanakajon et al., 2018; Z. Wang et al., 2015).

2.3.2.2 IMD pathway

Immune deficiency (IMD) pathway is the other essential signaling pathway of host defense against invading pathogens. Unlike the Toll pathway, the initiation of IMD pathway directly interact with the PNGs of Gram-negative bacterial to the transmembrane receptors to activate the pathway (Tassanakajon et al., 2018). The two related components in IMD pathway have been reported including, IMD and Relish. The IMD, death domain protein encoded by the immune deficiency gene participates in innate signaling to activate the expression of AMP genes. The IMD refers to a mutation that shows severe defects in resistance to Gram-negative bacteria but has normal response to fungi and Gram-positive bacteria. Other reported component, Relish, acts as NF-kB transcription factor that can translocate into the nucleus and immediately up-regulates the AMP genes (F. Li & Xiang, 2013a).
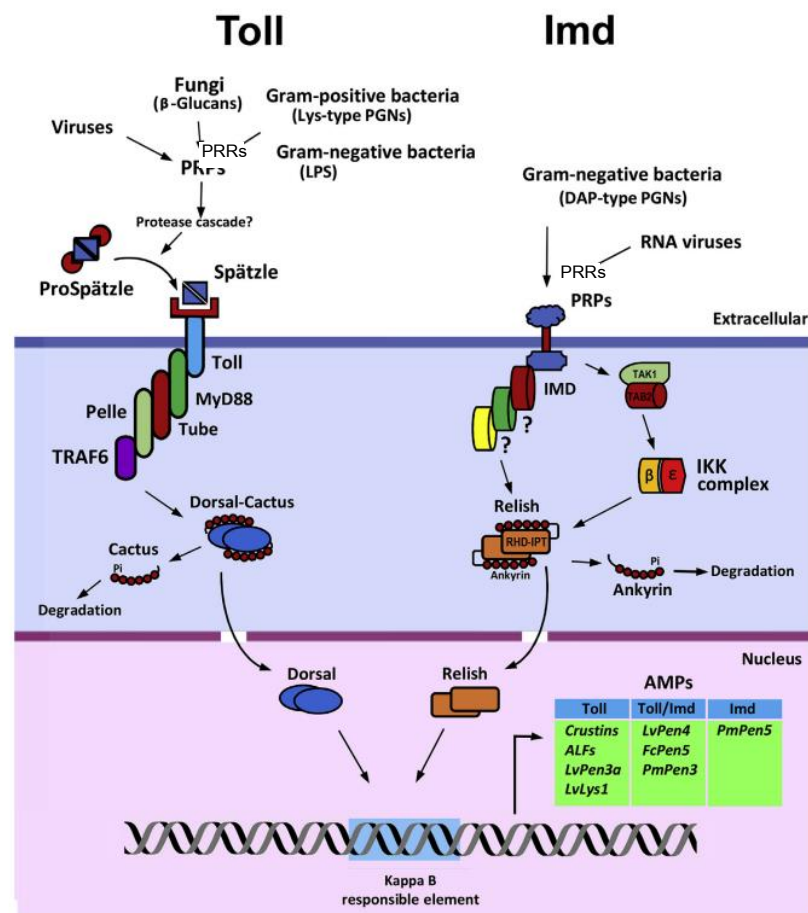
Figure 4 Schematic diagram of Toll and IMD signaling pathways in penaeid shrimp.

Source: Tassanakajon, A., Rimphanitchayakit, V., Visetnan, S., Amparyup, P., Somboonwiwat, K., Charoensapsri, W., & Tang, S. (2018). Shrimp humoral responses against pathogens: antimicrobial peptides and melanization. *Developmental & Comparative Immunology,* 80, 81-93.

2.3.3 Cellular immune response

The cellular immune response in penaeid shrimp is mediated directly by hemocytes that have the same biological functions as the macrophage in vertebrates and participate in phagocytosis, apoptosis, nodule formation and encapsulation of pathogens (Aguirre et al., 2009).

Phagocytosis, the engulfment of particles by cell, is a highly conserved process among the organisms that cells have ability to recognize and ingest small particles, including microbial pathogens (self/nonself-recognition). The phagocytosis is initiated by engagement of pathogen particles and cell surface receptors. The target particles are immediately uptake by intracellular vesicular transport to phagosomes which pathogens inside are destroyed by low pH, hydrolysis, and free-radicals (Pearson et al., 2003; Stuart & Ezekowitz, 2008; Xu et al., 2014). Apoptosis or programmed cell death is an important cellular process for removing cells that become sustained genetic damage or that undergo uncontrolled cellular proliferation (Bortner et al., 1995). Other cellular responses, apoptosis, the innate immune response that can be induced by viral infection and have ability to limit viral replication and destroy viral infected cells (Everett & McFadden, 1999; Xu et al., 2014) . Although various molecules related in apoptotic process have been characterized in crustaceans, the knowledge of the apoptosis pathway remains limited.

2.4 Tumor necrosis factor receptor-associated factors 6 (TRAF6)

Tumor necrosis factor receptor-associated factors (TRAFs) are a members of the Tumor necrosis factor receptor (TNFR) superfamily that have been identified as the major signal transducers for the TNF receptor superfamily and the Interleukin-1 receptor/Toll-like receptor (IL-1R/TLR) mediated a wide range of biological functions including both adaptive and innate immunity, development and stress response (Arch et al., 2000; Magnusson & Vaux, 1999). To date, TRAF1-TRAF6 have been identified (firstly in mammals) and found conserved across other animals (Mali & Frank, 2004).

Similar to other TRAFs, TRAF6 presents all the unique characteristics of TRAFs proteins including a novel TRAF domain at the C-terminus (a coiled-coil domain followed by a highly conserved TRAF-C domain) and a RING finger (several putative Zinc-finger motifs) at the N-terminus (Chung et al., 2002; Rothe et al., 1994; Wajant et al., 2001). The RING finger motif of TRAF6 possesses the ubiquitin (E3) ligase catalytic domain, which is important for activating the downstream signaling cascades (Budhidarmo et al.,

2012). A coiled-coil domain is crucial for auto-ubiquitination process and activating NF-kB signaling pathway (Yang et al., 2004). The TRAF-C domain at the C-terminus can catalyze the oligomerization of TRAF6 and is used for receptor binding (Megas et al., 2010).

TRAF6 is the only TRAFs member that can associate with both TNFR superfamily and IL-1R/TLR family due to its distinct receptor-binding specificity, and plays an important role in the regulation of several signaling cascades in adaptive and innate immunity (Cao et al., 1996; Ye et al., 2002).

Besides mammalian TRAF6s, there are several studies reported on the characterization of TRAF6 homologs in other invertebrates as well as determination of its role in innate immunity. As an illustrate, in 2009, Qiu and others identified *TRAF6* from Zhikong Scallop, *Chlamys farreri,* the first functional identified *TRAF6* in marine invertebrates, which was given a name of *CfTRAF6*, and examined the role of *Chlamys farreri TRAF6* (*CfTRAF6*) in regulation of PGN infection. The results showed that the full-length of *CfTRAF6* consisted of 2,510 bp with an open reading frame (ORF) encoding a polypeptide of 655 amino acids. The putative amino acid sequence presented all characteristic motifs of the TRAF proteins. The *CfTRAF6* is constitutively expressed in all examined tissues. After treating with different concentrations of PGN, *CfTRAF6* found down-regulated within 3 hour post-injection (Qiu et al., 2009). Another TRAF6 from mollusks, Japanese scallop (*Mizuhopecten yessoensis*), was identified and characterized by He and colleagues in 2013. The results revealed that *Mizuhopecten yessoensis TRAF6* (*MyTRAF6*) was highly expressed in hemocytes of normal adult *M. yessoensis* and was up-regulated after challenging with *Vibrio anguilarumn* (He et al., 2013). Later in 2018, Dandan and colleagues identified *TRAF6* from pearl mussel (*Hyriopsis cumingii*) and found that *HcTRAF6* could enhance the activity of the NF-kB in a dose-dependent manner. Silencing of *HcTRAF6* further decreased the ability to clear bacteria infecting cells (Huang et al., 2018). All these findings together prove that *TRAF6* in mollusks involved in signal transduction and immune response of innate immune mechanisms against invading pathogens.

The first identified and characterized *TRAF6* from swimming crab, *Portunus trituberculatus* was reported by Zhou and colleagues in 2015. The *Portunus trituberculatus TRAF6* (*Pt-TRAF6*) exhibited all characteristic domains of TRAFs. The *Pt-TRAF6* was down-regulated in hemocytes and up-regulated in gills after *V. alginolyticus* or LPS challenge suggesting that *Pt-TRAF6* may respond to Gram-negative bacterial infections (Zhou et al., 2015). Later in 2017, Sun and colleagues identified *TRAF6* from mud crab, *Scylla paramamosain* as well as examined the role of *Sp-TRAF6* in regulation of Anti-lipopolysaccharide factors (ALFs) expression. The results indicated that *Sp-TRAF6* transcripts were significantly up-regulated after *V. parahemolyticus* and LPS challenges. Silencing of *Sp-TRAF6* by siRNA showed the effect on expression of *ALFs* genes. After *Sp-TRAF6* was completely suppressed, the *SpALF5* and *SpALF6* expression were inhibited in hemocytes and hepatopancreas. These findings indicated that *TRAF6* plays an important role in host defense against pathogen invasions via regulation of *ALF*s expression (Sun et al., 2017).

In shrimp, the first functional *TRAF6* was identified from *Litopenaeus vannamei* by Wang and colleagues in 2011. The full-length *LvTRAF6* consisted of an ORF encoding a putative protein of 594 amino acids, including a RING-type Zinc finger, two TRAF-type Zinc fingers, a coiled–coil region, and a MATH domain. Dual luciferase reporter assays demonstrated that *Lv*TRAF6 could activate the expression of AMPs responsible for eliminating invading pathogens. *LvTRAF6* transcripts significantly responded to bacterial and viral infection such as down-regulation in intestine after *V. alginolyticus* challenge and up-regulation in gills and hepatopancreas after white spot syndrome virus (WSSV) challenge. These results suggested that *LvTRAF6* plays a crucial role in antibacterial and antiviral responses via regulation of *AMP* gene expression (Wang et al., 2011). In 2014, Deepika and colleagues identified *TRAF6* and also *MyD88* and *Toll* from *Penaeus monodon* and characterized its role in antiviral response via Toll-pathway. After challenging with WSSV, *Pm*Toll, *PmTRAF6*, and *PmMyD88* were all up-regulation significantly. Up-regulated expression of *PmTRAF6* was detected in hemocytes and lymphoid organ, whereas there was no significant

change after inducing with poly I:C (Deepika et al., 2014). Recently in 2017, Cai and colleagues investigated the functions of *TRAF6* from *Fenneropenaeus penicillatus* as a regulator of another AMP, *peroxinectin*, gene expression. The results demonstrated that the changes of *FpTRAF6* expression could be observed with the different patterns in examined tissues after WSSV and *V. alginolyticus* injection. Silencing of *FpTRAF6* gene could inhibit *peroxinectin* expression *in vivo*, and enhance the sensitivity of shrimps to WSSV and *V. alginolyticus* challenge, suggesting that *FpTRAF6* could play a crucial role in antibacterial and antiviral responses (Cai et al., 2017).

2.5 Rapid Amplification of cDNA Ends (RACE)

Rapid Amplification of cDNA Ends (RACE) is a molecular biology technique for obtaining the full-length cDNA of the gene of interest when the sequence is only partially identified (Yeku, 2011). RACE primarily utilizes reverse transcription converted mRNA to cDNA (RACE-Ready cDNA). The specific cDNA is then directly amplified by PCR using a gene-specific primers (GSPs) derived from the known partial sequence within an internal region of the mRNA of interest. The nested RACE-PCR using nested gene-specific primers (NGSPs) is required to generate a specific amplification product (Frohman, 1993).

The 3'- RACE begins with the first-strand cDNA synthesis using reverse transcriptase with modified oligo(dT) primer (Oligo(dT)-adaptor primer). After elimination of mRNA, the RACE-PCR reaction is then performed using GSP coupled with universal primer which is complementary to adaptor primer sequence (Figure 5) (Frohman, 1994; Scotto -Lavino et al., 2006).
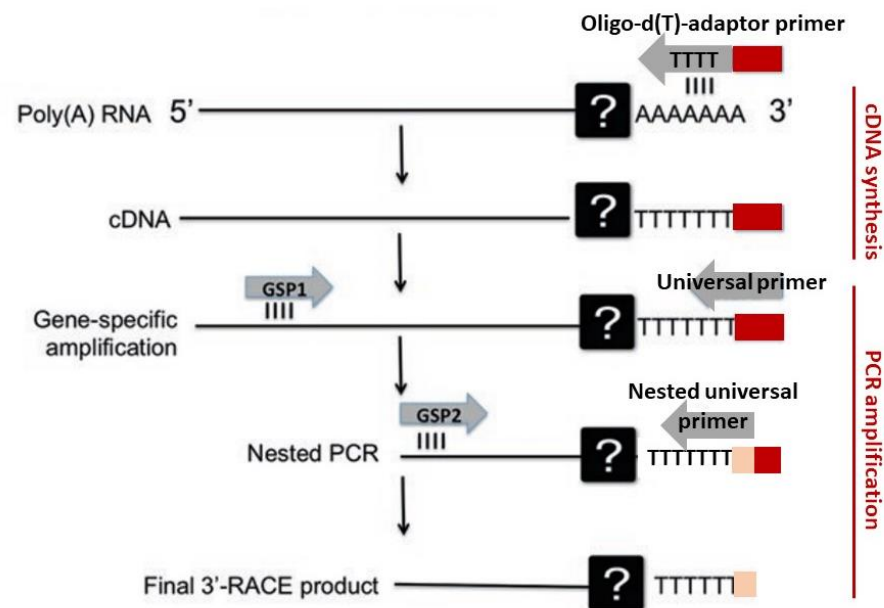
Figure 5 Schematic representation of 3' RACE.

The process of first-strand cDNA synthesis begins at the poly(A) tail of the RNA molecule, utilizing an Oligo-(dT) primer tagged with an adaptor (highlighted in red). The first round of PCR amplification involves the use of two primers: a gene-specific primer (GSP) 1 designed by the user and a universal primer that targets the sequence introduced by the adaptor primer during cDNA synthesis. A nested PCR is then employed to generate a specific amplification product using a GSP2 and a Nested universal primer. The question boxes [?] represent the unknown sequence of the gene.

Source: Modified from: C. Pastori, D. Velmeshev, V. Peschansky. (2017). Deep-RACE: Comprehensive Search for Novel ncRNAs Associated to a Specific Locus. 1543. 129-143.

In the case of 5'- RACE, the first-strand cDNA is synthesized using reverse transcriptase with another GSP followed by addition of homopolymeric tail at the 3'-end of the first-strand cDNA by terminal deoxynucleotidyl transferase (TdT). This synthetic tail provides a primer-binding site. The RACE-PCR reaction is then performed using GSP

coupled with universal primer that specific to the homopolymeric tail (Figure 6) (Frohman, 1994; Scotto-Lavino et al., 2006).
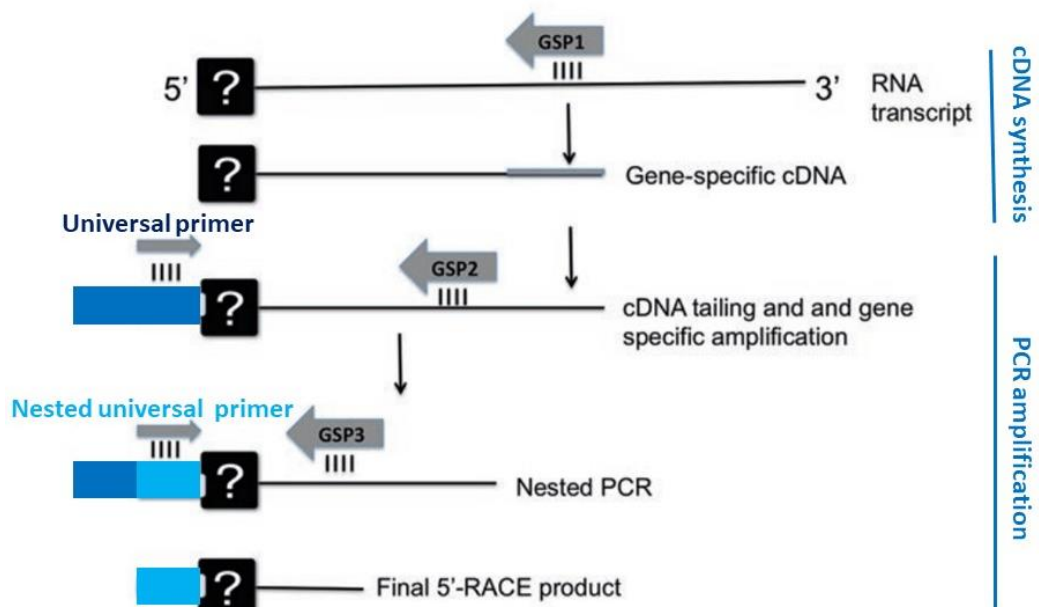
Figure 6 Schematic representation of 5' RACE.

The initiation of first-strand cDNA synthesis occurs with the use of a gene-specific primer (GSP1) in conjunction with an Oligo-d(T) primer tagged with an adaptor (highlighted in red). The first round of PCR amplification is conducted using a GSP2 and a nested universal primer. Subsequently, a nested PCR is employed to generate a specific amplification product using GSP3 and a Nested universal primer. The question boxes [?] represent the unknown sequence of the gene.

Source: Modified from: C. Pastori, D. Velmeshev, V. Peschansky. (2017). Deep-RACE: Comprehensive Search for Novel ncRNAs Associated to a Specific Locus. 1543. 129-143.

2.6 RNA interference (RNAi)

RNA interference (RNAi) is a conserved regulatory mechanism or post transcriptional gene silencing (PTGS) mechanism that most eukaryotic organisms possess for controlling gene expression which mediates suppression of gene expression triggered by small double-strand RNA (dsRNA). The RNAi process is being considered to be a powerful tool in studies of gene function on a whole-genome scale as well as in therapeutic applications for the treatment of diseases (Hamilton et al., 2002; Hannon, 2002; Kim & Rossi, 2008).

Based on genetic and molecular analysis, the mechanism of gene silencing through RNAi has been divided into two stages including initiation and effector stages (Jaronczyk et al., 2005).

The initiation stage involves the generation of short interfering RNA (siRNA) guided to degradation of target mRNA. Double-stranded RNA (dsRNA) is cleaved to generate the siRNA which is approximately 21-26 nucleotides long with two-nucleotide 3' overhangs by the action of RNaseIII enzyme named Dicer (Hamilton et al., 2002; Jaronczyk et al., 2005). Dicer contains a conserved dual RNase III motifs, dsRNA-binding domain (dsRBD) and helicase C domain. Most, but not all, Dicer proteins also contain PAZ (Piwi/Zwille/ARGONAUTE) domains (Bernsteinet al., 2001).

The effector stage begins immediately after the siRNA incorporates into the effector complex known as RNA-induced silencing complex (RISC). As the duplex siRNAs is unwound, the complex becomes activated. The RISC then uses the unwound siRNA (single-strand antisense siRNA) as a guide targeted to a specific region of the complementary mRNA. The endonuclease then cleaves the target mRNA at the central nucleotide of mRNA:siRNA heteroduplex. The degradation by exonuclease is occurred allow target mRNA to cleave into a small fragment. (Bernstein et al., 2001; Hannon, 2002). The PPD (PAZ protein domain) protein such as *Arabidopsis thaliana* AGO, a member of the *Argonaute* gene family, and ZWILLE has well-established function in RNAi process. PPD proteins contain a PAZ domain located at the central and Piwi domain at the C-terminus. PAZ domain is responsible for binding to the 3' overhang of

siRNA, whereas Piwi domain possesses the binding site for Dicer (Jaronczyk et al., 2005).

In nature, amplification of the silencing signal requires RNA-directed RNA polymerase (RdRP)-dependent for synthesis of new dsRNA (Hannon, 2002).
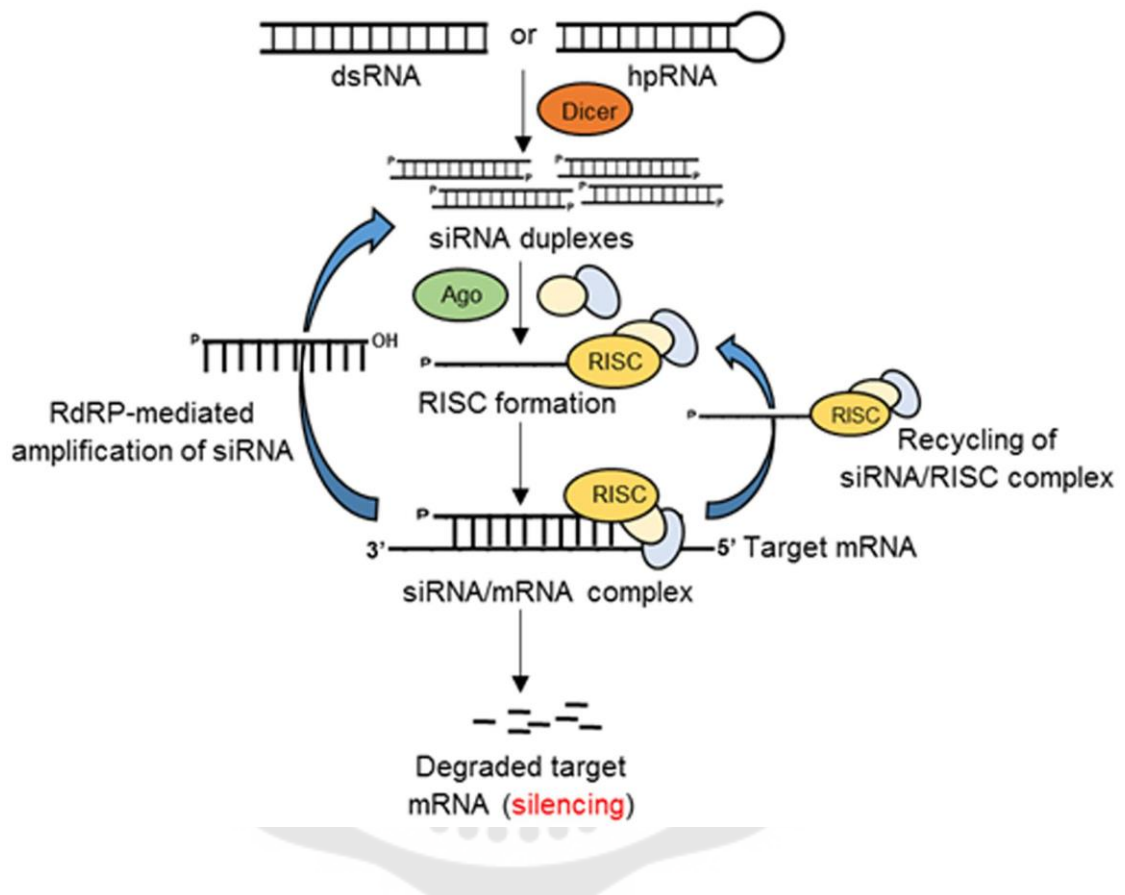
Figure 7 Schematic of RNAi-mediated gene silencing in eukaryotes.

Source: Majumdar, R., Rajasekaran, K., & Cary, J. W. (2017). RNA Interference (RNAi) as a Potential Tool for Control of Mycotoxin Contamination in Crop Plants: Concepts and Considerations. *Frontiers in Plant Science, 8*(200).

CHAPTER 3

MATERIALS AND METHODS

This research approach was divided into five major parts including (1) molecular isolation and identification of a full-length *Macrobrachium rosenbergii tumor necrosis factor associated factor 6* (*MrTRAF6*) gene using Rapid Amplification of cDNA Ends (RACEs), (2) characterization and bioinformatics analysis of *MrTRAF6*, (3) tissue expression and distribution analysis of *MrTRAF6* in normal prawns, (4) temporal expression of *MrTRAF6* in response to bacterial infection, and (5) investigation of the functional role of *MrTRAF6* innate immune response using RNA interference (RNAi) The procedure flowchart was illustrated in Figure 8.
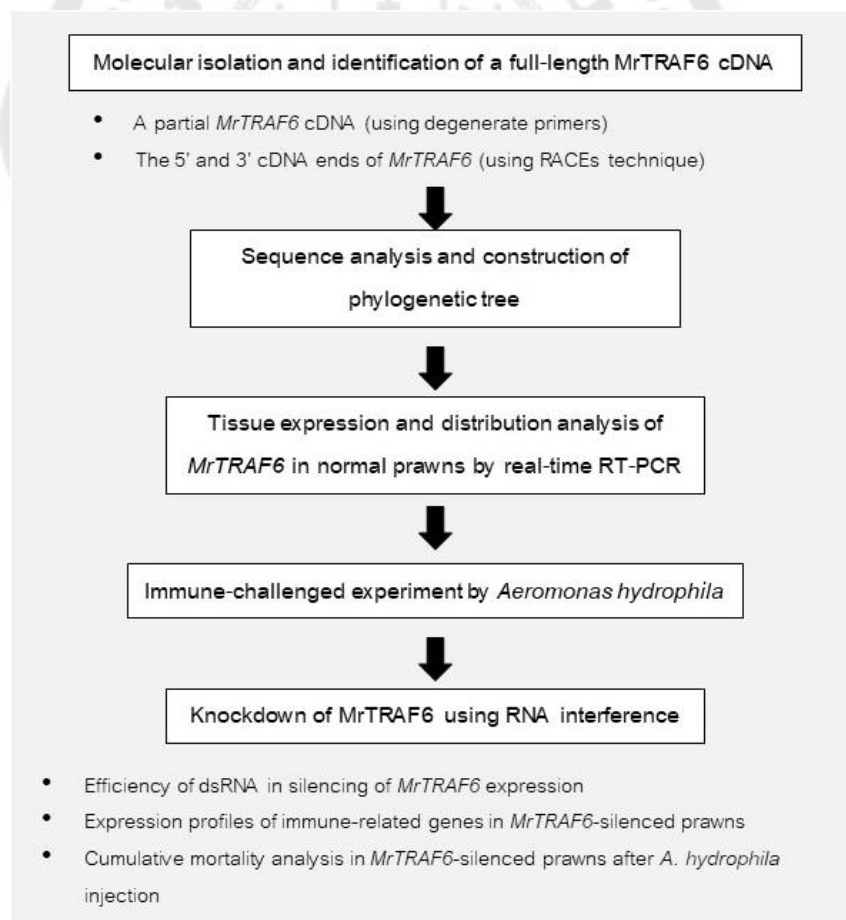
Figure 8 Experimental overview.

3.1 Molecular isolation of *MrTRAF6*

The full-length of *MrTRAF6* was identified from giant freshwater prawn, *Macrobrachium rosenbergii*. The sample prawns with approximated weight of 50 g were obtained from local farm at Suphanburi Province, Thailand. The tissue of a prawn was used to extract the total RNA. The extracted RNA was then utilized to generate cDNA. This cDNA synthesis was performed to isolate a partial sequence of the MrTRAF6 gene by employing degenerate primers that were designed based on conserved regions found in related species. The RACEs reactions were performed to generate the remaining 3' and 5' ends of *MrTRAF6*.

3.1.1 Total RNA extraction

The muscle tissues were used to extract total RNA following the manufacturer's protocol for the NucleoSpin® RNA XS total RNA isolation kit (Macherey-Nagel, Germany). In summary, 5 mg of collected muscle tissue was lysed and homogenized in 200 µL of RA1 buffer along with 4 µL of TCEP (tris(2-carboxyethyl)phosphine). To the lysate, 5 µL of a working solution containing carrier RNA (prepared as described in Table 2) was added. The mixture was then mixed by vortexing and briefly spinning down.

Table 2 Components of RNA working solution.

Components	Volume (µL)
RA1 buffer	99
Carrier RNA stock solution (100 ng/µL)	1
Total volume	100

The mixed lysate was passed through a NucleoSpin® Filter via centrifugation at 11,000 $x\ g$ for 30 seconds. Next, 70% ethanol was added to the filtered lysate and gently mixed by pipetting. The resulting mixture was transferred to the NucleoSpin® RNA XS Column and centrifuged at 11,000 $x\ g$ for 30 seconds. Following

centrifugation, 100 µL of Membrane Desalting Buffer (MDB) was added to the column and centrifuged again at 11,000 x g for 30 seconds. Once the column was dried, 25 µL of a rDNase reaction mixture (prepared as in Table 3) was directly applied to the center of the column and incubated at room temperature for 15 minutes.

Table 3 Components of rDNase reaction mixture.

Components	Volume (µL)
Reaction Buffer for rDNase	27
rDNase	3
Total volume	30

After the incubation step, the column was supplemented with 100 µL of RA2 buffer and allowed to incubate for 2 minutes at room temperature. Subsequently, the column was centrifuged at 11,000 x g for 30 seconds. Afterward, a wash step was performed by adding 400 µL of RA3 buffer to the column and centrifuging it at 11,000 x g for 30 seconds. The washing step was repeated using 200 µL of RA3 buffer and centrifugation at 11,000 x g for 2 minutes. Finally, the RNA within the column was eluted into a nuclease-free tube by adding 10 µL of RNase-free water to the center of the column, followed by centrifugation at 11,000 x g for 30 seconds. The extracted RNA was quantified using a NanoDrop Lite Spectrophotometer (Thermo Fisher Scientific, USA) and stored at -70°C until further use.

3.1.2 First-stranded cDNA synthesis

The synthesis of first-strand cDNA was carried out using the SuperScript® III First-Strand Synthesis System for RT-PCR (Invitrogen, USA) following the instructions provided by the manufacturer. Initially, the RNA mixture was prepared using the extracted RNA mentioned in section 3.1.1 as a template, with the specific components listed in Table 4.

Table 4 Components RNA mixture for First-Strand cDNA synthesis.

Components	Volume (µL)
Total RNA (500 ng/µL)	5
50 µM oligo(dT)$_{20}$	1
10 mM dNTPs mix	1
DEPC-treated water	3
Total volume	10

After that, the prepared RNA mixture was subjected to incubation at 65°C for 5 minutes, after which the tube was cooled on ice for at least 1 minute. Subsequently, the 2X reaction mixture was prepared using the components as listed in Table 5.

Table 5 Components of 2X reaction mixture for first-strand cDNA synthesis.

Components	Volume (µL)
RNA mixture (from Table 4)	10
10X RT buffer	2
25 mM MgCl$_2$	4
0.1 M DTT	2
RNaseOUT™ (40 U/µL)	1
SuperScript® III RT (200 U/µL)	1
Total volume	20

After preparation, the reaction mixture was incubated at 42°C for 50 minutes followed by terminating reaction at 85°C for 5 minutes, and then reaction tube was placed on-ice for at least 1 minute. To eliminate the RNA that is complementary to the cDNA, 1 µL of *E. coli* RNaseH (2 U/µL) was added to the reaction mixture. The mixture

was then incubated at 37°C for 20 minutes. Subsequently, the cDNA was stored at -20°C until use.

3.1.3 Molecular isolation and identification of the partial sequence of *MrTRAF6* gene

The partial sequence of *MrTRAF6* was obtained by PCR using degenerate primers designed from conserved regions of the other TRAF6s sequences from related species. The cDNA synthesized in section 1.2 was used as the template in PCR reaction.

3.1.3.1 PCR amplification using degenerate primers

To amplify the partial cDNA fragment of *MrTRAF6*, the sequences of TRAF6 proteins from related species, including *Litopenaeus vannamei*, *Fenneropenaeus chinensis*, *Penaeus monodon*, *Portunus trituberculatus*, and *Scylla paramamosain* were aligned (Figure 9) using Clustal Omega software (https://www.ebi.ac.uk/Tools/msa/clustalo/). The specific degenerate primers were designed based on amino acids in conserved regions. The sequences of two degenerate primers, degTRAF6-F and degTRAF6-R, used in this experiment were listed in Table 6.

```
L.vennamei        MESVEES-------ITILSRQEGFDYEFVPPLDPKYECAICLLGLRSPIQTTCGHRFCKD
F.chinensis       MESVEES-------ITILSRQEGFDYEFVPPLDPKYECAICLLGLRSPIQTTCGHRFCKD
P.monodon         MECVEES-------ITILSRQEGFDYEFVPPLDPKYECAICLLGLRSPIQTTCGHRFCKD
P.trituberculatus MECHNSLTDTPLGESVVLPRAQGYDYEFVPALDPKYECPICLLALRAPLQTACGHRFCKD
S.paramamosain    MACHNSLNDGHLGESVVLPRTQGYDYEFVPTLDPKYECPICLLALRAPLQTACGHRFCKD
                  * . :.          .:*.* :*:******.*******.****.**:*:**:********

L.vennamei        CIFNCMSESSSRCPVDNTPLTEADLFPDSCAEREILQLSVKCPNHGLGCRRTVDLMYIEH
F.chinensis       CIFNCMSESSSRCPVDNTPLTEVDLFPDSCAEREILQLSVKCPNHGLGCRRTVDLMYIEH
P.monodon         CIFNCMSESSSRCPVDNTPLTEVDLFPDSCAEREILQLSVKCPNHGLGCRRTVDLMYIEH
P.trituberculatus CIYNSLSESSRRCPIDNTPLKETDLFPDSCAEREVLQLRVRCPNTSLGCTQVLDLMYIEH
S.paramamosain    CIYNSLSESSRRCPIDNTPLKETDLFPDSCAEREVLQLRVRCPNTSLGCSQVLDLMYIEH
                  **:*.:**** ***:*****.*.************:*** *:*** .*** :.:*******

L.vennamei        EMS-GKYCNGDYVWGIKNFSQFCAELQNKPGRVCHSPSFYTSQFGYKFCLRTNITWK---
F.chinensis       EMS-GKYCNGDYVWRIKNFSQFCAELQNKPGRVCHSPSFYTSQFGYKFCLRTNITWK---
P.monodon         EMS-GKYCNGNYVWRIKNFSQFCAELQNRPGRVCHSPSFYTSQFGYKFCLRTNITWK---
P.trituberculatus EAARGRYCQGEYVWRLKDFPGTLAELREKPTRVFHSPGFYTSPFGYKFCLRLNLTRNGQG
S.paramamosain    EAARGKYCQGEYVWRLKDFPGTLAELREKPTRVIHSPGFYTSPFGYKFCLRLNLTRG--S
                  * : *:**:*:*** :*:*.   ***::* ** ***.**** ******** *:*

L.vennamei        -----SEQYFLTLFIHGMQSENDDFLDWPFSGRITLSVLDCDISLPKNHITETMVTKPGL
F.chinensis       -----SEQYFLTLFIHGMQSENDDFLDWPFSGRITLSVLDCDTSLPKNHITETMVTKPGL
P.monodon         -----SDQYFLTLFIHGMQSENDDFLDWPFSGRITLSVLDCDTSLPKKHITETMVTKPGL
P.trituberculatus GQGGPAGEEWLSLFIHGMQGENDAFLDWPFAGVITFALLDCSVGKPKAHITETLQSSPDR
S.paramamosain    GKGERGGEEWLSLFIHGMQGENDDFLDWPFSGIITFSLLDCGAGRPKAHITETLHSSPDR
                  . : :*:*******.*** ******:* **:::***. . ** *****: :.*.

L.vennamei        QAFKRPDVARNPKGFGFTEFVPLAKILQPS-TGTFLKNDTLCIRATVCPNTWNHESSQSM
F.chinensis       QAFKRPDVARNPKGFGFTEFVPLAKILQPS-IGTFLKNDTLCIRATVCPNTWNHESSQST
P.monodon         QAFKRPDVARNPKGFGFTEFVPLAKILQPS-IGTFLKNDTLCIRATVCPNTWNHESSQSM
P.trituberculatus QAFSRPQTHRNPKGFGYTEFAPVRKVVDGSGRAEYLHEGTLHIRATVKLLQHHQGPAGKA
S.paramamosain    QSFSRPQMHRNPKGFGYTEFAPLSKVVEGSGRAEYVHEGTLHIRATVRLQQQHQGSTGKT
                  *:*.**: *******:***.*: *::: *  . :::::.** *****    :: .: .

L.vennamei        EKLGIYKEKLHIEKQSCV
F.chinensis       EKLGIFKEKLHIEKQSCV
P.monodon         EKLGIFKEKLHIEKQSCV
P.trituberculatus GCICQHQQKAQKVG----
S.paramamosain    GCICQHQQKSQKV-----
                  :  .::* :
```

Figure 9 Multiple sequence alignments of TRAF6s from related species to design

degenerate primers.

The various TRAF6s were included: *L. vannamei* TRAF6 (ADM26237.1),

F. chinensis TRAF6 (AFU51810.1), *P. monodon* TRAF6 (AIS92907.1), *P. trituberculatus*

TRAF6 (AKD94181.1) and *S. paramamosain* TRAF6 (CRI06483.1).

The regions used to design the forward and reverse degenerate primers are indicated in

red and blue characters, respectively.

Table 6 Degenerate primers used in PCR reaction for amplification of partial *MrTRAF6.*

Primer name	Sequence (5'-3')	Amplicons (bp)
degTRAF6-F	GGI TTYGAYTAYGARTTYGTICC	550
degTRAF6-R	RAAYTCNGTRAANCCRAANCCYTTNGG	

The PCR amplification was carried out using Platinum™ *Pfx* DNA Polymerase (Invitrogen, USA). The cDNA obtained from section 3.1.2 was utilized as the template for the PCR reaction. The PCR reaction mixture was prepared as listed in Table 7.

Table 7 Components PCR reaction mixture for amplification of *partial MrTRAF6*.

Components	Volume (µL)
10X *Pfx* Amplification Buffer	10.0
10 mM dNTPs mixture	1.5
50 mM $MgSO_4$	1.0
50 µM degTRAF6-F	1.0
50 µM degTRAF6-R	1.0
cDNA template	1.0
Platinum™ *Pfx* DNA Polymerase	0.4
Sterilized distilled water	33.1
Total volume	50

After mixing, the reaction mixture was placed in a Thermal Cycler (Bio-Rad, USA). The amplification conditions used were as follows:

Step 1 Denaturation 94°C for 30 seconds

Step 2 Annealing 50°C for 30 seconds

Step 3 Extension 72°C for 30 seconds

Step 4 Repeat steps 1 - 3 for 34 cycles

Step 5 Final extension 72°C for 10 minutes

The PCR products obtained were analyzed using agarose gel electrophoresis, utilizing a 1.0% agarose gel stained with SYBR® Safe DNA gel stain (Invitrogen, USA). The gel was visualized under UV light using the GelView Master Gel Documentation System (Dynamica, UK). The PCR product of the expected size was

excised from the gel and purified using the NucleoSpin® Gel and PCR Clean-up kit (Macherey-Nagel, Germany) according to the manufacturer's protocol. In summary, the gel containing DNA was dissolved by incubating in 200 μL of NTI buffer at 50°C until complete dissolution. The dissolved mixture was then transferred to a NucleoSpin® Gel and PCR Clean-up column, and centrifuged at 11,000 *x g* for 30 seconds. Subsequently, the column was washed with 700 μL of NT3, centrifuged at 11,000 x g for 30 seconds, and dried by centrifugation at 11,000 *x g* for 1 minute. After drying the column, the DNA was eluted by adding 20 μL of NE elution buffer to the center of the column and centrifuging it at 11,000 *x g* for 1 minute. The purified PCR product was then stored at -20°C until use.

3.1.3.2 Cloning of partial *MrTRAF6* fragment

In order to identify the partial *MrTRAF6* sequence, the purified PCR product in section 1.3.1 was cloned into the pCR-Blunt II-TOPO plasmid (as shown in Figure 10) using the Zero Blunt® TOPO® PCR Cloning Kit (Invitrogen, USA). The ligation mixture was prepared according to the manufacturer's protocol, and the specific components used are listed in Table 8.

Table 8 Components of pCR™-Blunt II-TOPO® ligation mixture.

Components	Volume (μL)
Purified PCR product	4
Salt solution	1
pCR™II-Blunt-TOPO	1
Total volume	6

After mixing, the ligation mixture was incubated at room temperature for 30 minutes. Following the incubation, the mixture was transformed into 200 μL of *E. coli* strain TOP10 competent cells using a heat shock method at 42°C for 2 minutes, immediately followed by placing the cells on ice for 20 minutes. Subsequently, the

mixture was combined with 600 µL of LB broth and incubated at 37°C for 2 hours while shaking at 225 rpm. After the incubation, the bacterial culture was centrifuged at 6,000 *x g* for 3 minutes, and the resulting pellet was spread onto an LB agar plate supplemented with kanamycin at a final concentration of 100 µg/mL and 25 µL of 40 µg/mL X-gal for blue-white screening. The LB agar plate was then incubated overnight at 37°C.
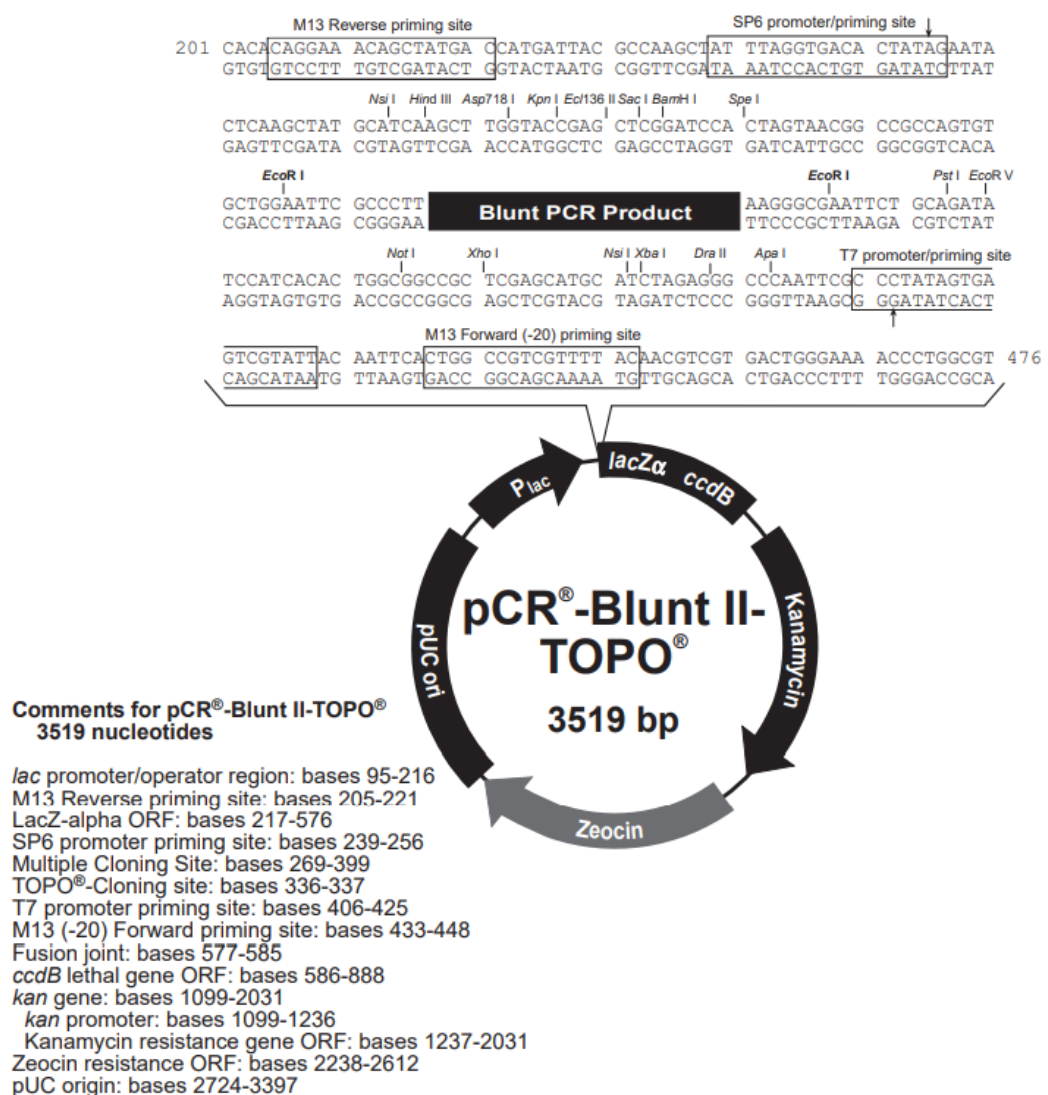
Figure 10 pCR™-Blunt II-TOPO® (Thermofisher, USA) circle map and sequence reference points.

After incubation, the bacteria that harbored recombinant plasmid, partioal*MrTRAF6*- pCR™ II-Blunt-TOPO® were grown as white colonies, whereas the others that carried vector without inserted DNA was as blue colonies. The white colony was sub-cultured in 4 mL of LB broth supplemented with kanamycin at a final concentration of 100 μg/mL. The sub-culture was then incubated overnight at 37°C with shaking at 225 rpm. Following the incubation, the plasmid DNA was extracted from the overnight bacterial culture using the NucleoSpin® Plasmid kit (Macherey-Nagel, Germany) according to the manufacturer's protocol.

Briefly, the bacterial culture was transformed to 1.5 mL sterile microcentrifuge tube. Bacterial cells were harvested by centrifugation at 11,000 x g for 30 seconds. The supernatant was discarded, and the bacterial pellet was lysed in 250 μL of A1 buffer. After the bacterial pellet completely re-suspended, the lysate was added with 250 μL of A2 buffer, mixed gently by converting tube, and incubated the tube at room temperature for 5 minutes. Next, 300 μL of A3 buffer was added to the lysate, mixed gently, and subjected to centrifugation at 11,000 x g for 10 minutes. Subsequently, the supernatant containing the plasmid DNA was carefully loaded onto a NucleoSpin® Plasmid column. The column was then centrifuged at 11,000 x g for 1 minute to allow for the binding of DNA to the column. Following this, the column was washed with 600 μL of A4 buffer and centrifuged at 11,000 x g for 1 minute. The washing step was performed to remove any impurities. The column was then centrifuged at 11,000 x g for 2 minutes to dry the membrane. Lastly, the plasmid DNA was eluted from the column using 50 μL of AE elution buffer, incubated the column at room temperature for 1 minute, and finally centrifuged at 11,000 x g for 1 minute.

To verify the presence of the recombinant plasmid in the extracted sample, a restriction digestion step was performed using *Eco*RI-HF (New England, UK). The digestion reaction was prepared as listed in Table 9.

Table 9 The restriction endonuclease reaction of *Eco*RI-HF.

Components	Volume (µL)
Extracted plasmid	4
rCutSmart™ Buffer	1
*Eco*RI-HF	1
Total volume	6

The prepared mixture was incubated at a temperature of 37°C for 2 hours to facilitate the digestion process. Subsequently, the digested products were analyzed via agarose gel electrophoresis using 1.5% agarose gel stained with SYBR® Safe DNA gel stain (Invitrogen, USA). The separated fragments resulting from the digestion were then visualized under UV light using the GelView Master Gel Documentation System (Dynamica, UK).

The verified recombinant plasmid was further sequenced to identify the partial *MrTRAF6* sequence. The obtained sequence was identified using BLASTX program (https://blast.ncbi.nlm.nih.gov/Blast.cgi). Subsequently, the identified partial sequence of *MrTRAF6* was utilized to identify the remaining 3' and 5' ends of the *MrTRAF6* gene.

3.1.4 Molecular isolation and identification of the full-length *MrTRAF6* gene using Rapid amplification of cDNA ends (RACEs)

The full-length *MrTRAF6* cDNA was isolated using the rapid amplification of cDNA ends (RACEs). The template cDNA for RACE was synthesized from extracted RNA using SMARTer™ RACE cDNA Amplification Kit (Takara, Japan). The gene specific primers for RACE reaction were designed from the partial *MrTRAF6* sequence. The remaining 3' and 5' RACEs were performed separately.

3.1.4.1 Preparation of 5' and 3' RACE-Ready cDNA

For the synthesis of the 5' and 3' RACE-Ready cDNA, separate reactions were performed using the SMARTer™ RACE cDNA Amplification Kit (Takara, Japan)

following the manufacturer's protocol. The 5'-RACE CDS Primer A (5'-(T)25VN-3') was used for 5' cDNA reaction mixture, and 3'-RACE CDS Primer A (5'–AAGCAGTGGTATCAACGCAGAGTAC(T)30VN–3') was used for 5' cDNA reaction mixture (N = A, C, G, or T; V = A, G, or C). The RNA reaction mixture for the 5' and 3' RACE-Ready cDNA synthesis was prepared using the total RNA obtained from section 3.1.1 as the template, with the components listed in Table 10.

Table 10 Components of RNA mixture for 5' and 3' RACE-Ready cDNA synthesis.

Components	Volume (µL)
Total RNA	10
12 µM 3'-RACE CDS Primer A / 5'-RACE CDS Primer A	1
Total volume	11

After preparation, the RNA mixture was subjected to incubation at 72°C for 3 minutes, followed by 42°C for 2 minutes using a Thermal Cycler (Bio-Rad, USA). Subsequently, the RACE-Ready cDNA synthesis reaction mixture was prepared using the specific components listed in Table 11. In case of 5'-RACE-Ready cDNA synthesis, 1 µL of SMARTer II A Oligonucleotide (5'–AAGCAGTGGTATCAACGCAGAGTACXXXXX–3') was required for the RACE-Ready cDNA preparation.

Table 11 Components of RACE-Ready cDNA synthesis reaction mixture.

Components	Volume (µL)
RNA Mixture	11
5X First-Strand Buffer	4
100 mM DTT	0.5
20 mM dNTPs Mix	1
RNase inhibitor (40 U/µL)	0.5
SMARTScribe Reverse Transcriptase (100 U)	2
Nuclease-free water (or SMARTer II A Oligonucleotide for 5' RACE-Ready cDNA)	1
Total volume	20

The reaction mixture was gently mixed and incubated at 42°C for 90 minutes. This was followed by a final incubation step at 70°C for 10 minutes using a Thermal Cycler (Bio-Rad, USA). Lastly, the RACE-Ready cDNA was diluted with 10 µL of Tricine-EDTA Buffer (10 mM Tricine, KOH, pH 8.5, and 1.0 mM EDTA) and stored at -20°C until use.

3.1.4.2 Rapid amplification of cDNA ends (RACEs)

To generate the remaining 3' and 5' ends of *MrTRAF6*, the primary RACE-PCR were first performed, followed by the nested RACE-PCE to increase the specificity and sensitivity of the PCR. The *MrTRAF6*-specific primers for RACE reaction were designed from partial *MrTRAF6* sequence and listed in Table 12. The GSP001 was designed for 5'-RACE-PCR, and NGSP001 was designed for nested 5'-RACE-PCR. Whereas the GSP002 and NGSP002 were designed for 3'-RACE-PCR and nested 3'-RACE-PCR, respectively.

Table 12 Gene specific primers used for RACE-PCR.

Primer name	Sequence (5'-3')
GSP001	CACATCACCGGCTGACAGGAACATGCCTGTG
GSP002	CGCAGTGCATCTTGCGGGTTACCAGGTGTG
NGSP001	ACTGTGACGTGCGAGATGTGTGGAGC
NGSP002	CCTGTCCTAGAGTCGTAGTTGCCTG

The primary 3' and 5' RACE-PCR was performed using SeqAmp™ DNA Polymerase (Clontech, USA). Firstly, the reaction mixture for primary RACE-PCR was prepared separately as listed in Table 13.

Table 13 Components of reaction mixture using SeqAmp™ DNA Polymerase.

Components	Volume (µL)
2X SeqAmp PCR	25
10 µM GSP001 or GSP002	1
10X UMP*	5
5' or 3' RACE-Ready cDNA	5
SeqAmp DNA Polymerase (1.25 U/µL)	1
Sterilized distilled water	13
Total volume	50

*Universal primer mix (UPM) provide from the kit

UMP: 5'-CTAATACGACTCACTATAGGGCAAGCAGTGGTATCA ACGCAGAGT-3'

Following the preparation of the reactions, the tubes were placed in a Thermal Cycler (Bio-Rad, USA) to perform the touchdown PCR. The program used for the touchdown PCR is as follows:

Step 1 Denaturation $\quad\quad\quad\quad\quad\quad$ 94°C $\quad$ for 30 seconds

Step 2 Annealing and Extension $\quad\quad$ 72°C $\quad$ for 3 minutes

Step 3 Repeat steps 1 and 2 for 4 cycles

Step 4 Denaturation $\quad\quad\quad\quad\quad\quad$ 94°C $\quad$ for 30 seconds

Step 5 Annealing $\quad\quad\quad\quad\quad\quad\quad$ 70°C $\quad$ for 30 seconds

Step 6 Extension $\quad\quad\quad\quad\quad\quad\quad$ 72°C $\quad$ for 3 minutes

Step 7 Repeat steps 4 - 6 for 4 cycles

Step 8 Denaturation $\quad\quad\quad\quad\quad\quad$ 94°C $\quad$ for 30 seconds

Step 9 Annealing $\quad\quad\quad\quad\quad\quad\quad$ 68°C $\quad$ for 30 seconds

Step 10 Extension $\quad\quad\quad\quad\quad\quad$ 72°C $\quad$ for 3 minutes

Step 11 Repeat steps 9 - 11 for 24 cycles

The PCR products obtained were subjected to analysis through agarose gel electrophoresis using 1.0% agarose gel stained with SYBR® Safe DNA gel stain (Invitrogen, USA). The separated DNA fragments were then visualized under UV light using the GelView Master Gel Documentation System (Dynamica, UK).

After that, the primary RACE-PCR products 3' and 5' reactions were 50-fold diluted with Tricine-EDTA buffer. The 1:50 diluted-PCR products were used as a template for nested RACE-PCR reactions that were prepared as listed in Table 14 using SeqAmp™ DNA Polymerase (Takara, Japan).

Table 14 Components of nested RACE-PCR reaction mixture.

Components	Volume (µL)
2X SeqAmp PCR	25
10 µM NGSP001 or NGSP002	1
10X UPM short*	5
Diluted PCR product	1
SeqAmp DNA Polymerase	1
Sterilized distilled water	17
Total volume	50

* UMP short: 5'-CTAATACGACTCACTATAGGGCAAGCAGTGGTATCAACGCAGAGT-3'

After preparation of reaction mixture, the nested RACE-PCR was carried out in a Thermal Cycler (Bio-Rad, USA). The program used for the nested PCR is as follows:

Step 1 Denaturation   94°C   for 30 seconds

Step 2 Annealing   68°C   for 30 seconds

Step 3 Extension   72°C   for 3 minutes

Step 4 Repeat steps 1 - 3 for 24 cycles

The PCR products obtained were subjected to analysis through agarose gel electrophoresis using 1.0% agarose gel stained with SYBR® Safe DNA gel stain (Invitrogen, USA). The separated DNA fragments were then visualized under UV light using the GelView Master Gel Documentation System (Dynamica, UK). The PCR product with the expected size was carefully excised from the gel and subsequently purified using the NucleoSpin® Gel and PCR Clean-up kit (Macherey-Nagel, Germany) as described in section 3.1.3.2.

3.1.4.3 Cloning and identification of 5' and 3' ends of *MrTRAF6*

To identify the full-length *MrTRAF6* cDNA, the purified 3' and 5' nested RACE products from section 3.1.4.2 were cloned into pCR™ -Blunt II-TOPO® plasmid

using Zero Blunt® TOPO® PCR Cloning Kit (Invitrogen, USA) and then transformed to *E. coli* TOP10. The plasmid was extracted and verified by restriction endonuclease *Eco*RI-HF. The processes of ligation, transformation, plasmid extraction, and plasmid verification were described in section 3.1.3.2. The recombinant plasmid, 3'*MrTRAF6*-pCR-BluntII-TOPO, and 5'*MrTRAF6*-pCR-BluntII-TOPO were further sequenced to obtain the 3' and 5' ends of *MrTRAF6* sequences. The sequencing data was identified using BLASTX program (https://blast.ncbi.nlm.nih.gov/Blast.cgi). The full-length cDNA of *MrTRAF6* was obtained by overlapping the sequences of 3' and 5' cDNA ends.

3.1.5 Molecular verification of *MrTRAF6*

To confirm the accuracy of the *MrTRAF6* sequence, a PCR amplification was performed using Platinum™ *Pfx* DNA Polymerase (Invitrogen, USA) to verify the full-length *MrTRAF6* gene. The primers used for this verification process, as listed in Table 15 were designed from the untranslated regions (UTRs) in order to amplify the complete coding sequence (CDS) of the gene.

Table 15 Primers used for verification of *MrTRAF6*-Coding sequence.

Primer name	Sequence (5'-3')	Amplicon size (bp)
TRAF6-CDS-F	CAG ATC AAC TGC TTT TAA GCA	1,797
TRAF6-CDS-R	CTA AAC ATA CGA CGG AAC	

The reaction mixture for verification of full-length *MrTRAF6* was prepared as listed in Table 16 using the cDNA in section 3.1.2 as a template.

Table 16 Components of reaction mixture for PCR using Platinum™ *Pfx* DNA Polymerase.

Components	Volume (µL)
10X *Pfx* Amplification Buffer	10
10 mM dNTPs mixture	1.5
50 mM MgSO$_4$	1
10 µM TRAF6-CDS-F	1.5
10 µM TRAF6-CDS-R	1.5
cDNA template	1
Platinum™ *Pfx* DNA Polymerase	0.4
Sterilized distilled water	33.1
Total volume	50

After mixing, the PCR amplification was conducted in a Thermal Cycler (Bio-Rad, USA) using the following program:

Step 1 Denaturation   94°C   for 30 seconds

Step 2 Annealing   55°C   for 30 seconds

Step 3 Extension   68°C   for 3 minutes

Step 4 Repeat steps 1 - 3 for 29 cycles

The PCR products obtained were subjected to analysis through agarose gel electrophoresis using 1.0% agarose gel stained with SYBR® Safe DNA gel stain (Invitrogen, USA). The separated DNA fragments were then visualized under UV light using the GelView Master Gel Documentation System (Dynamica, UK). The PCR products with expected size was purified and cloned in to pCR-Blunt II-TOPO® plasmid described in section 3.1.3.2. The recombinant plasmid, TRAF6CDS-pCR-BluntII-TOPO, was then sequenced to identify the nucleotides sequence.

3.2 Bioinformatics analysis

After obtaining the identified full-length *MrTRAF6* sequence, the sequence and phylogenetic analysis of *MrTRAF6* was analyzed and identified. The nucleotide sequence and deduced amino acid sequence of full-length *Mr*TRAF6 were compared with the sequences of TRAF6 from other species reported in GenBank database using BLASTX program (https://blast.ncbi.nlm.nih.gov/Blast.cgi). The approximate molecular weight (MW) and isoelectric point (pI) of *Mr*TRAF6 protein were estimated by the Expasy Compute pI/Mw software (http://web.expasy.org/compute_pi/). The signal peptide sequence was predicted by SignalP-6.0 program (https://services.healthtech.dtu.dk /services/SignalP-6.0/). The prediction of domain topology was conducted by the Simple Modular Architecture Research Tool (SMART) program (http://smart.embl-heidelberg.de/). Multiple sequence alignment of *Mr*TRAF6 and TRAF6 from other species was performed using ClustalW and viewed in BioEdit software. Similarity/identity matrices protein sequences were generated from Matrix Global Alignment Tool (MatGAT) software. The phylogenetic tree was created using the Maximum Likelihood method with the LG model. The tree's reliability was assessed with 1,000 bootstrap replicates using the Molecular Evolutionary Genetics Analysis (MEGA) software version 11 (https://megasoftware.net/). The TRAF6s from 25 species were listed in Table 17.

Table 17 TRAF6s from various species used to construct phylogenetic tree.

No	Species	Molecules	Accession No.
Crustaceans			
1	*Cherax quadricarinatus*	TRAF6-A-like	XP_053628633.1
2	*Eriocheir sinensis*	TRAF6-like	XP_050739933.1
3	*Fenneropenaeus chinensis*	TRAF6	AFU51810.1
4	*Fenneropenaeus penicillatus*	TRAF6	APU52029.1
5	*Homarus americanus*	TRAF6-like	XP_042239384.1

Table 17 (Continued).

No	Species	Molecules	Accession No.
6	*Litopenaeus vannamei*	TRAF6	ADM26237.1
7	*Macrobrachium nipponense*	TRAF6	ASM46956.1
8	*Macrobrachium rosenbergii*	TRAF6	QDV59708.1
9	*Palaemon carinicauda*	TRAF6	AVG44185.1
10	*Penaeus japonicus*	TRAF6	QPI70527.1
11	*Penaeus monodon*	TRAF6	AIS92907.1
12	*Portunus trituberculatus*	TRAF6	AKD94181.1
13	*Procambarus clarkii*	TRAF6-like isoform X1	XP_045603665.1
14	*Scylla paramamosain*	TRAF6	CRI06483.1
Insects			
15	*Anopheles cruzii*	TRAF6	XP_052865094.1
16	*Bactrocera oleae*	TRAF6	XP_014091704.1
17	*Drosophila melanogaster*	TRAF6	AAD47895.1
18	*Glossina fuscipes*	TRAF6	XP_037895574.1
19	*Lucilia sericata*	TRAF6	XP_037812196.1
20	*Scaptodrosophila lebanonensis*	TRAF6	XP_030378054.1
Mollusks			
21	*Bulinus truncatus*	TRAF6	KAH9518846.1
22	*Crassostrea gigas*	TRAF6	ASK05289.1
23	*Octopus bimaculoides*	TRAF6	XP_052825543.1
24	*Patella vulgata*	TRAF6-like	XP_050409809.1
Fish (outgroup)			
25	*Ctenopharyngodon idella*	TRAF6	XP_051756020.1

3.3 Tissue expression and distribution analysis of *MrTRAF6*

To analyze the expression and tissue distribution of *MrTRAF6*, the real-time RT-PCR was performed. The normal prawns, with approximated weight of 30-40 g, were kindly provided from Kanokpol Farm in Suphanburi Province, Thailand. Prawns were first subjected to detection of *Mr*NV and XSV infection to verify that they were viral-free. After verification, total RNA was extracted from various tissues of normal prawns, including gill, heart, hepatopancreas, hemocyte, muscle, stomach, and intestine, and reverse-transcribed to cDNA. The cDNA was subjected to expression analysis by real-time RT-PCR. Subsequently, the relative expression pattern of *MrTRAF6* in tissues was determined and normalized with the internal control gene, elongation factor (EF) 1α.

3.3.1 Detection of viral infection in normal prawns

In order to investigate the tissue distribution of *MrTRAF6*, prawn samples were first subjected to *Mr*NV and XSV detections in order to eliminate the possibility of any confounding effects on the subsequent expression analysis. This step was taken to ensure that the prawns were free from viral contamination that could potentially impact the accuracy and reliability of the results obtained.

Firstly, the viral nucleic acids were extracted from the muscle of all three prawns using High Pure Viral Nucleic Acid Kit (Roche, USA) according to the manufacturer's protocol with some modifications. Briefly, the 5 mg of muscle tissues were lysed and homogenized in 200 µL of lysis buffer (50 mM Tris-HCl (pH 9), 100 mM EDTA, 50 mM NaCl, and 2% SDS), and the lysate was centrifuged at 2,000 x g for 3 minutes. After centrifugation, 200 µL of supernatant was loaded to a new 1.5 mL-tube and added with 200 µL of working solution which were prepared as in Table 18.

Table 18 Components of working solution for extraction of viral nucleic acids.

Components	Volume (µL)
Binding buffer	200
Poly(A)	4
Total volume	204

After that, 50 µL of proteinase K was added to the mixture and then incubated the tube at 75°C for 10 minutes. After incubation, 100 µL of isopropanol was added, then, the mixture was transferred to a High pure filter tube and centrifuged at 6,000 x g for 1 minute. Next, 500 µL of inhibitor removal buffer was added to the filter tube and centrifuged at 6,000 x g for 1 minute. To remove the residual impurities, the filter tube was washed with 450 µL of wash buffer and centrifuged at 6,000 x g. After centrifugation, the tube was centrifuged again at 14,000 x g for 30 seconds to dry the filter membrane. The viral nucleic acids were eluted from the column by adding 50 µL of elution buffer, incubating at room temperature for 2 minutes, and centrifugation at 6,000 x g for 30 seconds. The extracted viral nucleic acids were subjected to amplification of *Mr*NV and XSV targets by RT-PCR.

To detect the presence of *Mr*NV and XSV in samples, the RT-PCR was performed using SuperScript™ III One-Step RT-PCR System with Platinum™ *Taq* DNA Polymerase (Invitrogen, USA). The specific primers to *Mr*NV and XSV were from Senapin et al. (2012), which were listed in Table 19.

Table 19 Primers used for *Mr*NV and XSV detection.

Primer name	Sequence (5'-3')	Amplicon size (bp)
Mr-RdRp-F	GCATTTGTGAAGAATGAACCG	279
Mr-RdRp-R	CATGTTCAACTTTCTCCACGT	
XSV-F	GGAGAACCATGAGATCACG	507
XSV-R	CTGCTCATTACTGTTCGGAGTC	

The reaction mixture of RT-PCR amplifications of *Mr*NV and XSV were prepared separately as listed in Table 20 and used the extracted viral nucleic acid as the template.

Table 20 Components of RT-PCR reaction mixture for detection of *Mr*NV and XSV.

Components	Volume (µL)
2X *2X* Reaction Mix	25
10 µM RdRP-F or XSV-F	1
10 µM RdRP-R or XSV-R	1
Extracted viral nucleic acids	5
SuperScript III RT/Platinum Taq Mix	1
Sterilized distilled water	17
Total volume	50

After mixing, the PCR amplification was conducted in a Thermal Cycler (Bio-Rad, USA). The condition for RT-PCR amplification is as follows the:

Step 1 cDNA synthesis   45°C   for 20 minutes

Step 2 Pre-denaturation   95°C   for 2 minutes

Step 3 Denaturation   95°C   for 30 seconds

Step 4 Annealing   55°C   for 30 seconds

Step 5 Extension   72°C   for 1 minute

Step 6 Repeat steps 3 - 5 for 34 cycles

Step 7 Final extension   72°C   for 10 minutes

The PCR products obtained were subjected to analysis through agarose gel electrophoresis using 1.0% agarose gel stained with SYBR® Safe DNA gel stain (Invitrogen, USA). The separated DNA fragments were then visualized under UV light using the GelView Master Gel Documentation System (Dynamica, UK).

3.3.2 Tissue collection and RNA extraction

The different organs, including gill, heart, hepatopancreas, muscle, stomach, and intestine were collected from three normal prawns. To obtain the hemocytes, hemolymph was collected from the ventral sinus and mixed with an equal volume of modified Alsever's solution (0.79% sodium citrate, 1.66% sodium chloride, and 0.34% EDTA (w/v)). The mixture was then subjected to centrifugation at 2,000 x g for 10 minutes. The resulting pellet was washed twice with 1 mL of Alsever's solution and centrifuged at 2,000 x g for 5 minutes each time. Total RNA was extracted from the collected tissues using the NucleoSpin® RNA XS total RNA isolation kit (Macherey-Nagel, Germany), following the procedure described in section 3.1.1. The extracted RNA from each organ was quantified using a NanoDrop Lite Spectrophotometer (Thermo Fisher Scientific, USA) and stored at -70°C until further use.

3.3.3 cDNA synthesis for real-time PCR

The extracted RNA from each organ were adjusted to final concentration of 1,000 ng/µL, and reverse-transcribed to cDNA using SensiFAST™ cDNA Synthesis Kit (BioLine, UK). The reaction mixture for cDNA synthesis was prepared as listed in Table 21.

Table 21 Components of cDNA reaction mixture for real-time PCR.

Components	Volume (µL)
Total RNA	1-15
5X TransAmp Buffer	4
Reverse Transcriptase	1
Sterilized distilled water	0-14
Total volume	20

After preparation, the reactions were placed in a Thermal Cycler (Bio-Rad, USA) and incubated following the manufacturer's program as follows:

Step 1   Primer annealing   25°C   for 10 minutes

Step 2   Reverse transcription   42°C   for 15 minutes

Step 3   Inactivation   85°C   for 5 minutes

The cDNA was quantified using NanoDrop Lite Spectrophotometer (Thermo Fisher Scientific, USA) and diluted to concentration of 500 ng/µL and stored at -20°C until use.

3.3.4 Expression analysis using real-time PCR

The expression of *MrTRAF6* in various tissues was determined by real-time PCR using SensiFAST™ SYBR® No-ROX kit (BioLine, UK) to investigate the distribution of *MrTRAF6* among tissues. The cDNA (500 ng/µL) of each organ was used as a template for real-time PCR. Two sets of specific primers were used in the PCR reaction, including *MrTRAF6* specific primers and EF1α specific primers for an internal control gene (Table 22).

Table 22 Primers used for expression analysis of *MrTRAF6.*

Primer name	Sequence (5'-3')
qTRAF6-F	TCT GGA TTG TGG TCC CAC TG
qTRAF6-R	ATG GGT CGC TGA AAT GCT TG
EF1α-F	TGC GCT GTG TTG ATT GTA GC
EF1α-R	ACA ATG AGC TGC TTG ACA CC

The PCR amplifications of *MrTRAF6* and EF1α were performed using cDNA from each organ as a template. The reaction mixtures of *MrTRAF6* and EF1α were prepared separately as listed in Table 23.

Table 23 Components of reaction mixture for real-time PCR.

Components	Volume (µL)
2X SensiFAST SYBR® No-ROX Mix	10
10 µM qTRAF6-F or EF1α-F	0.8
10 µM qTRAF6-R or EF1α-R	0.8
cDNA (500 ng/µL)	2
Sterilized distilled water	6.4
Total volume	20

After preparation, the reactions were placed in the CFX connect real-time PCR system (Bio-Rad, USA) with real-time PCR program as follows:

Step 1   Pre-denaturation   95°C   for 2 minutes

Step 2   Denaturation   95°C   for 5 seconds

Step 3   Annealing   60°C   for 10 seconds

Step 4   Extension   72°C   for 15 seconds

Step 5   Repeat steps 2 – 4 for 39 cycles

Step 6   Melt curve analysis   65°C to 95°C

(with an increment of 0.5°C for 5 seconds)

The results were analyzed by Bio-Rad CFX Maestro. The experiment was performed in triplicates and the relative expression of *MrTRAF6* was calculated by $2^{-\Delta\Delta ct}$ normalized with EF1α.

3.4 Immune-challenged experiment with *Aeromonas hydrophila*

The immune-challenged experiment was conducted to study the response of *MrTRAF6* against bacterial infection by injection of Gram-negative bacteria, *A. hydrophila*, into prawns and monitoring *MrTRAF6* expression by real-time RT-PCR. The expression of *MrTRAF6* in bacterial-challenged prawns was analyzed and compared to the control group (2X PBS) at different time points.

3.4.1 Confirmation of *A. hydrophila* strain

A. hydrophila 1234 (VMARC) was re-streaked onto Tryptone Soy Agar (TSA) plate and then was incubated at 37°C for 18 hours. The single colony grown in the incubated plate was selected, cultured in 4 mL of Tryptone Soy Broth (TSB), and incubated overnight at 37°C.

To confirm the bacteria strain, colony PCR was performed according to Rozi's protocol (Rozi et al., 2018). A pair of primers used in PCR reaction targeted *A. hydrophila* hemolysin gene were listed in Table 24.

Table 24 Primers used for identification of *A. hydrophila*.

Primer name	Sequence (5'-3')	Amplicon size (bp)	Reference
Hyl-F	GGCCGGTGGCCCGAAGATACGGG	592	(Rozi et al.,
Hyl-R	GGCGGCGCCGGACGAGACGGGG		2018)

Firstly, the colony PCR was carried out using Platinum® *Taq* DNA Polymerase (Invitrogen, USA). The reaction mixture was prepared as listed in Table 25.

Table 25 Components of PCR reaction mixture for identification of *A. hydrophila.*

Components	Volume (µL)
10X PCR Buffer	5
10 mM dNTPs mix	1
50 mM MgCl$_2$	1.5
10 µM Hyl-F	1
10 µM Hyl-R	1
Template DNA	1
Platinum$^®$ *Taq* DNA Polymerase	0.2
Sterilized distilled water	39.3
Total volume	50

After preparation of reaction mixture, the tube was incubated in a Thermal Cycler (Bio-Rad, USA) to perform PCR amplification using the following program:

Step 1 Pre-denaturation   95°C for 5 minutes

Step 2 Denaturation   95°C for 2 minutes

Step 3 Annealing   55°C for 1 minute

Step 4 Extension   72°C for 1 minute

Step 5 Repeat steps 2 – 4 for 29 cycles

Step 6 Final extension   72°C for 7 minutes

The PCR products obtained were subjected to analysis through agarose gel electrophoresis using 1.0% agarose gel stained with SYBR® Safe DNA gel stain (Invitrogen, USA). The separated DNA fragments were then visualized under UV light using the GelView Master Gel Documentation System (Dynamica, UK). The PCR product with the expected size was carefully excised from the gel and subsequently purified using the NucleoSpin® Gel and PCR Clean-up kit (Macherey-Nagel, Germany) as described in section 3.1.3.1. The purified PCR product was further sequenced to verify sequence of *A. hydrophila.*

3.4.2 Preparation of *A. hydrophila* inoculum

To prepare *A. hydrophila* for the immune-challenged experiment, the identified bacteria were initially cultured in 4 mL of TSB and incubated at 37°C for 18 hours. Subsequently, the bacterial culture was sub-cultured in 20 mL of TSB and incubated at 37°C with shaking at 225 rpm for 2 hours, or until the optical density at 600 nm (OD600) reached a range of 0.5 - 0.7. The bacterial cells were then collected by centrifugation at 2,000 x g for 20 minutes, and the resulting cell pellet was re-suspended in sterile 2X PBS solution. Then, the cell suspension was adjusted to an OD600 of 1, which corresponded to a concentration of bacterial cells at 1×10^9 CFU/mL. The bacterial cell suspension was further diluted to a concentration of 5×10^3 CFU/μL.

3.4.3 Immune-challenged experiment

The immune-challenged experiment was conducted to examine the response of *MrTRAF6* to bacterial infection. The prawns with approximate weights of 15-20 g were from Kanokpol Farm at Suphanburi Province. The experimental prawns were reared in 100 L-concrete tanks filled with air-pump circulating dechlorinated fresh water at room temperature (28°C), fed twice a day with the commercial pellets, and acclimated for 7 days before the experiment. Total 10 of prawns were randomly sampled to detect *Mr*NV and XSV infection as described in section 3.3.1. The *Mr*NV-XSV-free prawns were used for expression analysis of *MrTRAF6* expression in response to *A. hydrophila*.

In immune-challenged experiment, the prawns were divided into 2 groups (N=21 each), including the *A. hydrophila*-challenged prawns and the 2X PBS-challenged prawns (control group). In *A. hydrophila*-challenged group, each individual prawn was injected with 50 μL of *A. hydrophila* (5×10^3 CFU/μL), which was freshly prepared as described previously using 1 mL insulin syringe. In control group, the prawns were injected with 50 μL of sterile 2X PBS.

For monitoring the expression of *MrTRAF6* after immune challenge, the prawns from each group were randomly selected for organs collection including gill, hepatopancreas, hemocyte, and muscle at 0, 3, 6, 12, 24, 36 and 48 hours post-

injection (hpi) (N=3 per timepoint). The hemocytes were collected as described in section 3.1.1.

To confirm *A. hydrophila* infection in challenged-prawns, the 10 μL of collected hemocyte was mixed with 90 μL of sterile 2X PBS and 10-fold diluted to 10^{-3} and 10^{-4}. Each of dilutions was spread onto TSA plate for bacterial cultivation. After incubation at 37°C for 18 hours, colonies grown on the plate were subjected to PCR identification as described previously in section 3.4.1.

3.4.4 Expression analysis of *MrTRAF6* after bacterial-challenged experiment

The total RNA from each collected tissue was isolated using the NucleoSpin® RNA XS total RNA isolation kit (Macherey-Nagel, Germany), following the protocol outlined in section 3.1.2. Subsequently, the extracted RNA was utilized for cDNA synthesis, as described in section 3.3.3. Real-time PCR analysis was then performed using the synthesized cDNA, following the procedure detailed in section 3.3.4.

The real-time PCR was carried out in triplicates per sample. The relative mRNA expression of *MrTRAF6* in this experiment was normalized with those in 2X PBS control group at each time point. Data obtained from real-time PCR was analyzed by a two-tailed Student's *t*-test using Microsoft Excel 2017. All data were presented as means ± SE. Differences were considered to be significant at $p < 0.05$.

3.5 *MrTRAF6* knockdown experiment using RNAi

To further examine the role of *MrTRAF6* in innate immune system of prawns, the knockdown experiment was conducted using dsRNA. In which *MrTRAF6* expression was suppressed, the mortality rate after *A. hydrophila* injection was observed.

3.5.1 Construction of DNA template for *in vitro* transcription

For the generation of a DNA template to be used in *in vitro* transcription, PCR amplification was conducted. The specific primers for dsRNA-MrTRAF6 were designed using the E-RNAi Webservice (http://www.dkfz.de/signaling/e-rnai3/), and were based on the coding sequence of the gene. Additionally, dsRNA of the RNA-directed RNA polymerase (RdRP) gene from the infectious myonecrosis virus (IMNV)

was employed as an unrelated control gene. The primers for the control gene were modified from those used in the study by Senapin et al. (2007). The sense and antisense strands of *MrTRAF6* gene and *RdRP* gene of IMNV were separately amplified using a pair of primers which one of the primers used for each gene amplification was designed to include the T7 promoter sequence (5'-GGATCCTAATACGACTCACTATAGG-3') at the 5'-end.

The sense strand of *MrTRAF6*, for instance, was amplified using TRAF6-RNAi-T7-F (T7-added one) combined with TRAF6-RNAi-R (normal one). The antisense strand was amplified using TRAF6-RNAi-F (normal one) combined with TRAF6-RNAi-T7-R (T7-added one). Similarly, for *RdRP* gene of IMNV, the sense stand was constructed using IMNV-RNAi-T7-F combined with IMNV-RNAi-R, while for the antisense, IMNV-RNAi-F combined with IMNV-RNAi-T7-R were used. The primers for amplification of *MrTRAF6* and *RdRP* template for RNAi were listed in Table 26.

Table 26 Primers used in the construction of DNA template for *in vitro* transcription.

Primer name	Sequence (5'-3')	Amplicon size (bp)
TRAF6-RNAiT7-F	ggatcctaatacgactcactataggTCAAAATAAACCAGGCAGGG	431
TRAF6-RNAi-R	TTTGGAGAAACAATTGCACG	
TRAF6-RNAi-F	TCAAAATAAACCAGGCAGGG	431
TRAF6-RNAiT7-R	ggatcctaatacgactcactataggTTTGGAGAAACAATTGCACG	
F13N-IMNV-T7	ggatcctaatacgactcactataggTGTTTATGCTTGGGATGGAA	307
*R13N-IMNV	TCGAAAGTTGGCTGATG	

Table 25 (Continued).

Primer name	Sequence (5'-3')	Amplicon size (bp)
*F13N-IMNV	TGTTTATGCTTGGGATGGAA	307
R13N-IMNV-T7	ggatcctaatacgactcactataggTCGAAAGTTGGCTGATG	

Nucleotides in lowercases indicate T7 promoter sequence

*From Senapin et al., (2007)

     The PCR amplification of sense and antisense strands of both *MrTRAF6* and *RdRP* were performed using KOD One™ PCR Master Mix (TOYOBO, Japan) which were prepared as described in Table 27. The recombinant plasmid, TRAF6CDF-pcR Blunt II TOPO (in section 3.1.5) was used as the template for *MrTRAF6* gene, and plasmid, pDrive-IMNV region13, which was kindly provided from the Center of Excellence for Shrimp Molecular Biology and Biotechnology (CENTEX Shrimp), was used as the templates for *RdRp* gene of IMNV.

Table 27 Components of PCR reaction for amplification of dsRNA templates.

Components	Volume (µL)
10X KOD One Master Mix	25
10 µM Primer-F*	2
10 µM Primer-R**	2
Plasmid	2
Sterilized distilled water	19
Total volume	50

    * Forward primers: TRAF6-RNAiT7-F (*MrTRAF6* sense), TRAF6-RNAi-F (*MrTRAF6* antisense), F13N-IMNV-T7 (*RdRP* sense), F13N-IMNV (*RdRp* antisense)

** Reverse primers: TRAF6-RNAi-R (*MrTRAF6* sense), TRAF6-RNAiT7-R (*MrTRAF6* antisense), R13N-IMNV (*RdRP* sense), R13N-IMNV-T7 (*RdRp* antisense)

The PCR products obtained were subjected to analysis through agarose gel electrophoresis using 1.0% agarose gel stained with SYBR® Safe DNA gel stain (Invitrogen, USA). The separated DNA fragments were then visualized under UV light using the GelView Master Gel Documentation System (Dynamica, UK). The PCR product with the expected size was carefully excised from the gel and subsequently purified using the NucleoSpin® Gel and PCR Clean-up kit (Macherey-Nagel, Germany). The purified DNA was quantified using NanoDrop Lite Spectrophotometer (Thermo Fisher Scientific, USA) and stored at -20°C until use.

3.5.2 *In vitro* transcription and dsRNA purification

In order to synthesize dsRNA, the sense and antisense ssRNA was firstly transcribed *in vitro* using T7 RiboMAX™ Express Large Scale RNA Production System (Promega, USA) according to manufacturer's protocol. The two *in vitro* transcription reactions (sense and antisense) were separately prepared using the purified products in section 3.5.1 as templates with total amount of 1 µg. The reaction mixtures were listed in Table 28.

Table 28 Components of reaction mixture for *in vitro* transcription.

Components	Volume (µL)
RiboMAX™ Express 2X Buffer	10
DNA template (sense or antisense) (500 ng/µL)	2
Enzyme mix, T7 Express	2
DEPC-treated H_2O	6
Total volume	20

The prepared reaction mixture was mixed gently and incubated at 37°C for 30 minutes. Subsequently, the sense and antisense mixtures were combined together to produce double-stranded RNA (dsRNA). The resulting dsRNA mixture was then incubated at 70°C for 10 minutes to ensure denaturation, followed by a gradual cooling from 70°C to 25°C within 20 minutes to facilitate annealing. After annealing, the dsDNA mixture was added with 2 μL of RQ1 DNase (RNase free) (1 U/ μL) and incubated at 37°C for 30 minutes to remove DNA templates. To purify dsRNA by removal of protein residues, 42 μL of phenol:chloroform:isoamyl alcohol (25:24:1) (Sigma-Aldrich, USA) was added to dsRNA mixture. The resulting mixture was vigorously vortexed for 1 minute to ensure proper mixing of the organic and aqueous phases. Subsequently, the mixture was centrifuged at 14,000 x g and 4°C for 15 minutes. The centrifugation step could separate the phases, with the dsRNA remaining in the aqueous phase while proteins and other contaminants were extracted into the organic phase. After centrifugation, the aqueous phase was carefully transferred to a new tube. To precipitate the dsRNA, 4.2 μL of 3M sodium acetate (pH 5.2) and 42 μL of isopropanol were added to the transferred solution. The mixture was gently mixed and incubated at -20°C for 20 minutes. Subsequently, the mixture was subjected to centrifugation at 14,000 x g and 4°C for a duration of 15 minutes. The resulting dsRNA pellet was washed with 1 mL of 70% ethanol by centrifuging it again at 14,000 x g and 4°C for 15 minutes. The ethanol was then removed, and the pellet was air-dried at room temperature. Next, the dsRNA pellet was re-suspended in 100 μL of nuclease-free water. After re-suspension, the dsRNA was quantified using a NanoDrop Lite Spectrophotometer (Thermo Fisher Scientific, USA). For the *in vivo* knockdown experiment, the dsRNA was diluted in sterile 2X PBS solution.

3.5.3 Validation of dsRNA

After the synthesis of dsRNA, the integrity of the dsRNA was validated through three enzymatic tests. These tests include DNA digestion using DNase I, single-stranded RNA (ssRNA) digestion using RNase A, and double-stranded RNA (dsRNA) digestion using RNase III. These enzymes specifically targeted and digested their

respective nucleic acid substrates. After the enzymatic digestion, the resulting products were analyzed by agarose gel electrophoresis using 1.0 % agarose with SYBR® safe DNA gel stain (Invitrogen, USA).

3.5.3.1 DNA digestion using DNase I

The DNA digestion was performed to ensure the complete removal of DNA templates using DNase I, RNase-free (NewEngland Biolabs, USA). The DNase I digestion mixture was prepared using the specific components listed in Table 29. The mixture was then incubated at a temperature of 37°C for 30 minutes. After incubation, the reaction was terminated by adding 1 µL of 50 mM EDTA and incubating it at 65°C for 10 minutes.

Table 29 Components of DNase I digestion mixture.

Components	Volume (µL)
dsRNA (500 ng)	2
10X reaction buffer with MgCl$_2$	1
DNase I, RNase-free (1 U/µL)	0.5
Nuclease-free water	6.5
Total volume	10

3.5.3.2 ssRNA digestion using RNase A

To confirm the successful annealing of the dsRNA, a digestion step was performed to remove any remaining unannealed single-stranded RNA (ssRNA) using RNase A (Vivantis, Malaysia). The components of RNase A digestion mixture were as listed in Table 30. The mixture was gently mixed and incubated at room temperature for 5 minutes.

Table 30 Components of RNase A digestion mixture.

Components	Volume (µL)
dsRNA (500 ng)	2
RNase A (0.1 mg/ µL)	0.5
20X Saline-Sodium Citrate buffer (SSC)	1
Nuclease-free water	6.5
Total volume	10

3.5.3.3 dsRNA digestion using RNase III

The dsRNA digestion step was conducted to confirm the successful synthesis of dsRNA using ShortCut® RNase III from New England Biolabs (USA). ShortCut® RNase III is an enzyme that digests dsRNA by converting long dsRNA molecules into a mixture of shorter oligonucleotides. The RNase III digestion mixture was prepared using the specific components listed in Table 31. The mixture was gently mixed and incubated at 37°C for 30 minutes. After that, the reaction was terminated by adding 1 µL of 10X EDTA solution.

Table 31 Components of RNase III digestion mixture.

Components	Volume (µL)
dsRNA (500 ng)	2
10X ShortCut® Reaction Buffer	1
10X MnCl$_2$	1
ShortCut® RNase III (2 U/µL)	1
Nuclease-free water	5
Total volume	10

3.5.4 Silencing *MrTRAF6 in vivo* by dsRNA-mediated RNA interference

To suppress the expression level of *MrTRAF6*, the knockdown experiment was performed using dsRNA. The juvenile prawns with approximate weight of 1.5-2.0 g were kindly provided from Lukkungsetthi Farm at Chachoengsao Province, Thailand. The experimental prawns were reared in 100 L-concrete tanks filled with air-pump circulating dechlorinated fresh water at room temperature (28°C), fed twice a day with the commercial pellets, and acclimated for 7 days. Before the experiment, total of 10 prawns were first subjected to detection of *Mr*NV-XSV infection by RT-PCR using SuperScript™ III One-Step RT-PCR System with Platinum™ *Taq* DNA polymerase (Invitrogen, USA) as described in section 3.3.1. The *Mr*NV-XSV-free prawns were used in the knockdown experiment.

For the *in vivo* knockdown experiment, the prawns were divided into three groups including dsRNA-TRAF6, dsRNA-IMNV and 2X PBS groups (N=21 each). Prawns in dsRNA-TRAF6 and dsRNA-IMNV groups were injected with 15 µg/g of dsRNA-TRAF6 and 15 µg/g of dsRNA-IMNV, respectively. On the other hand, prawns in the 2X PBS control group were injected with 40 µL of sterile 2X PBS. To enhance the efficiency of dsRNA, the second injection was given 24 hours after first injection using the same treatments. All injections were intramuscular injections at the third abdominal segment using a 1 mL syringe (0.33 x 13 mm). The gill tissues of prawns in each group were randomly collected at 0, 2, 3, 4, 5, 6, and 7 days post-first injection (three prawns per timepoint).

3.5.5 Efficiency of dsRNA in knocking down *MrTRAF6*

The efficiency of dsRNA in knocking down *MrTRAF6* was evaluated through real-time RT-PCR analysis of *MrTRAF6* mRNA levels in the samples treated with dsRNA-*MrTRAF6*, dsRNA-IMNV (as an unrelated dsRNA samples), and 2X PBS control samples.

Total RNA was extracted from the collected gill tissues at 0, 2, 3, 4, 5, 6, and 7 days post injection (in section 3.5.4) using NucleoSpin® RNA XS total RNA isolation kit (Macherey-Nagel, Germany) as described in section 3.1.1. After RNA

extraction, the cDNA was synthesized from extracted RNA and subjected to real-time PCR analysis as described in section 3.3.3 and 3.3.4, respectively. The reaction was performed in triplicates using the primers, qTRAF6-F and qTRAF6-R (Table 23). The relative expression level of *MrTRAF6* was calculated by $2^{-\Delta\Delta Ct}$ method (Livak et al., 2001). Data obtained from real-time PCR was analyzed one-way analysis of variance (ANOVA) followed by Duncan's multiple range tests. The knockdown efficiency was calculated as the percentage decrease in *MrTRAF6* mRNA levels in the treated samples compared to the control samples. Differences were considered to be significant at $p < 0.05$. The day on which *MrTRAF6* showed the most significant knockdown was chosen for use in the bioassay of bacterial injection.

3.5.6 Expression analysis of AMP genes in *MrTRAF6*-silenced *M. rosenbergii*

To assess the impact of *MrTRAF6* knockdown on downstream antimicrobial peptide (AMP) genes, an expression analysis of the relevant AMP genes was conducted after the knockdown experiment. The relevant AMP genes were included including crustin, anti-lipopolysaccharide factor 5 (ALF5), and mannose-binding lectin (MBL).

In this experiment, the expression levels of crustin, ALF5, and MBL were detected in the gill samples from all three groups, including dsRNA-TRAF6, dsRNA-IMNV, and 2X PBS (in section 3.5.4) by real-time RT-PCR as described previously in section 3.3.4 with the primers listed in Table 32.

Table 32 Primers used in expression analysis of AMP genes by real-time RT-PCR.

Primer name	Sequence (5'-3')	References
*Mr*Crs-F	AACGACTTCAAGTGCTTCGGGTCT	(Arockiaraj et al., 2012)
*Mr*Crs-R	AAGCTTAGTGGTTTGCAGACGTGC	
MBL-F3	TGGCACATCGATACCCTACT	(Arockiaraj et al., 2015)
MBL-R3	GGACTGAGAGAGGGACCTTATT	
ALF5(2)-F	GCACACGTGTCAGTACAGCGTTAA	(Ren et al., 2012)
ALF5(2)-R	GAAGGCTTTCCTGACGAAGTCTTG	

The reaction was performed in triplicates. The relative expression level of each gene was normalized to EF1α itself and compared to those in 2X PBS control group. Data obtained from real-time PCR was analyzed one-way ANOVA followed by Tukey test. Differences were considered to be significant at $p < 0.05$.

3.5.7 Cumulative mortality rate analysis in *MrTRAF6*-silenced *M. rosenbergii* after *A. hydrophila* challenge

To investigate the role of *MrTRAF6* in resistance to bacterial infection, the mortality rates analysis was conducted after the knockdown experiment. Firstly, a total of 120 healthy prawns (average 1.5-2 g body weight) were randomly divided into three independent groups, including dsRNA-TRAF6-injected, dsRNA-IMNV-injected, and 2X PBS-injected groups (N=40 each) which were intramuscularly injected twice with 15 µg/g of dsRNA-TRAF6, dsRNA-IMNV (unrelated control dsRNA) and 50 µL of 2X PBS (control treatment), respectively (the second injection was performed at 24 h after first injection). On the day that *MrTRAF6* was mostly significant knockdown, prawns in each group were divided into two subgroups (N=20 each). In the first subgroup, the prawns were challenged with an *A. hydrophila* suspension at a dose of 10^5 CFU/g body weight. In another subgroup, the prawns were injected with a 2X PBS solution. The cumulative mortality rates were monitored at 0, 6, 12, 24, 48, 72, 96, 120, 144, and 168 hour post-injection. The experiment was performed in triplicates.

CHAPRER 4
RESULS

The present study aimed to isolate and identify a novel tumor necrosis factor receptor-associated factor 6 (*TRAF6*) gene, designated as *MrTRAF6*, from the giant freshwater prawn, *M. rosenbergii*. Bioinformatics tools were employed for sequence analysis, and the expression pattern of *MrTRAF6* in healthy prawns was investigated across different tissues. The response of *MrTRAF6* to bacterial infection was evaluated by challenging the prawns with *A. hydrophila*. Moreover, to investigate the involvement of *MrTRAF6* in antibacterial activity, RNAi was employed to silence *MrTRAF6*, followed by bacterial infection to observe the resistance to bacteria in *MrTRAF6*-depleted prawns.

4.1 Molecular isolation of *MrTRAF6* cDNA

The full-length cDNA sequence was assembled from three fragments, which included a partial fragment, 5' fragment, and 3' fragment, using PCR-based methods.

4.1.1 Amplification of a partial *MrTRAF6* cDNA

To isolate the full-length cDNA of *MrTRAF6*, the partial fragment was first amplified by PCR using the degenerated primers which were designed based on the conserved sequences of TRAF6 proteins from related species. The result showed that the PCR product band of 600 bp could be observed on, as depicted in Figure 11.
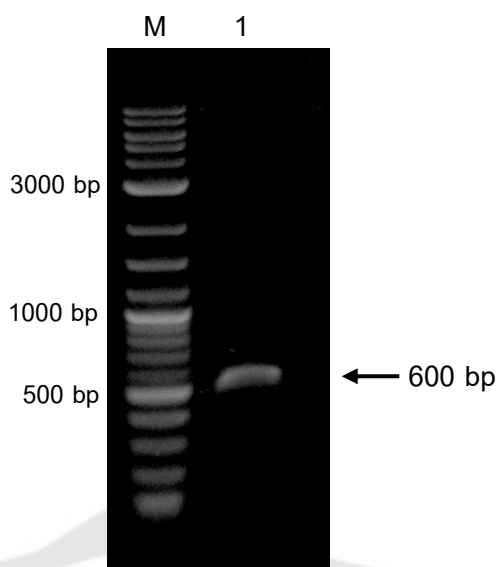
Figure 11 The representative gel of the amplification of partial *MrTRAF6* cDNA.

Lane M = DNA marker and Lane 1 = partial *MrTRAF6* cDNA.

The expected product size of 600 bp is indicated by arrow.

The purified product was then cloned into pCR-Blunt II-TOPO vector, and a positive clone was selected for sequencing. To confirm the presence of recombinant plasmid, partial*MrTRAF6*(600)-pCR-Blunt II-TOPO, the extracted plasmid was digested by restriction enzyme, *Eco*RI-HF. Agarose gel electrophoresis of the digested plasmid showed two distinct DNA bands, including a 600-bp target product, and a vector band of approximately 3,500 bp, as shown in Figure 12. After verification, the recombinant plasmid was sequenced, and obtained data was used to further design the specific primers for amplification of 5' and 3' ends of the *MrTRAF6* cDNA sequence.

Figure 12 The representative gel of verification of recombinant plasmid,

partial*MrTRAF6*(600)-pCR-Blunt II-TOPO by digesting with *Eco*RI-HF.

Lane M = DNA Marker, and Lane 1 = digested products of recombinant plasmid.

The digested products are indicated by arrows.

4.1.2 Amplification of a full-length *MrTRAF6* cDNA

The remaining 5' and 3' ends of *MrTRAF6* cDNA were then amplified separately by rapid amplification of cDNA ends (RACEs)-PCR. The primary RACE-PCR was first performed followed by the nested RACE-PCR. For the 5' cDNA end, the primary-RACE result showed no detectable band, and the nested-RACE result yielded a 600-bp band on agarose gel, as illustrated in Figure 13.

Figure 13 The representative gel of amplification of 5' RACE cDNA.
Lane M = DNA marker, Lane 1 = Primary 5' RACE-PCR, and Lane 2 = Nested 5' RACE-
PCR. The expected product size of 600 bp is indicated by arrow.

     The nested product was purified, ligated to pCR-Blunt II-TOPO vector, and transformed into *E. coli* TOP10. The plasmid was extracted from overnight culture, and the recombinant plasmid was verified by digesting with restriction enzyme, *Eco*RI-HF before sequencing. Verification of recombinant 5'TRAF6(600)-pCR-Blunt II-TOPO showed the two distinct bands, including a 600-bp nested-RACE product, and approximately 3,500-bp vector, as shown in Figure 14.
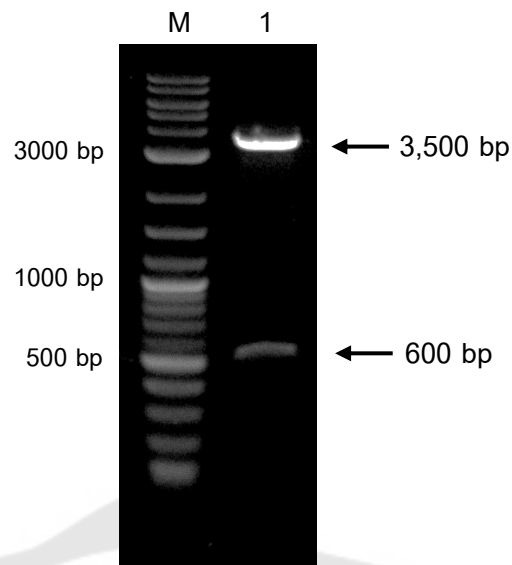
Figure 14 The representative gel of verification of recombinant plasmid 5'TRAF6(600)-

pCR-Blunt II-TOPO by digesting with *Eco*RI-HF.

Lane M = DNA marker and Lane 1 = Digested products of recombinant plasmid.

The digested products are indicated by arrows.

    Similarly, the primary 3' RACE-PCR was first carried out which yielded no detectable band, while a band of 1,300 bp was detected in the nested 3' RACE-PCR, as shown in Figure 15.
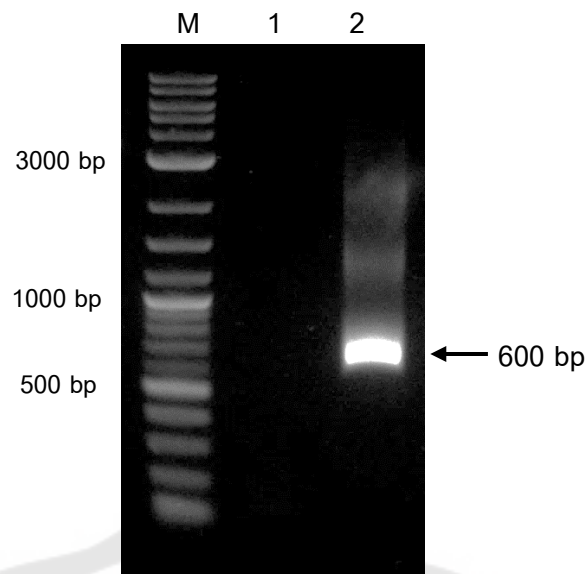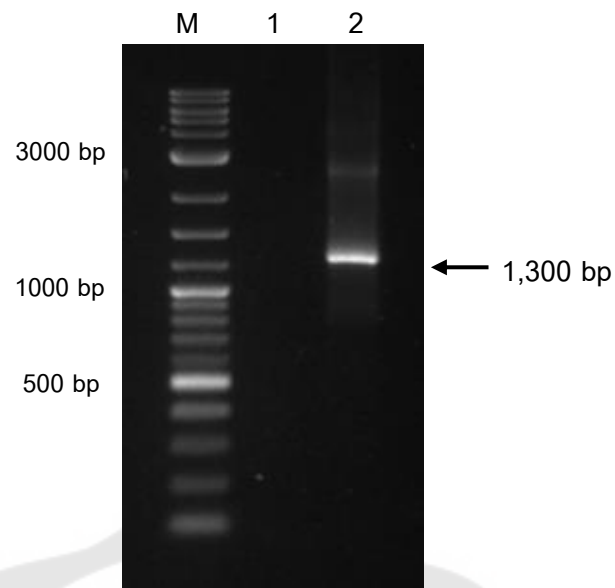
Figure 15 The representative gel of amplification of 3' RACE cDNA.
Lane M = DNA marker, Lane 1 = Primary 3' RACE-PCR, and Lane 2 = Nested 3' RACE-
PCR. The expected product size of 1,300 bp is indicated by arrow.

      For sequencing, the nested product (1,300 bp) was cloned to pCR-Blunt II-
TOPO and transformed into *E. coli* TOP10. The plasmid was extracted and verified by
digesting with restriction enzyme, *Eco*RI-HF. The verification of recombinant
3'TRAF6(1300)-pCR-Blunt II-TOPO showed the two distinct bands, including a nested-
RACE product of 1,300-bp, and a vector of approximately 3,500-bp, as illustrated in
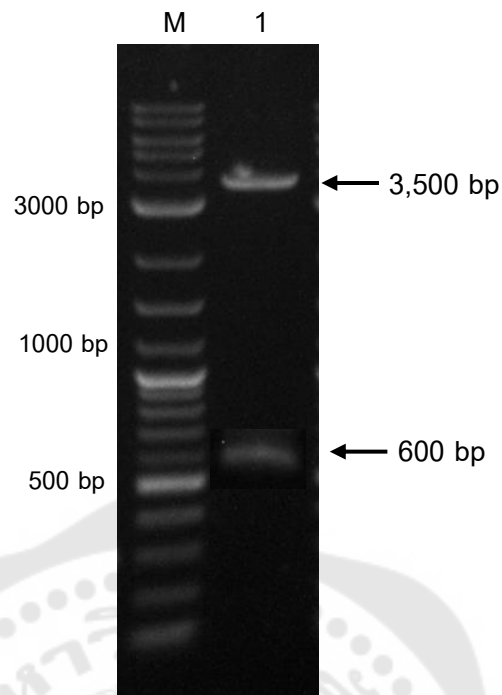Figure 16.

Figure 16 The representative gel of verification of recombinant plasmid 3'TRAF6(1300)-

pCR-Blunt II-TOPO by digesting with *Eco*RI-HF.

Lane M = DNA marker and Lane 1 = Digested products of recombinant plasmid.

The digested products are indicated by arrows.

After sequencing, the complete cDNA of *MrTRAF6* was obtained from the overlapping of 5' and 3' ends sequences.

4.1.3 Verification of full-length *MrTRAF6* cDNA

The full-length *MrTRAF6* sequence obtained from three fragments, including partial cDNA, 5' cDNA end, and 3' cDNA end was verified by PCR using the desired specific primers to confirm the coding sequence (CDS) of the full-length *MrTRAF6* cDNA. The PCR result showed the DNA band of approximately 1,700 bp detected under UV light after agarose gel electrophoresis analysis, as illustrated in Figure 17.
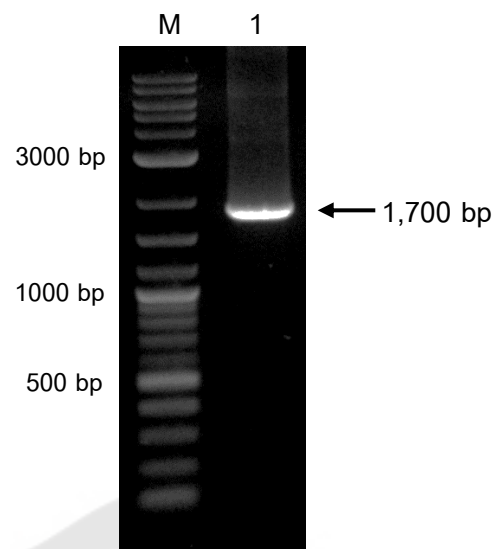
Figure 17 The representative gel of amplification of full-length *MrTRAF6* cDNA covering

the coding sequence (CDS) of the gene.

Lane M = DNA Marker and Lane 1 = *MrTRAF6*-CDS.

The expected product of 1,700 bp is indicated by arrow.

The 1,700-bp product was purified and ligated to pCR-Blunt II-TOPO vector followed by being transformed into *E. coli* TOP10. The plasmid was extracted and verified by digesting with restriction enzyme, *Eco*RI-HF before sequencing. The verification of recombinant TRAF6-CDS(1700)-pCR-Blunt II-TOPO showed the two distinct bands, including a 1,700-bp target product, and approximately 3,500-bp vector (Figure 18). The verified recombinant plasmid was used for sequencing to verify the full-length cDNA fragment.
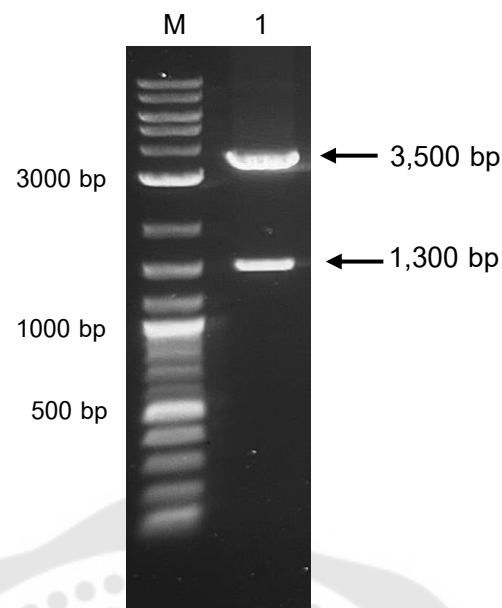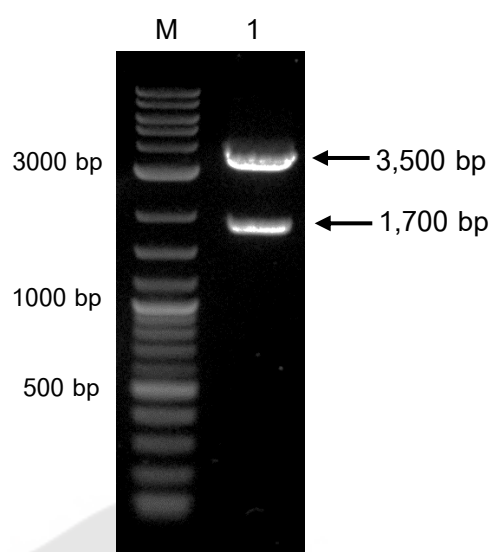
Figure 18 The representative gel of verification of recombinant plasmid, *MrTRAF6*-
CDS(1700)-pCR-BluntII-TOPO, by digesting with *Eco*RI-HF.

Lane M = DNA Marker and Lane 1 = digested products of recombinant plasmid.

The digested products are indicated by arrows.

The resulting sequence obtained from re-identification of full-length *MrTRAF6* cDNA was compared to the sequence obtained from RACE results. The obtained sequence was then analyzed by various bioinformatics tools.

4.2 Sequence analysis

4.2.1 Full-length *MrTRAF6* nucleotide and protein

The full-length *MrTRAF6* cDNA was submitted and deposited in NCBI GenBank database under accession number MH507502. According to sequencing results identified by BLASTX (https://blast.ncbi.nlm.nih.gov/Blast.cgi), the full-length cDNA of *MrTRAF6* consisted of 2,114 nucleotides including the 5'-untranslated region (UTR) of 21 nucleotides, the 3' UTR of 398 nucleotides, and the open reading frame (ORF) of 1,695 nucleotides encoding the 564-amino acid protein with no signal peptides. The full sequences of *MrTRAF6* cDNA and the deduced amino acids were illustrated in Figure 19. The predicted theoretical isoelectric point (pI) and molecular weight of mature *Mr*TRAF6 were 5.92 and 63.1 kDa, respectively.

```
-21    cagatcaactgctttttaagca

1      ATG GAA GGC TCG GAC GGG AGT TCG ATA ACC CTG ATA TCT AGG CAA    45
1       M   E   G   S   D   G   S   S   I   T   L   I   S   R   Q     15
46     GAG GGG TTT GAT TAC GAC TTC GTG CCC CCC TTA GAT AGC AAG TAT    90
16      E   G   F   D   Y   D   F   V   P   P   L   D   S   K   Y     30
91     GAG TGT GCC ATA TGT CTC TTA GGC CTC AGA TCT CCA ATG CAG ACA   135
31      E   C   A   I   C   L   L   G   L   R   S   P   M   Q   T     45
136    ACC TGT GGG CAC CGA TTT TGT AAA GAC TGC ATC TTC AAT TGC CTA   180
46      T   C   G   H   R   F   C   K   D   C   I   F   N   C   L     60
181    AGT GAG AGC AGC AGT CGG TGT CCT GTT GAC AAT ACA CCA CTG TTG   225
61      S   E   S   S   S   R   C   P   V   D   N   T   P   L   L     75
226    GAG AGT GAC TTG TTT GCT GAT TCT TGT GCT GAA AGA GAA ATA CTA   270
76      E   S   D   L   F   A   D   S   C   A   E   R   E   I   L     90
271    CAG CTT AAA GTA AAG TGT CCA AAC CAT GCA CTT GGT TGT TCA ACA   315
91      Q   L   K   V   K   C   P   N   H   A   L   G   C   S   T    105
316    GTG GTA GAT CTC ATG TAC ATA GAA CAT CAC ACA CAG GCA TGT TCC   360
106     V   V   D   L   M   Y   I   E   H   H   T   Q   A   C   S    120
361    TGT CAG CCG GTG ATG TGC CCT AAT GAG TGT TCA GCA ACA GTT CTG   405
121     C   Q   P   V   M   C   P   N   E   C   S   A   T   V   L    135
406    CAA AAG GAA CTT GAA CAG CAC CTC ACA TCG CAG TGC ATC TTG CGG   450
136     Q   K   E   L   E   Q   H   L   T   S   Q   C   I   L   R    150
451    GTT ACC AGG TGT GCA CTG TGT GAC CAG CCT TTC ACT TTT AAT CAA   495
151     V   T   R   C   A   L   C   D   Q   P   F   T   F   N   Q    165
496    GAG CAG CTC CAT CTC TTG AGT TGT TCG CGG GTG ACT GTG ACG TGC   540
166     E   Q   L   H   L   L   S   C   S   R   V   T   V   T   C    180
541    GAG ATG TGT GGA GCT ATG ATG CCC CGA GGT GAA GTG CCA TCC CAT   585
181     E   M   C   G   A   M   M   P   R   G   E   V   P   S   H    195
586    ACC ACA GAA TCC TGT CCT AGA GTC GTA GTT GCC TGT ACA TTT GCA   630
196     T   T   E   S   C   P   R   V   V   V   A   C   T   F   A    210
631    GAA CAT GGA TGC CAT CAT AAA ATG ACA AGA TCT GAC CTT GAT CAG   675
211     E   H   G   C   H   H   K   M   T   R   S   D   L   D   Q    225
676    CAT ATG GAA CAA GCA ATC CAG TAC CAT CTC CAG CTT CTT TCA TCA   720
226     H   M   E   Q   A   I   Q   Y   H   L   Q   L   L   S   S    240
721    GCC AAC AAA AAG ATG AAT GCA TTT GTT TCT GAC TTA AGC CGA ACA   765
241     A   N   K   K   M   N   A   F   V   S   D   L   S   R   T    255
766    GTA GGA CTC ATT CAG TCT CCT TAT GGA AAC TTT AGC CGG CAA CCA   810
256     V   G   L   I   Q   S   P   Y   G   N   F   S   R   Q   P    270
811    AGT CTT CGA AGC CAG ATG TCA GCA ACT TCG CCC ATA CCT GAA AAT   855
271     S   L   R   S   Q   M   S   A   T   S   P   I   P   E   N    285
856    CAT TCA AGC CCA TCA CAG CAT GAC AGA AAT CTT GAG AAA TCT TTT   900
286     H   S   S   P   S   Q   H   D   R   N   L   E   K   S   F    300
```

Figure 19 Sequence analysis of full-length sequences of *MrTRAF6* gene. The nucleotides (upper row) and deduced amino acids (lower row) of *MrTRAF6*. The initiation codon (ATG) and stop codon (TGA) are in bold. The nucleotides shown in uppercase represent the open reading frame (ORF) of the gene, and the lowercases represent the untranslated regions (UTRs). An asterisk (*) mark indicates the end of the translated protein sequence produced by a stop codon. The left and right numbers specify the position of sequences, where the minus numbers indicate the upstream region of *MrTRAF6*. Amino acids in RING fingers regions are underline, and the MATH domain is shaded.

```
901   GGT GCT TAT GGA GGA ACT ATT AGT CTC AAT GAT AGA TCA TCA TTA   945
301    G   A   Y   G   G   T   I   S   L   N   D   R   S   S   L    315
946   ACT CCA CAG AGT GAT GAA TTG GGA AAT GAA ATC AAT AAG CTG GAG   990
316    T   P   Q   S   D   E   L   G   N   E   I   N   K   L   E    330
991   CTC CAG TTA AAC AAT CTA AGT GCG AGT GAA ACA AAG AGT GGG TCT   1035
331    L   Q   L   N   N   L   S   A   S   E   T   K   S   G   S    345
1036  AAA ATT CCA AAC ACT ATT ACT CAT CAG GAA ATC ATT TTA CGG GAT   1080
346    K   I   P   N   T   I   T   H   Q   E   I   I   L   R   D    360
1081  GTT AGT GAA AAG ACA GTA GAC TTA AAT CAG AGG ATG TTA GAG GAA   1125
361    V   S   E   K   T   V   D   L   N   Q   R   M   L   E   E    375
1126  ACT ATA AAG TTA AGC AAT CTG AGT AAG AGA ATT GAG GAA GTT GAT   1170
376    T   I   K   L   S   N   L   S   K   R   I   E   E   V   D    390
1171  GCT ATG GTA GAA GTT CAG TTA GCA GAT GTG AGT GGT AAA TTT TGT   1215
391    A   M   V   E   V   Q   L   A   D   V   S   G   K   F   C    405
1216  AAT GGA GAG TAT GTC TGG AAA ATC AAG CAT TTC TCT CAT TTG TGT   1260
406    N   G   E   Y   V   W   K   I   K   H   F   S   H   L   C    420
1261  GTA GAG CTT CAA AAT AAA CCA GGC AGG GTG CTC CAC AGT CCA CCT   1305
421    V   E   L   Q   N   K   P   G   R   V   L   H   S   P   P    435
1306  TTT TAC ACA TCA CAA TTT GGA TAT AAA TTC TGT TTA CGT ACT AAT   1350
436    F   Y   T   S   Q   F   G   Y   K   F   C   L   R   T   N    450
1351  ATC ACG TGG AAG TCT AAT GAA TAC TTT TTT ACT TTG TTC ATA CAC   1395
451    I   T   W   K   S   N   E   Y   F   F   T   L   F   I   H    465
1396  TCA ATG CAA GGA GAA AAT GAT GAC TTT TTA GAA TGG CCT TTT AGT   1440
466    S   M   Q   G   E   N   D   D   F   L   E   W   P   F   S    480
1441  GGG GAA ATA ACT CTC TCA ATT CTG GAT TGT GGT CCC ACT GCA CCA   1485
481    G   E   I   T   L   S   I   L   D   C   G   P   T   A   P    495
1486  AAA AAA CAC ATT ACG GAA TCC ATG GTA AGC AAG CCA GAT CTG CAA   1530
496    K   K   H   I   T   E   S   M   V   S   K   P   D   L   Q    510
1531  GCA TTT CAG CGA CCC ATG GTA TCA AGA AAT CCT AAA GGT TTT GGT   1575
511    A   F   Q   R   P   M   V   S   R   N   P   K   G   F   G    525
1576  TAC ACT GAA TTT GTA CCC TTG GCC AAG TTA CTG AAA TCT GAA GGG   1620
526    Y   T   E   F   V   P   L   A   K   L   L   K   S   E   G    540
1621  GGA AGT TAC ATC AAC AGT GAT GTT CTG TGT ATC CGT GCA ATT GTT   1665
541    G   S   Y   I   N   S   D   V   L   C   I   R   A   I   V    555
1666  TCT CCA AAA GCA CCA AAA TCA TCA AGT TGA                      1695
556    S   P   K   A   P   K   S   S   S   *                       565
1696  tgtatgagcaatatgtacagtattatctttttttctactcagttttttctttctctacctgc   1755
1756  attgatttgtatgctgccttgcatctatgtttgttgatatttggctgaatttaaaaggaa   1815
1816  aagtgcagttcaatacattcctctttgtgtgattgcttctttcaattatatagcaattta   1875
1876  taccctattttttatatatggtaatggcactctgctttatactttaatgtttaaagtttat   1933
1934  acattgttgtgtacagtattacagtggcttcaaagggaccatttagctcattttttaatg   1991
1992  ttacatattctttaaaattatatgtatatttacagcgaaaaaaaaaaaaaaaaaaaaaaa   2051
2052  agtactctgcgttgataccactgcttaagggcgaattc
```

Figure 18 (Continued).

Furthermore, domain topology analysis revealed that the putative amino acids of *Mr*TRAF6 possesses the characteristic motifs of TRAF family including two RING-type Zinc fingers at the position 32-70 and 154-203, and a meprin and TRAF homology (MATH) domain at the position of 411-535 which was the highly conserved domain at C-terminal as shown in Figure 20.

Figure 20 Predicted domains of *Mr*TRAF6 protein by SMART program.

4.2.2 Multiple sequences alignments

The *Mr*TRAF6 and other TRAF6s from shrimp species included were aligned by ClustalW to analyze the similarities and identities between these TRAF6s. The result revealed the highly conserved of TRAF6 among shrimp species with sharing 365 identical amino acids and 77 similar amino acids, as demonstrated in Figure 21.
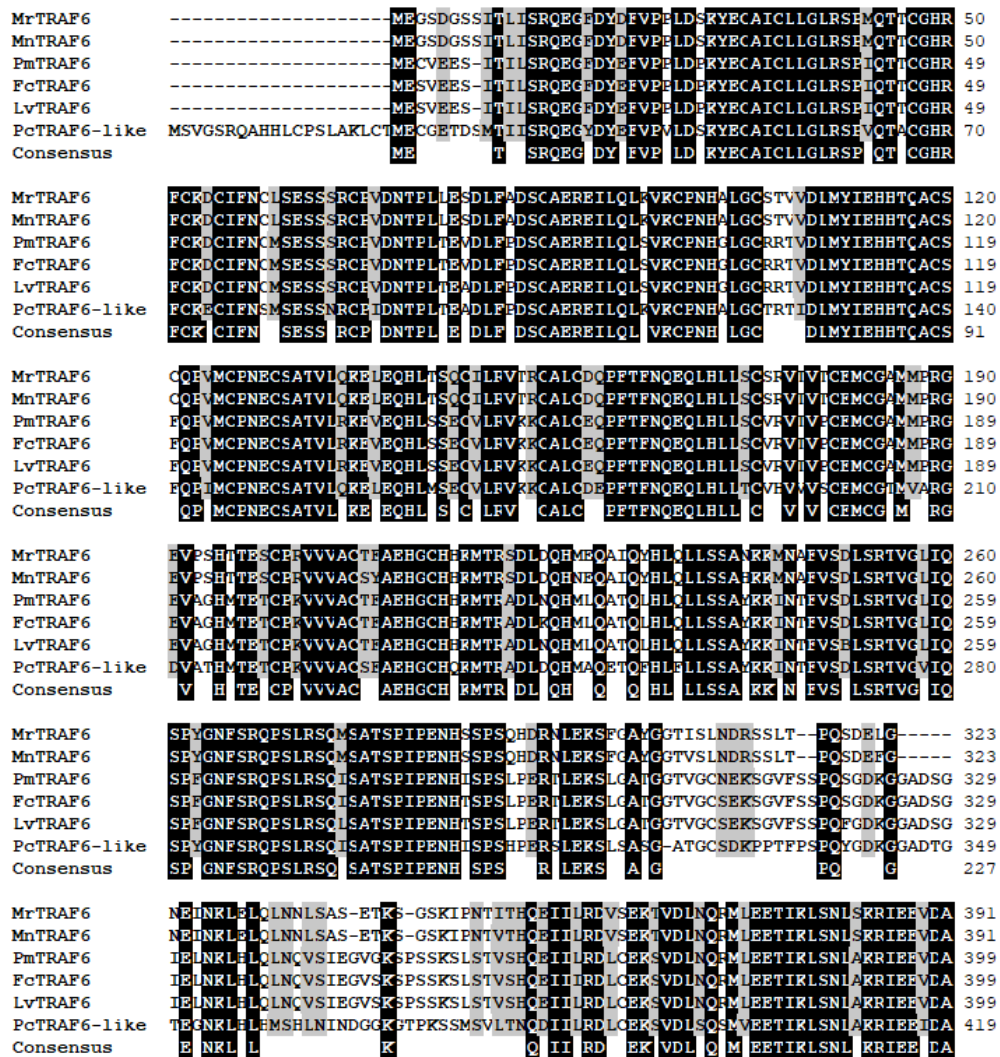
Figure 21 Multiple sequence alignment of *Mr*TRAF6 and other TRAF6s

from related species, including *Macrobrachium nipponense* TRAF6 (Accession no.

ASM46956.1), *Penaeus monodon* TRAF6 (Accession no. AIS92907.1), *Fenneropenaeus*

chinensis (Accession no. AFU51810.1), *Litopenaeus vannamei* TRAF6 (Accession no.

ADM26237.1), and *Procambarus clarkii* TRAF6 like (Accession no. XP_045603665.).

Numbers on the right indicate amino acid positions, and dashes (-) represent gaps in

the sequence. The identical amino acids between these species are highlighted in black

and the similar amino acids are in grey with the threshold of shading of 100%.

```
MrTRAF6        MVEVQLADVSGKFCNGEYVWKIKHFSHLCVELQNKPGFVLHSPEFYTSQFGYRFCLRTNITWKSNEYFFT 461
MnTRAF6        MVEVQLADVTGKFCNGEYVWKIKHFSHLCTELQNKPGFVLHSPAFYTSQFGYRFCLRTNITWKSNEYFFT 461
PmTRAF6        LVEAQLMEMSGKYCNGNYVWRIKNFSQFCAELQNKPGFVGHSPSFYTSQFGYRFCLRTNITWKSDQYFLT 469
FcTRAF6        LVEAQLMEMSGKYCNGNYVWRIKNFSQFCAELQNKPGFVGHSPSFYTSQFGYRFCLRTNITWKSEQYFLT 469
LvTRAF6        LVEAQLTEMSGKYCNGDYVWRIKNFSQFCAELQNKPGFVGHSPSFYTSQFGYRFCLRTNITWKSEQYFLT 469
PcTRAF6-like   YVEAQLTEVSGKFCNGEYVWRIRNFSQLCAELQNKPGFVGHSPEFYTSQFGYRFCLRTNITRRSDEHFLA 489
Consensus       VE QL   GK CNG YVW I  FS  C ELQN PGFV HSP FYTSQFGYRFCLRTNIT  KS    F

MrTRAF6        LFIHSMQGENDDFLEWPFSGEITLSILDCGPTAPKKHITESVVSKPDLCAFKRPMVSRNPKGFGYTEFVP 531
MnTRAF6        LFIHSMQGENDDFLEWPFSGEITLSILDCGPNVPKKHITESMVSKPDLCAFKRPVVSRNPKGFGYTEFVP 531
PmTRAF6        LFIHCMQSENDDFLDWPFSGRITLSVLDCDTSLPKKHITETVVTKPGLCAFKRPDVARNPKGFGETEFVP 539
FcTRAF6        LFIHCMQSENDDFLDWPFSGRITLSVLDCDTSLPKKHITETVVTKPGLCAFKRPDVARNPKGFGETEFVP 539
LvTRAF6        LFIHCMQSENDDFLDWPFSGRITLSVLDCDISLPKKHITETVVTKPGLCAFKRPDVARNPKGFGETEFVP 539
PcTRAF6-like   LFIHTMQGDNDDFLDWPFSGRITISVLDCGKILPKKHITETMMSKPDRCAFKRPEVSRNPKGFGTDFVP 559
Consensus      LFIH MQ  NDDFL WPFSG IT S LDC    PK HITE M  RP  CAF RP V RNPKGFG T FVP 356

MrTRAF6        LAKLLKSEGGSYINSDVLCIFALVSPKAPKSSS--------------------- 564
MnTRAF6        LAKLLKSQGGSYINSDVLCIFAVVSPKAP------------------------- 560
PmTRAF6        LAKILQPSIGTFLKNDTLCIFAIVCPNTWNHESSQSMEKLGIFKEKLHIEKQSCV 594
FcTRAF6        LAKILQPSIGTFLKNDTLCIFAIVCPNTWNHESSQSTEKLGIFKEKLHIEKQSCV 594
LvTRAF6        LAKILQPSTGTFLKNDTLCIFAIVCPNTWNHESSQSMEKLGIYKEKLHIEKQSCV 594
PcTRAF6-like   LNKLLEAKHGMYIRNDVLCIFAVVCPEALTTKQIECN----------------- 596
Consensus      L KL   G   D LCIFA V P                                368
```

Figure 21 (continued).

Furthermore, the pairwise alignment result showed that *Mr*TRAF6 shared the highest identity to *Mn*TRAF6 (96.6%), and relatively high (67.3-87.6%) with other shrimp species, including *Palaemon carinicauda* TRAF6 (87.6%), *Penaeuse monodon* TRAF6 (72.1%), *Litopenaeus vannamei* TRAF6 (71.6%), *Fenneropenaeus chinensis* TRAF6 (71.8%), and *Procambarus clarkii*-TRAF6 like (67.3%). While in other crustaceans, *Mr*TRAF6 shared 53.5% identity to *Scylla paramamosain* TRAF6, 51.1% to *Portunus trituberculatus*, and 46.1% to *Eriocheir sinensis* TRAF6-like, as presented in Figure 22.

% Identity / % Similarity	1	2	3	4	5	6	7	8	9	10
1. *M. rosenbergii* TRAF6		96.6	72.1	71.8	71.6	67.3	87.6	53.5	51.1	46.1
2. *M. nipponense* TRAF6	98.4		71.6	71.3	71.1	67.3	86.7	53.2	51.2	45.5
3. *P. monodon* TRAF6	82.8	82.8		98.1	97.1	72.5	69.6	53	51.8	45.8
4. *F. chinensis* TRAF6	82.8	82.8	99		98	71.7	69.6	53.2	51.8	45.6
5. *L. vannamei* TRAF6	82.8	82.8	98.3	98.7		71.7	69.4	53	51.9	45.3
6. *P. clarkii* TRAF6-like	81.4	81.2	85.2	84.7	85.2		66.3	52	51.4	46.7
7. *P. carinicauda* TRAF6	93.3	92.9	79.6	79.6	79.6	78.7		51.6	50.2	45.1
8. *S. paramamosain* TRAF6	69.4	68.6	71.7	72.1	71.7	71.2	69.1		87.8	60.7
9. *P. trituberculatus* TRAF6	66.8	66.4	69.8	69.6	69.9	70.1	66.3	93		60.8
10. *E. sinensis* TRAF6	59.4	59.4	61.2	61.3	61.5	61.6	58.4	70.5	70.3	

Figure 22 Identity/Similarly matrix of amino acids pairwise alignment of *Mr*TRAF6 and
other TRAF6s from crustacean species generated by MatGAT software.
The upper right (blue area) indicates identity (%) and the lower left (red area) indicates
similarity (%). The numbers at the top of the table represent the TRAF6s from different
crustacean species corresponding to those listed in the leftmost of the matrix table.

4.2.3 Phylogenetic tree analysis

A phylogenetic tree of *Mr*TRAF6 and TRAF6s from other species was
constructed by Maximum likelihood method with a bootstrap of 1,000 replicates. The NJ
tree revealed that *Mr*TRAF6 belonged to the crustaceans group. The result also showed
that *Mr*TRAF6 exhibited the close relationship with TRAF6 of Palaemonid prawn,
*Mn*TRAF6 with a strong bootstrap and was clustered in the distinct subgroup with
penaeid shrimps and was classified as the different clades of TRAF6s from insects and
mollusks, as illustrated in Figure 23.
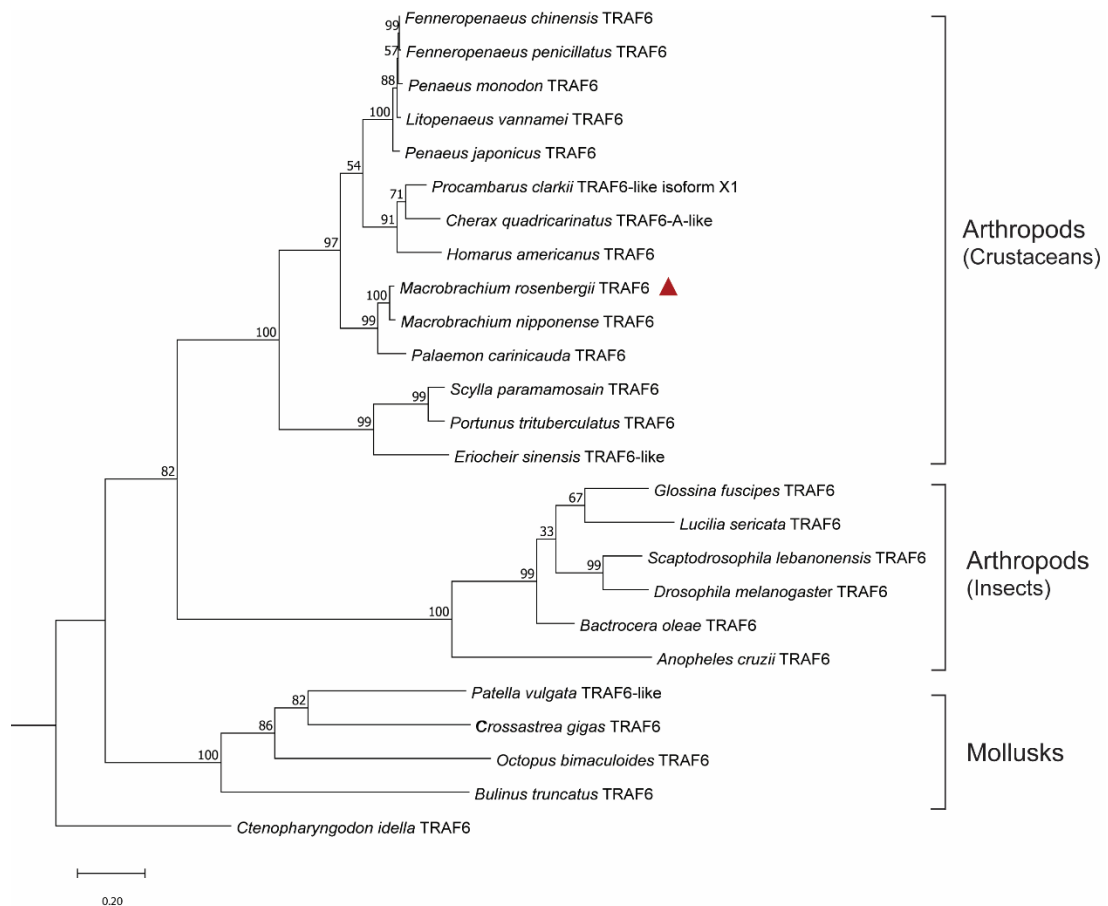
Figure 23 The rooted ML-tree constructed via the maximum likelihood method with

bootstraps of 1,000 replicates using MEGA11 software.

The TRAF6s of selected invertebrates are included: *A. cruzii* TRAF6 (Accession

no. XP_052865094.1), *B. oleae* TRAF6 (Accession no. XP_014091704.1), *B. truncatus*

TRAF6 (Accession no. KAH9518846.1), *C. gigas* TRAF6 (Accession no. ASK05289.1),

C. quadricarinatus TRAF6-A-like (Accession no. XP_053628633.1), *D. melanogaster*

TRAF6 (Accession no. AAD47895.1), *E. sinensis* TRAF6-like (Accession no.

XP_050739933.1), *F. chinensis* TRAF6 (Accession no. AFU51810.1), *F. penicillatus*

TRAF6 (Accession no. APU52029.1), *G. fuscipes* TRAF6 (Accession no.

XP_037895574.1), *H. americanus* TRAF6-like (Accession no. XP_042239384.1), *L.*

vannamei TRAF6 (Accession no. ADM26237.1), *L. sericata* TRAF6 (Accession no.

XP_037812196.1*), M. nipponense* TRAF6 (Accession no. ASM46956.1), *M. rosenbergii*

TRAF6 (Accession no. QDV59708.1), *O. bimaculoides* TRAF6 isoform X1 (Accession no. XP_052825543.1), *P. carinicauda* TRAF6 (Accession no. AVG44185.1), *P. clarkii* TRAF6 isoform X1 (Accession no. XP_045603665.1), *P. japonicus* TRAF6 (Accession no. QPI70527.1), *P. monodon* TRAF6 (Accession no. AIS92907.1), *P. trituberculatus* TRAF6 (Accession no. AKD94181.1), *P. vulgata* TRAF6 (Accession no. XP_050409809.1), *S. lebanonensis* TRAF6 (Accession no. XP_030378054.1), *S. paramamosain* TRAF6 (Accession no. CRI06483.1), and the outgroup, *C. idella* TRAF6 (Accession no. XP_051756020.1).

4.3 Tissue expression and distribution analysis of *MrTRAF6*

The expression pattern of *TRAF6* in *M. rosenbergii* was investigated by analyzing the distribution of *MrTRAF6* transcript in various tissues using real-time RT-PCR. The tissues examined included gill, heart, hepatopancreas, hemocyte, muscle, stomach, and intestine of normal prawns.

4.3.1 Detection of viral infection in normal prawn samples

Before performing tissue distribution analysis, prawn samples were subjected to viral detection by RT-PCR to confirm that the samples were free of viral infections. The results showed that no positive amplicons of *Mr*NV target (729 bp), and XSV target (507 bp) could be observed in all samples tested (Figure 24A and 24B) indicating the *Mr*NV-XSV-free samples which were further used in tissue distribution analysis.

(A)

(B)
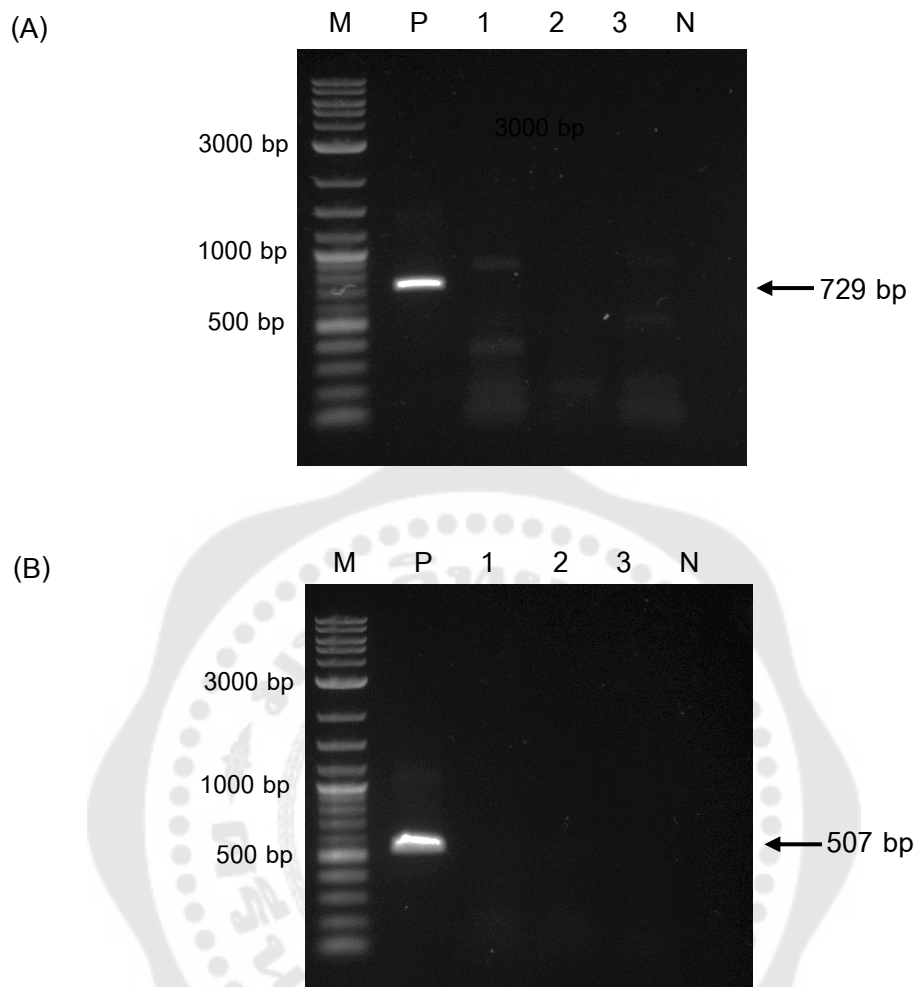
Figure 24 The representative gel of detection viral infections in healthy prawns

for normal distribution analysis. (A) *Mr*NV-detection and (B) XSV-detection. Lane M =

DNA marker, Lane P = positive control, Numbers (1-3) = prawn samples, and Lane N =

Negative control. Expected product sizes of 729 bp in *Mr*NV detection and 507 bp of

XSV detection are indicated by arrows.

4.3.2 Expression profile of *MrTRAF6* of normal prawns

The distribution of *MrTRAF6* transcript in different tissues was investigated by real-time RT-PCR. The results demonstrated that the expression of *MrTRAF6* was constitutively detected in all examined tissues. Among tissues, the highest expression was found in gill by 0.048-fold different from the baseline. Moderate expression was

found in the stomach (0.011-fold), hepatopancreas (0.021-fold), hemocyte (0.017), and intestine (0.029), while the relatively low expression was found in heart (0.0064-fold), and the lowest level in muscle (0.0025-fold). The expression profile of *MrTRAF6* was shown in Figure 25.
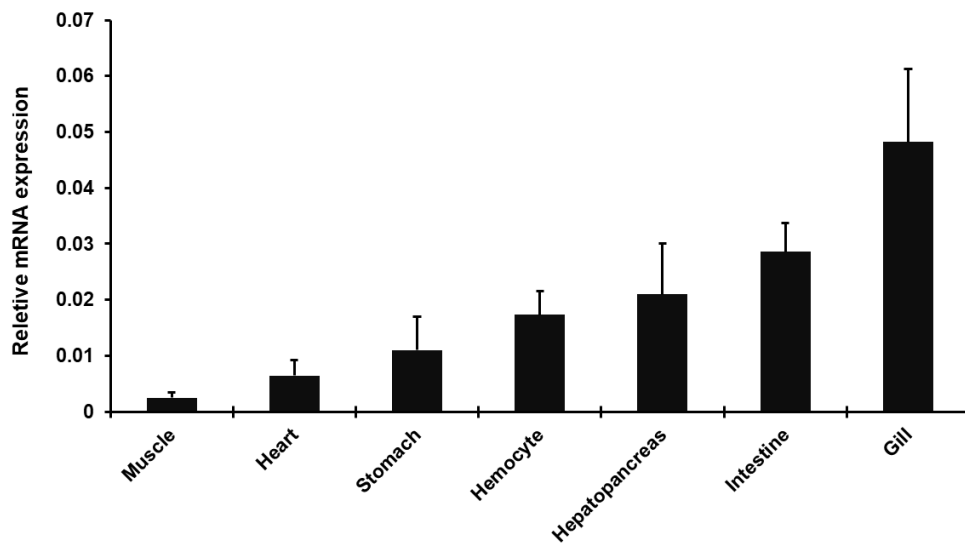

Figure 25 Tissue distribution of *MrTRAF6* in normal *M. rosenbergii*.
Real-time RT-PCR was performed in triplicates for each sample. The obtained data for were normalized to those EF1α in each tissue. The results were presented as the average fold changes (N = 3). The bars on the graph represent the standard errors.

4.4 *MrTRAF6* in response to bacterial infection in immune-challenged experiment

In order to investigate the mRNA expression profile of *MrTRAF6* during the innate immune response of prawns following a challenge with *A. hydrophila*, the temporal expression patterns of *MrTRAF6* were examined in the muscle, hemocyte, gill, and hepatopancreas tissues of the prawns. By challenging with *A. hydrophila*, the role of *MrTRAF6* in response to bacterial infection could be analyzed.

4.4.1 Detection of viral infection in 10 g-prawn samples

To ensure that the prawn samples were free of *Mr*NV and XSV viral infections before conducting the immune-challenged experiment, a total of 10 prawns

(10-15 g) were first sampled and subjected to RT-PCR viral detection. The results indicated that no positive amplicons of the *Mr*NV target (729 bp) or the XSV target (507 bp) were detected in any of the samples tested, as shown in Figure 26A and 26B. This could be confirmed that the samples were free from *Mr*NV and XSV infections and were therefore suitable for use in temporal expression analysis.
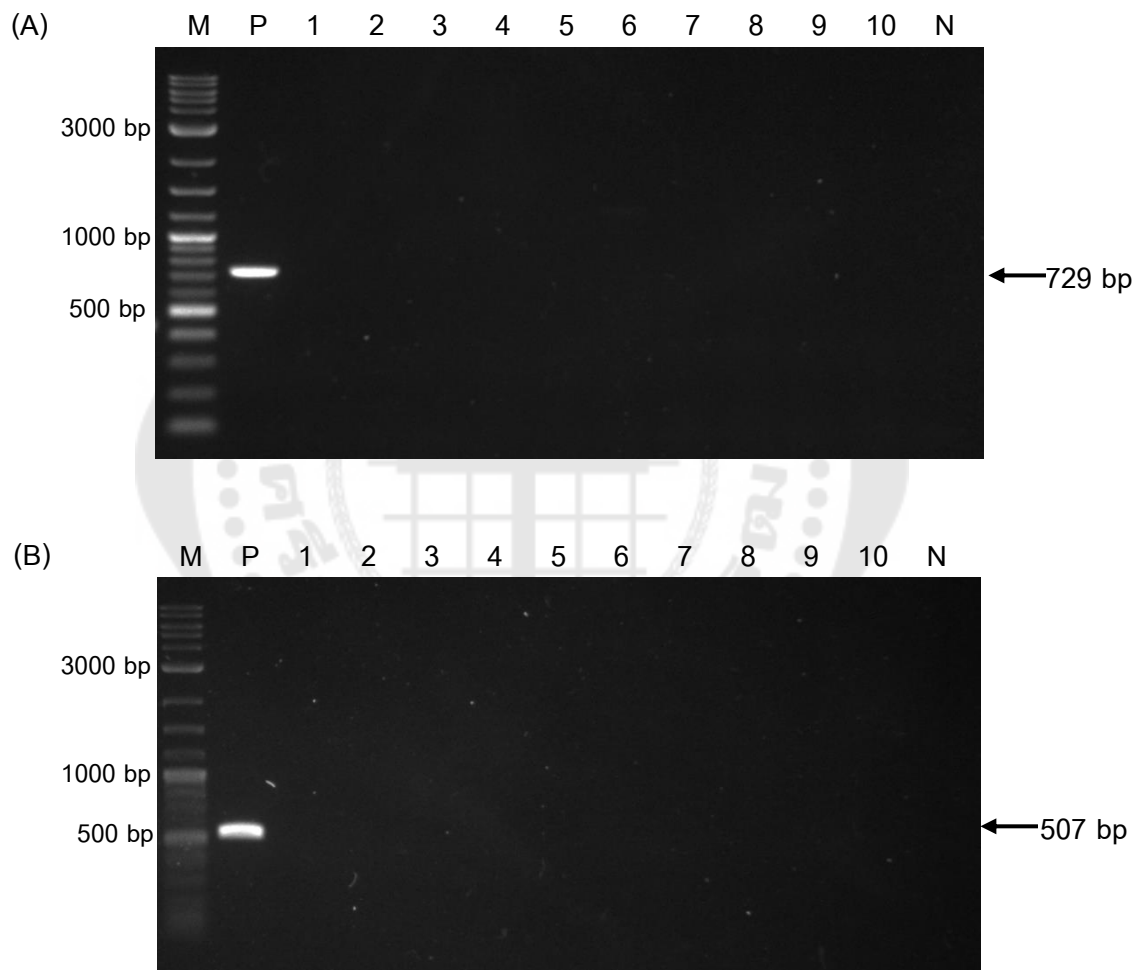

Figure 26 The representative gel of viral detection in prawn samples

for immune-challenged experiment.

(A) *Mr*NV-detection, and (B) XSV-detection. Lane M = DNA marker, Lane P = positive control, Lanes 1-10 = the PCR products from different prawn samples, and Lane N = Negative control. Expected product sizes of 729 bp in *Mr*NV detection and 507 bp of XSV detection are indicated by arrows.

4.4.2 Confirmation of *A. hydrophila* strain

Before performing the immune-challenged experiment, the bacterial strain *A. hydrophila* (VMARC1234) was identified using colony PCR. The results revealed the presence of a 592-bp amplicon specific to *A. hydrophila* (Figure 27). The PCR product was purified and subsequently subjected to sequencing analysis, which further confirmed the identification of the *A. hydrophila* hemolysin (accession no. AEE80943.1). The verified *A. hydrophila* strain was then used to prepare the bacterial inoculum for the subsequent immune-challenged experiment.
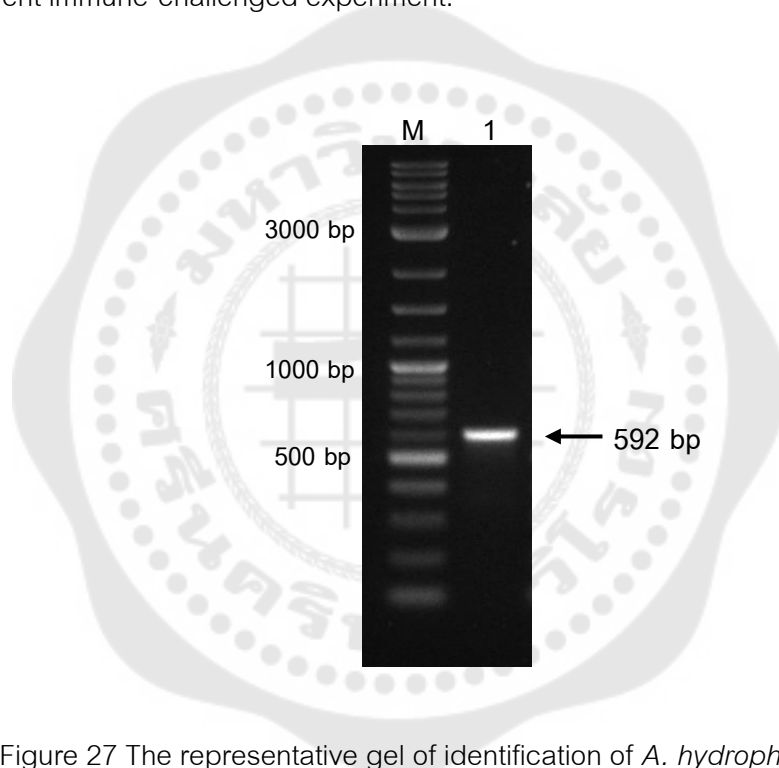
Figure 27 The representative gel of identification of *A. hydrophila* strain.

Lane M = DNA marker and Lane 1 = the PCR product from of *A. hydrophila* hemolysin gene. The expected product size of 592 bp is indicated by arrow.

4.4.3 Detection of *A. hydrophila* infection in immune-challenged prawns

To monitor the development of *A. hydrophila* infection in prawns, hemolymph samples were collected from the ventral sinus at different time points after injection (0, 3, 6, 12, 24, 36, and 48 hours post-injection), and diluted 10-fold in Tryptic Soy Broth (TSB) before being spread onto Tryptic Soy Agar (TSA) plates. The bacterial colonies grown on the TSA plates at each time point were then subjected to PCR

analysis to identify *A. hydrophila* infection. The results showed that a 592-bp amplicon specific to *A. hydrophila* was detected in all selected colonies, confirming the presence of *A. hydrophila* infection in the experimental prawn samples, as shown in Figure 28.
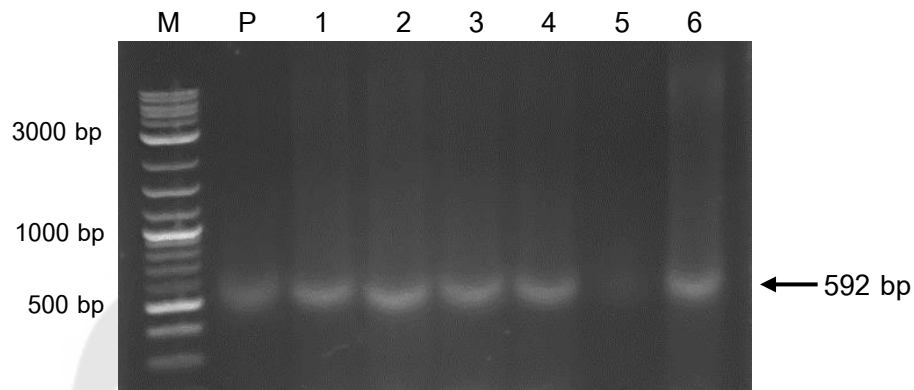
Figure 28 The representative gel of confirmation of *A. hydrophila* infection in AH-
challenged prawns at different timepoints.
Lane M = DNA marker,
Lane P = positive control,
Lanes 1-6 indicated the PCR products from bacterial colonies
PCR at 3, 6, 12, 24, 36, and 48 hour post-injection, respectively.
The expected product size of 592 bp is indicated by arrow.

4.4.4 Expression profile of *MrTRAF6* in immune-challenged *M. rosenbergii*

The immune-challenged experiment was performed to investigate the role of *MrTRAF6* in response to bacterial infection. The 10-15 g healthy prawns were intramuscularly injected with *A. hydrophila* suspension (5 x 10^3 CFU/µL) or 2X PBS (as a control group). The tissue selected, including gill, hepatopancreas, hemocyte, and muscle of prawns at 0, 3, 6, 12, 24, 36, and 48 hpi was collected, and subjected to real-time RT-PCR analysis. The results showed that The *MrTRAF6* mRNA transcripts levels differed between tissues after challenge with *A. hydrophila*. In muscle, the *MrTRAF6* transcript was significantly up-regulated in the early stage of stimulation by reaching the

highest level (about 14.2-fold) at 6 hours post-injection (hpi), and continuously declined to normal stage at 36 hpi (Figure 29A). In hemocytes, the expression level of *MrTRAF6* was up-regulated significantly at 6, 12, and 24 hpi. Interestingly, the significant up-regulation was found again at 48 hpi (Figure 29B). In gill, the *MrTRAF6* transcript was up-regulated significantly 3.78-fold and 3.56-fold at 12 and 24 hpi, respectively, and returned to normal stage after 36 hpi (Figure 29C). In hepatopancreas, however; the significant up-regulation of the *MrTRAF6* transcript was found only at 36 hpi with 1.85-fold difference from the base line (Figure 29D).
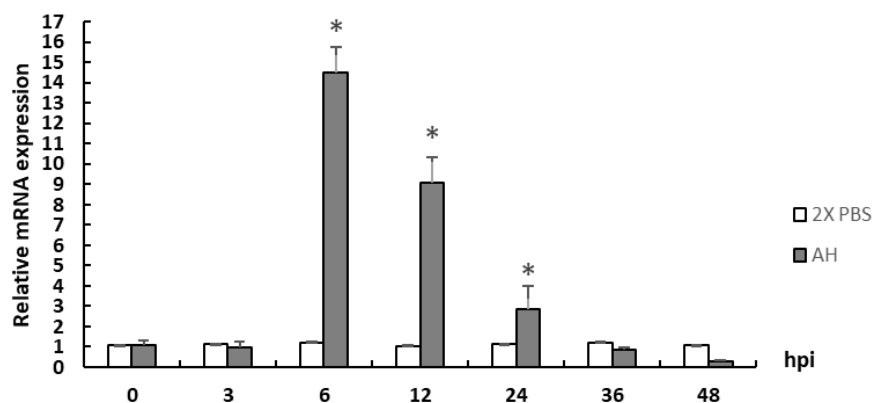
Figure 29 Temporal expression of *MrTRAF6* in different tissues:

(A) muscle, (B) hemocyte, (C) gill, and (D) hepatopancreas in response to bacteria *A. hydrophila*. The 2X PBS-injected prawns were used as the control group at each hour post-injection (hpi). The relative mRNA expressions were provided as mean fold changes (mean± SD., N = 3). Bars represent standard errors, and asterisks (*) indicate statistical significance at $p < 0.05$.

(B) **Hemocyte**
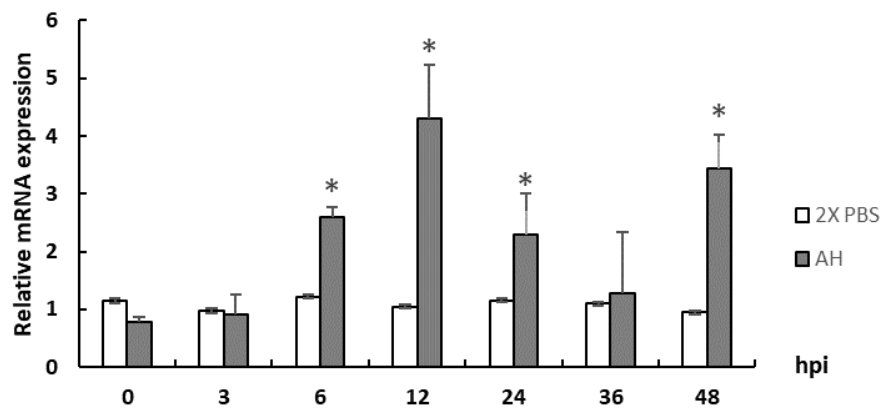
(C) **Gill**
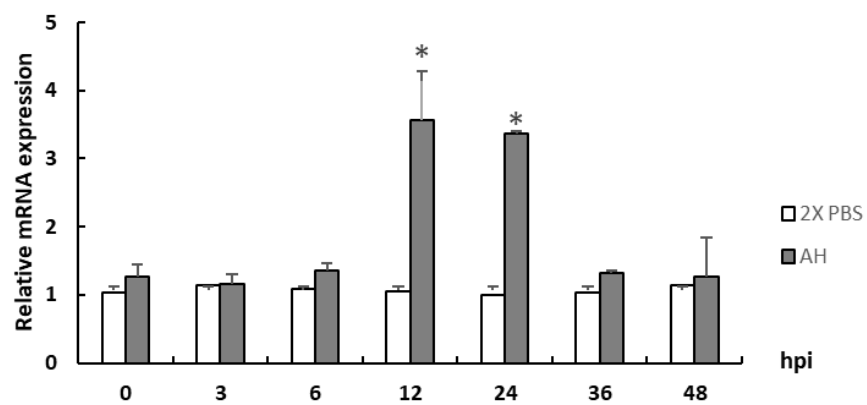
(D) **Hepatopancrease**
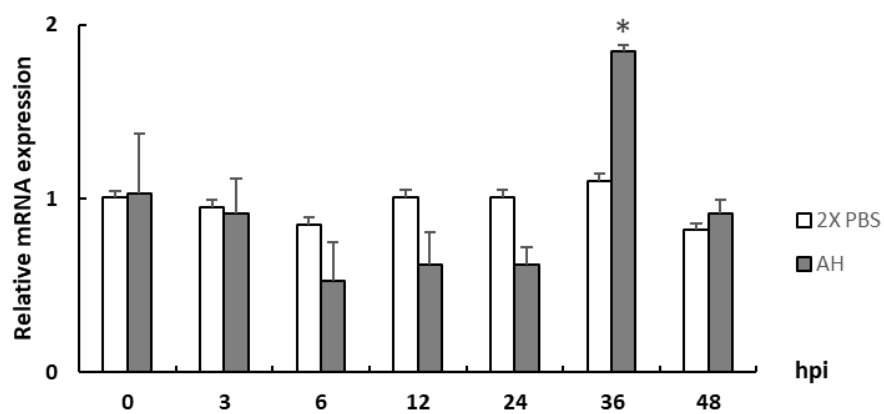
Figure 29 (Continued).

4.5 Silencing of *MrTRAF6* by dsRNA-mediated RNA interference

To investigate the specific role of *MrTRAF6* in the innate immune system of *M. rosenbergii*, RNA interference (RNAi) was used to knock down the expression of *MrTRAF6*. The knockdown efficiency was confirmed by detecting the mRNA expression levels of *MrTRAF6* using real-time RT-PCR. The knockdown prawns were then challenged with *A. hydrophila*, and the cumulative mortality rate was monitored over a specified time period following bacterial infection. By comparing the survival rates of the *MrTRAF6* knockdown prawns to those of the control group, the functional significance of *MrTRAF6* in the innate immune response of *M. rosenbergii* could be assessed.

4.5.1 Construction of DNA template for *in vitro* transcription

The desired DNA templates for *in vitro* transcription were constructed by PCR using the specific primers tagged with T7 promoter sequence at 5' end. The PCR yielded the products of 431 bp (including T7 promoter sequence) for both sense and antisense strands of *MrTRAF6*, as demonstrated in Figure 30.
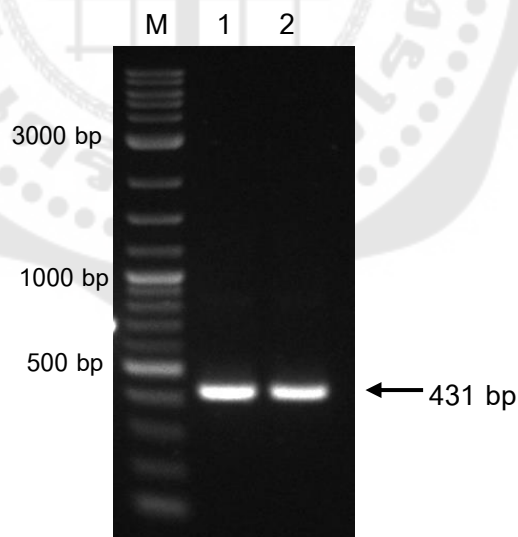
Figure 30 The representative gel of construction of *MrTRAF6* template

for *in vitro* transcription.

Lane M = DNA marker, Lane 1 = sense strand, and Lane 2= antisense strand of

*MrTRAF*6. The expected product of 431 bp is indicated by arrow.

Furthermore, the sense and antisense strands of IMNV, which was employed as unrelated-control gene, yielded products of 307 bp (including T7 promoter sequence), as illustrated in Figure 31.
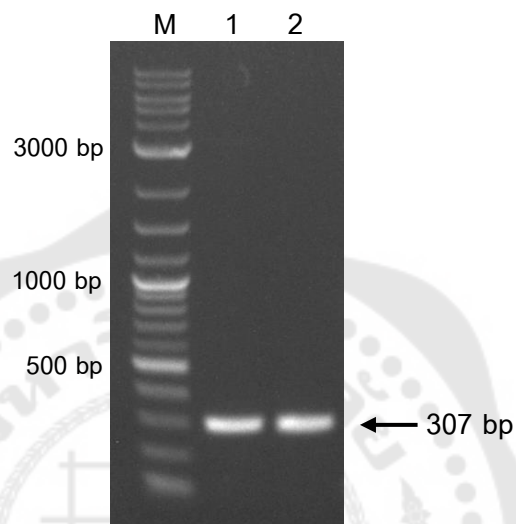
Figure 31 The representative gel of construction of IMNV template

for *in vitro* transcription.

Lane M = DNA marker,

Lane 1 = sense strand of IMNV,

Lane 2 = antisense strand of IMNV.

The expected product of 307 bp is indicated by arrow.

4.5.2 *In vitro* transcription and validation of dsRNA

The dsRNA of *MrTRAF6* and IMNV were synthesized *in vitro*. The synthesized dsRNAs were subjected to enzymatic digestions for validation. The results showed that after being digested with three enzymes, a 406-bp dsRNA-*MrTRAF6* (excluded T7 promoter sequence) was neither digested with DNase I nor RNase A (which are known to digest DNA and ssRNA, respectively). The complete digestion of dsRNA-*MrTRAF6* appeared only by digesting with RNase III (which is used specifically for the digestion of dsRNA), as indicated in Figure 32. Similarly, a 282-bp of dsRNA-

IMNV was completely digested by RNase III but remained unaffected by DNase I or RNase A digestion, as shown in Figure 33. These results demonstrated successful *in vitro* constructions of both dsRNA-*MrTRAF6* and dsRNA-IMNV.
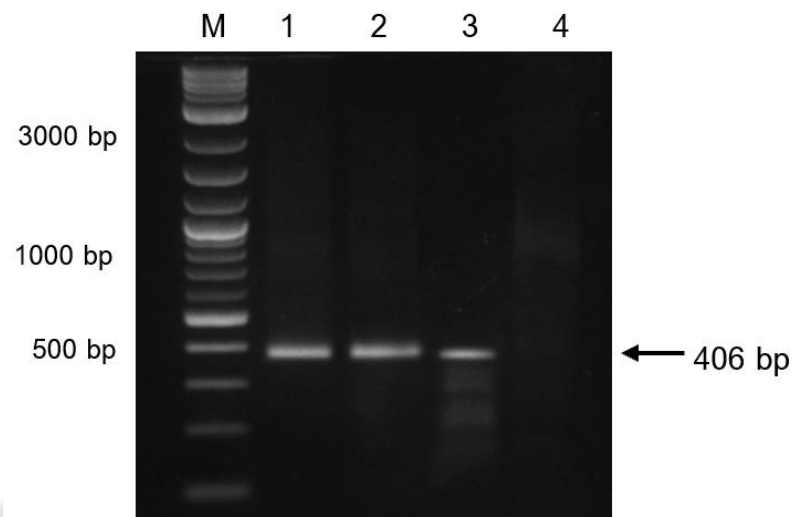
Figure 32 The representative gel of validation of dsRNA-*MrTRAF6*.

The synthesized dsRNA-*MrTRAF6* was validated by enzymatic digestions.

Lane M = DNA marker,

Lane 1 = dsRNA-*MrTRAF6*,

Lane 2 = DNase I digestion,

Lane 3 = RNase A digestion,

Lane 4 = RNase III digestion.

The expected product of 406 bp was indicated by arrow.
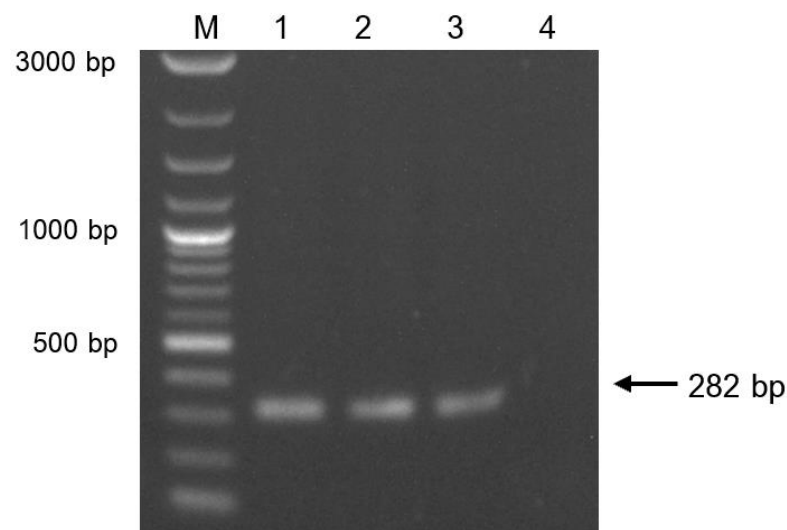
Figure 33 The representative gel of dsRNA-IMNV.

The synthesized dsRNA-IMNV was validated by enzymatic digestions.

Lane M = DNA marker,

Lane 1 = dsRNA-IMNV,

Lane 2 = DNase I digestion,

Lane 3 = RNase A digestion,

Lane 4 = RNase III digestion.

The expected product of 282 bp is indicated by arrow.

4.5.3 Detection of viral infection in 2 g-prawn samples

Before performing the knockdown experiment *in vivo*, a total of 10 prawns (1.5-2 g) were first sampled and subjected to RT-PCR viral detection to ensure that they were *Mr*NV- and XSV-free. The results indicated that no positive amplicons of the *Mr*NV or the XSV target were detected in all prawns tested, as indicated in Figure 34A and 34B. This confirmed the absence of *Mr*NV and XSV infections in the prawn samples and ensured that they were suitable for use in the knockdown experiment.
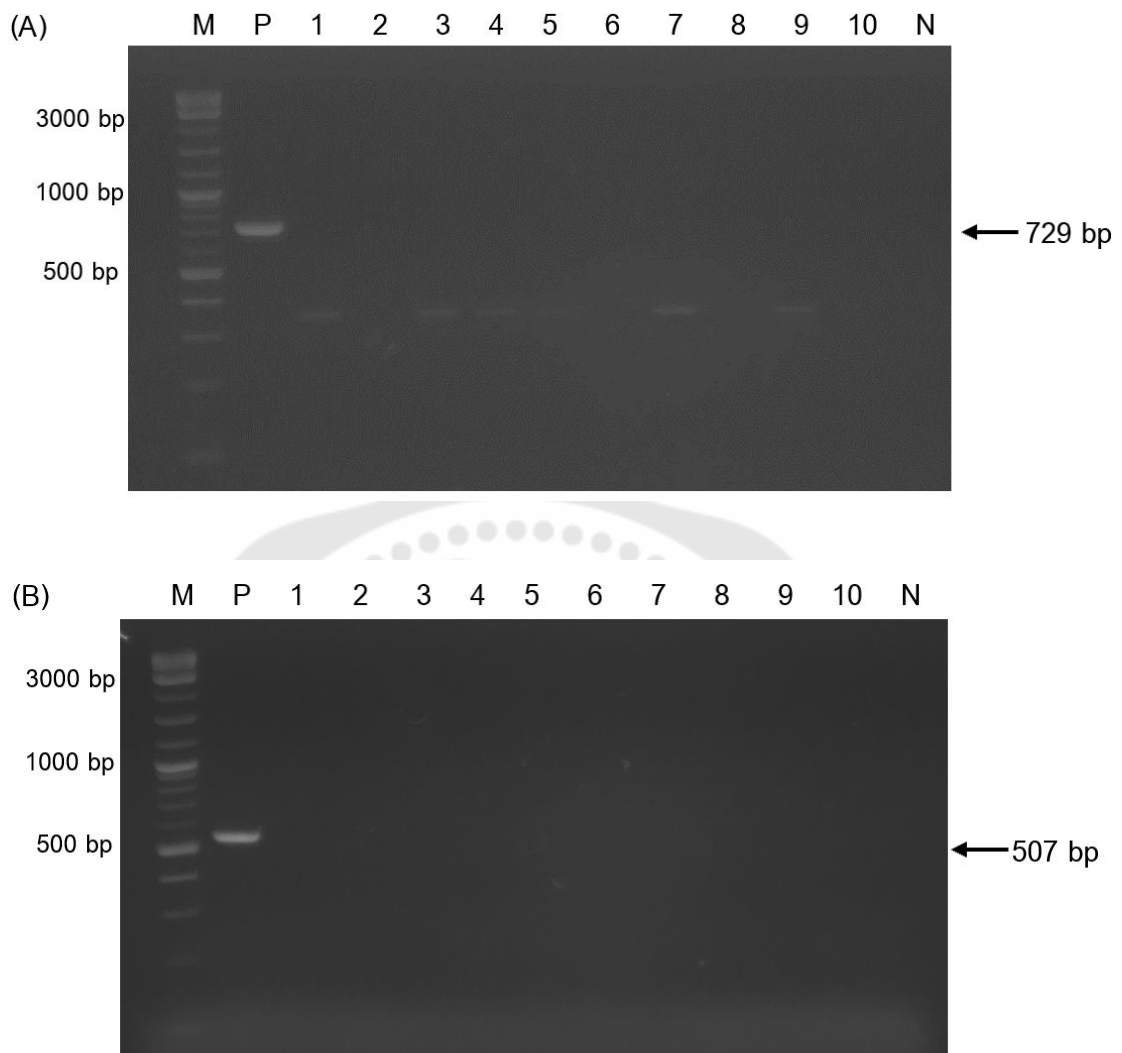
Figure 34 The representative gel of viral detection in prawn samples

for a knockdown experiment.

(A) *Mr*NV-detection, and (B) XSV-detection.

Lane M = DNA marker, Lane P = positive control,

Lanes 1-10 = the PCR products from different 2 g-prawn samples,

Lane N = Negative control.

Expected product sizes of 729 bp in *Mr*NV detection and 507 bp of XSV detection are

indicated by arrows.

4.5.4 Silencing of *MrTRAF6 in vivo* by dsRNA-mediated RNA interference

The dsRNA was utilized to knockdown the expression of *MrTRAF6 in vivo*. Prawns with an approximated weight of 1.5-2 g were injected twice with dsRNA-*MrTRAF6*, dsRNA-IMNV, or 2X PBS (as a control group). To confirm the efficiency of the knockdown, the mRNA expression levels of *MrTRAF6* were detected using real-time RT-PCR in gills tissues at days 0 to 7 after first injection to verify that the knockdown had effectively reduced the expression of *MrTRAF6*. The result revealed that the relative expression level of *MrTRAF6* in gill tissue after dsRNA-*MrTRAF6* injection was reduced from days 2 to 7 when compared to those in dsRNA-IMNV and the 2X PBS control group. In addition, the most significant effect of dsRNA-*MrTRAF6* knocking down was detected at days 3, 4, and 5 after first injection which their relative expressions accounted for 0.19-, 0.20-, and 0.15-fold, respectively. The expression of *MrTRAF6* decreased by 81.8%, 76.0%, and 85.4% at day 3, 4, and 5, respectively, compared to the expression levels in the control group treated with 2X PBS. In the late stage of experiment (days 6 to 7), the expression of *MrTRAF6* gradually recovered to 0.33- and 0.60-fold by the end of experiment. Nevertheless, there was no significant down-regulation of *MrTRAF6* expression in both dsRNA-IMNV and 2X PBS injected groups at all examined timepoints ($p < 0.05$). The expression of *MrTRAF6* from days 0 to 6 after knockdown experiment was illustrated in Figure 35.
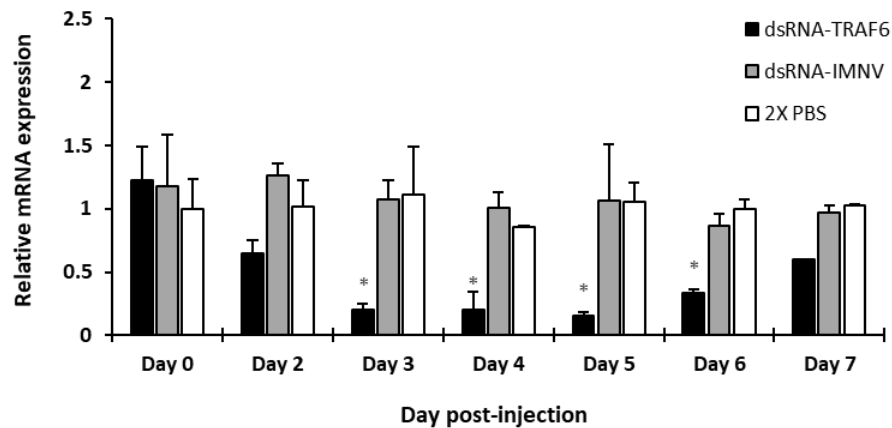
Figure 35 The knockdown efficiency of dsRNA-*MrTRAF6*.

The expression levels of *MrTRAF6* in the gills of knocked-down prawns were measured using real-time RT-PCR. The prawns were injected with either dsRNA or 2X PBS, and the expression levels were detected at day 0 to day 7 after the first injection. Relative expression values were normalized to EF1α. The expression in 2X PBS was used as the control (set as 1.00). The results are based on three independent experiments and provided as mean fold change (N=3). Bars represent standard errors. The asterisks indicate $p < 0.05$ compared to 2X PBS injection group.

4.5.5 The expression of AMP genes in silenced-*M.rosenbergii*

Following the *in vivo* knockdown experiment, the expression levels of downstream AMPs, including crustin, ALF5, and the antimicrobial peptide MBL were investigated by real-time RT-PCR in dsRNA-silenced *M. rosenbergii*. The results showed that the relative expression of crustin remarkably decreased in the dsRNA-*MrTRAF6*-injected group at 4 days post-injection by 1.92-fold compared to the control group (Figure 36A). For MBL expression, significant down-regulation was detected at day 3 to 6 after first injection in the dsRNA-*MrTRAF6*-injected group (Figure 36B). In contrast, no significant change of ALF5 expression level was observed in the dsRNA-*MrTRAF6*-injected group at all tested timepoints compared to those in dsRNA-IMNV-silenced group and the control group (Figure 36C).

(A)

(B)
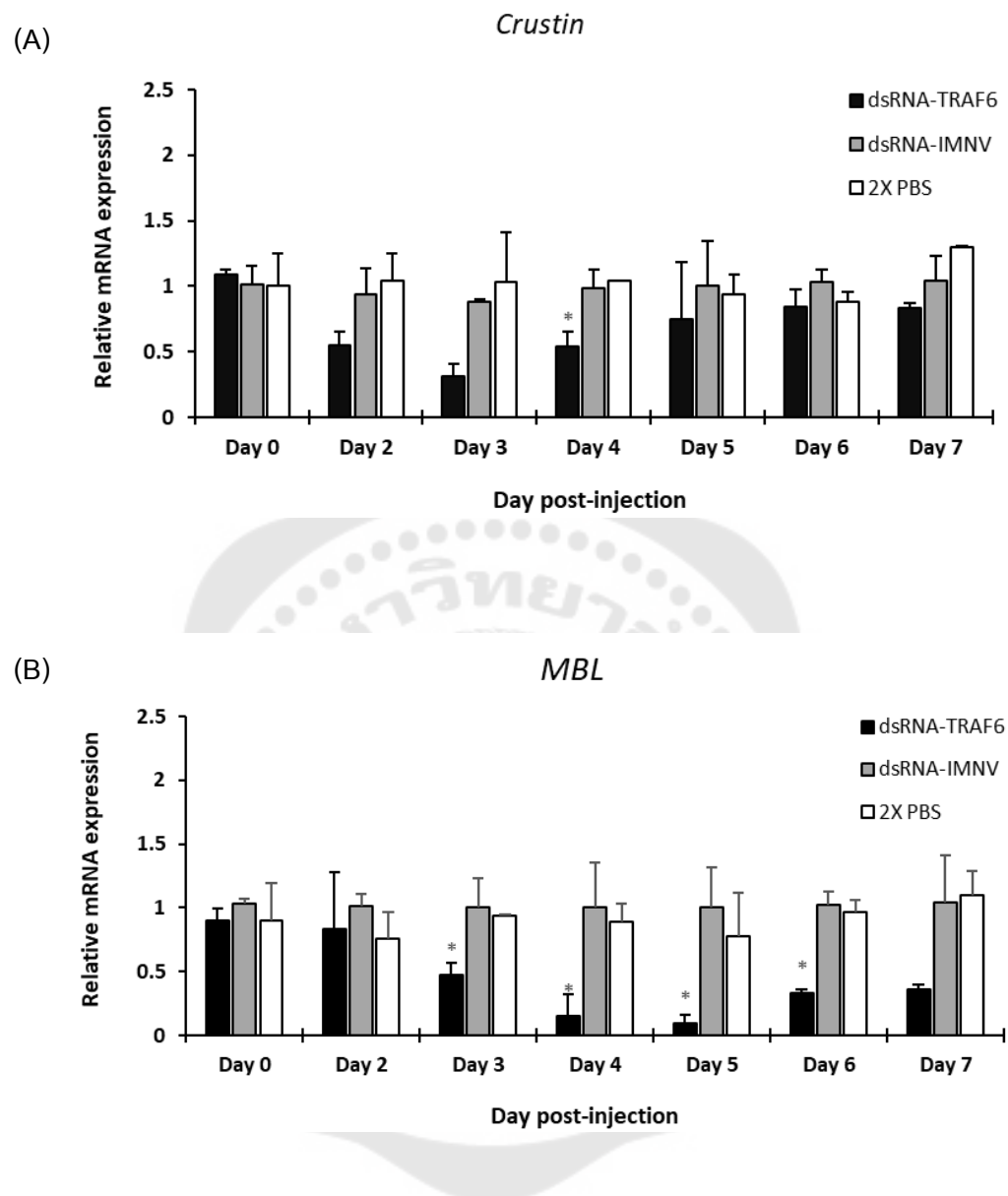
Figure 36 The expression profile of AMPs genes in the knockdown prawns.

(A) Crustin, (B) MBL, and (C) ALF5 in gill at day 0-7 after first injection of dsRNA or 2X

PBS. Relative expression values were normalized to EF1α. The 2X PBS was used as the

control group (set as 1). The results are based on three independent experiments and

provided as mean fold change (N=3). Bars represent standard errors. The asterisks

indicate $p < 0.05$ compared to 2X PBS injection group.

(C)

ALF5
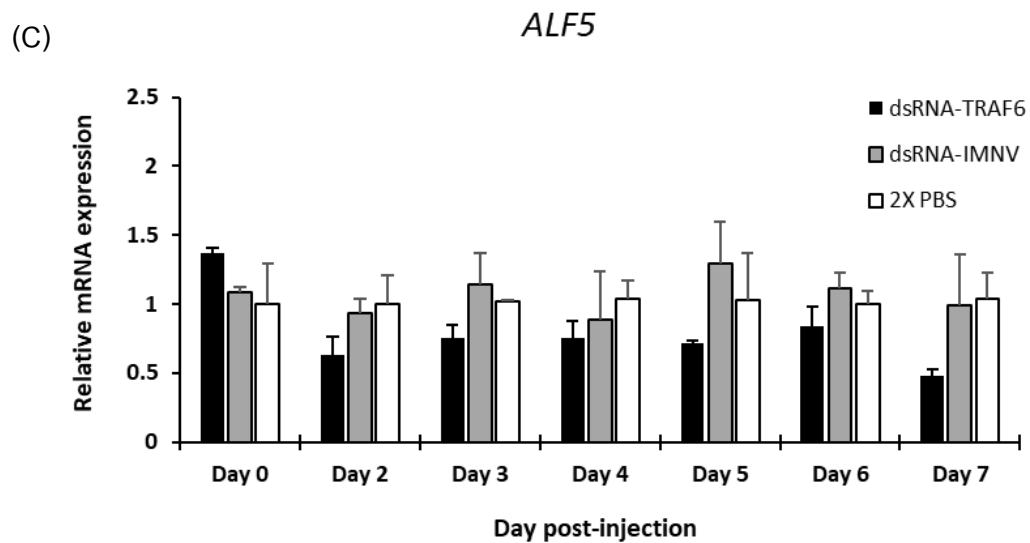
Figure 36 (Continued).

4.5.6 Cumulative mortality analysis of *MrTRAF6*-silenced prawns

To investigate the function of *MrTRAF6* in the innate immune against bacterial infection of *M. rosenbergii*, the microbial infection experiment was conducted in dsRNA-injected prawns. The prawns with approximate weight of 1.5-2.0 g were injected twice with dsRNA-*MrTRAF6*, dsRNA-IMNV, or 2X PBS, and then challenged with *A. hydrophila* (at a dose of LD25) or 2X PBS at days 4 post-dsRNA injection. The cumulative mortality rates of *M. rosenbergii* were monitored from 0 to 168 hour post-bacterial injection. The result revealed that after injection with *A. hydrophila*, the cumulative mortality was significantly increased in *MrTRAF6*-silenced prawns and reached 55% at 120 hpi. In comparison, the cumulative mortalities after *A. hydrophila* injection were 25% and 20% in the dsRNA-IMNV and 2X PBS control groups, respectively, as depicted in Figure 37A. After the prawns were injected with 2X PBS, the cumulative mortalities in the dsRNA-*MrTRAF6*, dsRNA-IMNV, and 2X PBS control groups were monitored and found to be 10%, 15%, and 15%, respectively, as shown in Figure 37B. These results indicate that the injection of 2X PBS had a lower mortality rate compared to bacterial infection, and there was no significant difference in mortality rate between the three experimental groups.

(A)

Accumulate mortality (%)

(B)

Accumulate mortality (%)
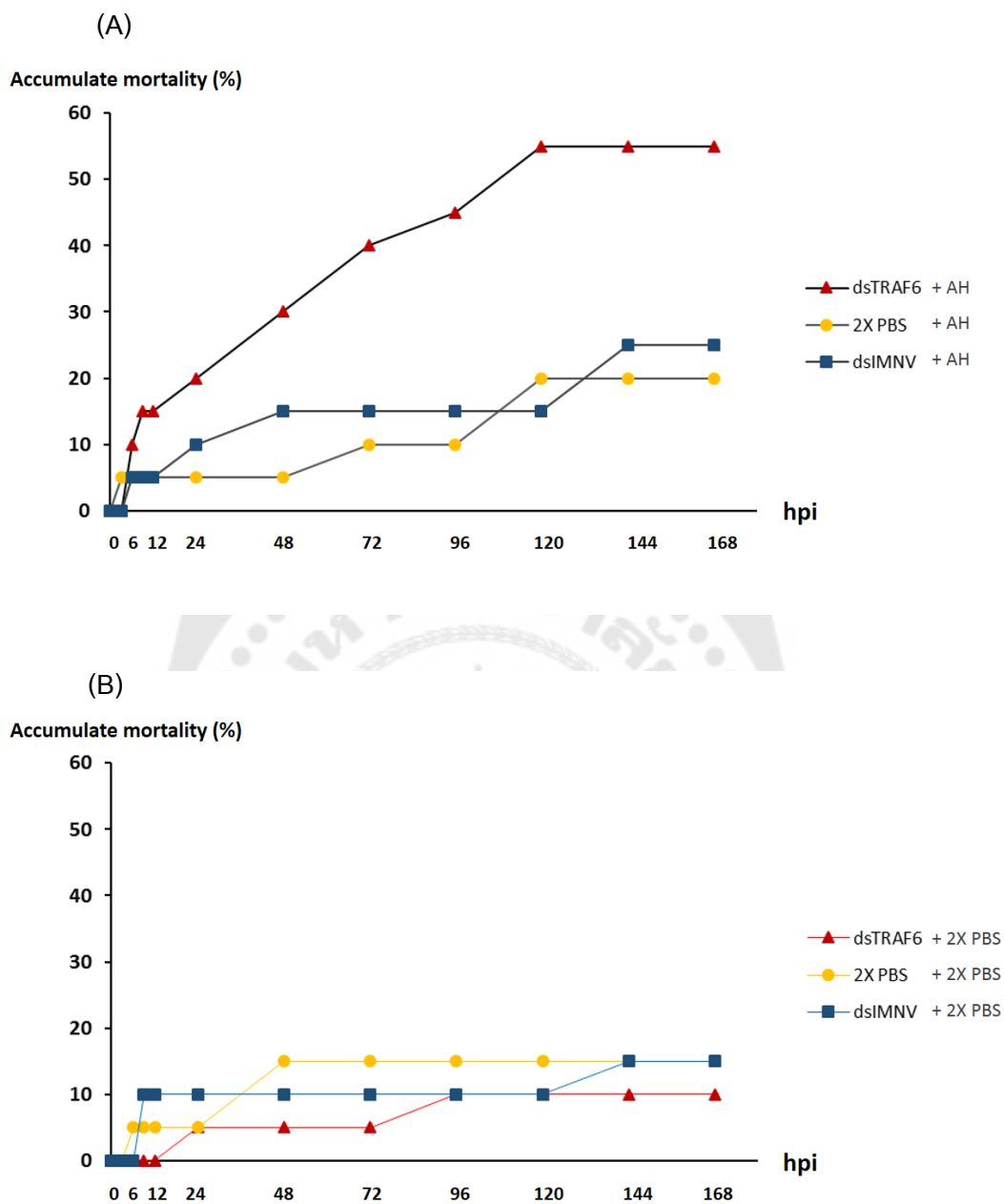
Figure 37 Cumulative mortality rates of *MrTRAF6*-silenced *M. rosenbergii*

after injection of (A) *A. hydrophila* and (B) 2X PBS.

Prawns were injected intramuscularly with 2X PBS or dsRNA corresponding to
MrTRAF6 or IMNV. At days 4 after dsRNA-*MrTRAF6*, dsRNA-IMNV, and 2X PBS first-
injection, the animals were injected with AH or 2X PBS (control group). Mortality was
monitored in each treatment group at 0 to 168 hour post-injection (hpi), N=20

CHAPTER 5

DISCUSSION AND CONCLUSION

5.1 Discussion

Toll-like receptors (TLRs) are critical components of the innate immune system that are responsible for responding to various pathogen-associated molecular patterns (PAMPs). By recognizing these PAMPs, TLRs activate signaling pathways that trigger the expression of immune and pro-inflammatory genes, which help to combat invading pathogens. Therefore, TLRs serve as the first line of defense against pathogens and play a critical role in initiating an effective immune response (Y. Huang & Ren, 2020; F. Li & Xiang, 2013a). In crustaceans, the Toll pathway plays crucial roles in immune response against Gram-positive bacteria, Gram-negative bacteria, and certain viruses (F. Li & Xiang, 2013a; Tassanakajon et al., 2018).

TRAF6 has been identified as a crucial mediator that connects the upstream TLRs, MyD88, and interleukin-1 receptor-associated kinases (IRAKs) with the downstream signaling pathways of NF-κB and Mitogen-Activated Protein Kinase (MAPK) (Walsh, Lee, & Choi, 2015). Additionally, some TRAF6s have been identified in shrimp species such as *Litopenaeus vannamei*, *Penaeus monodon*, *Fenneropenaeus penicilatus*, and *Procambarus clarkii* (Cai et al., 2017; Deepika et al., 2014; B. Li et al., 2020; P.-H. Wang, Wan, et al., 2011). To our knowledge, this study provides the first evidence of TRAF6 protein in *Macrobrachium rosenbergii* and sheds some light on its potential involvement in the innate immune system of this valuable freshwater prawn species.

In this study, we successfully isolated the full-length *TRAF6* gene from *M. rosenbergii*, designated as *MrTRAF6*. Structural analysis of the *Mr*TRAF6 protein illustrated that *Mr*TRAF6 also possessed the characteristic domains of TRAFs family including two RING fingers, and a highly conserved MATH domain. Similar to *Fp*TRAF6, *Pc*TRAF6-like (Cai et al., 2017; B. Li et al., 2020), and *Macrobrachium nipponense* TRAF6 (Accession No. ASM46956.1), *Mr*TRAF6 lacked a typical coiled-coil region found

in other shrimp TRAF6s, such as *Lv*TRAF6 and *Pm*TRAF6 (Deepika et al., 2014; P.-H. Wang, Wan, et al., 2011). However, the precise biological role of coiled-coil region in TLRs signaling pathway remains unclear in crustaceans.

The deduced amino acid of *MrTRAF6* shared the highest similarity with MnTRAF6 (96.6%) and relatively high among crustaceans (46.1-87.6%). The phylogenetic analysis revealed that *Mr*TRAF6 was clustered to the group of crustaceans and most closely related to *Mn*TRAF6. These findings supported the notion that *MrTRAF6* was a homolog derived from *M. rosenbergii* and was evolutionarily conserved from D*rosophila* to humans, which suggests that it may share similar functions as other TRAF6 proteins.

The *MrTRAF6* was constitutively expressed in all analyzed tissues including gill, heart, hepatopancreas, hemocyte, muscle, stomach, and intestine, although the level difference appeared among tissues. This universal distribution was also reported in several crustaceans' species such as *L. vannamei* TRAF6, *P. monodon* TRAF6, *P. trituberculatus* TRAF6, *F. penicillatus* TRAF6, *S. paramamosain* TRAF6, and *P. clarkii* TRAF6 (Cai et al., 2017; Deepika et al., 2014; B. Li et al., 2020; Sun et al., 2017; P.-H. Wang, Wan, et al., 2011; Zhou et al., 2015). These expression profiles of TRAF6s exhibited different patterns in shrimp species. *MrTRAF6* was predominantly expressed in gill where it regularly contacts with the external environment and, as a result, frequently encounters pathogenic microorganisms. This is in agreement with the *PcTRAF6*-like that exhibited relatively high expression level in gill, hepatopancreas and hemocytes (Li et al., 2020). Meanwhile, *LvTRAF6* transcript was highly expressed in epithelium, nerve, and muscle tissues (P.-H. Wang, Wan, et al., 2011), *PmTRAF6* was detected in the highest level at eyestalk followed by midgut and nerve tissues (Deepika et al., 2014), and the highest level in lymphoid organ was found in *FpTRAF6* (Cai et al., 2017). This is probably due to species-specific, genetic background, developmental stages, and external environment. Furthermore, the *MrTRAF6* transcript found in non-immune tissue could be implied that *MrTRAF6* may be involved in other physical processes besides the pivotal role in innate immune system. Other studies have

demonstrated that TRAF6 also involves in regulating a wide variety of biological functions in invertebrates, such as sac formation, development, and apoptosis (D. Huang, Bai, Shen, Zhao, & Jiale, 2018; Lin et al., 2020; Mishra, Sachan, Mutsuddi, & Mukherjee, 2014)

As TRAF6 has been identified as a crucial adaptor that links the upstream TLRs, MyD88, and IRAKs with the downstream signaling of NF-κB through the TLR signaling pathway, it may potentially play a role in response to invading viruses and bacteria as part of the immune defense of fish and shellfish (H.-Y. Kim & Rikihisa, 2002). To demonstrate the presence of that response in *M. rosenbergii*, the temporal expression of *MrTRAF6* was assessed post bacterial infection with the Gram-negative bacterial pathogen, *A. hydrophila*. According to real-time RT-PCR results, the significant up-regulation of *MrTRAF6* transcript was detected in gill, hemocyte, muscle, and hepatopancreas during challenge with *A. hydrophila* compared to that in 0 hpi and in 2X PBS control group suggesting that *MrTRAF6* could be induced and activated during the immune response against bacterial infection and plays different roles in different organs. The result was supported by previous studies that have been observed in some invertebrates. In pearl mussel (*Hyriopsis cumingii*), for instance, *HcTRAF6* was reported to be obviously induced in gill and hemocyte after stimulating with *A. hydrophila* (D. Huang, Bai, Shen, Zhao, & Jiale, 2018). In tiger shrimp (*P. monodon*) the expression of *PmTRAF6* intensively increased in hemocyte (Deepika et al., 2014). In redtail prawn (*F. penicillatus*), the expression of *FcTRAF6* was up-regulated in gill and hepatopancreas post *Vibrio alginolyticus* infection (Cai et al., 2017). For the red swamp crayfish (*P. clarkii*), the result showed significant up-regulation of *Pc-TRAF6* like during infection with two bacterial species; *Staphylococcus aureus* and *Edwardsiella ictaluri* (Li et al., 2020). Furthermore, *MrSpätzle*, *MrToll*, *MrMyD88*, and *MrDorsal* have also been induced by multiple pathogens and exhibited various temporal expression patterns (Gao et al., 2021; X. Huang et al., 2016; Srisuk et al., 2014; Vaniksampanna et al., 2019). These findings suggested that TLR-MyD88-TRAF6-Dorsal linkage exists in *M. rosenbergii* and mediates in the response to bacterial infection, especially Gram-negative bacteria.

Generally, in crustaceans, the Toll signaling pathway is activated after recognition of PAMPs by PRRs, which triggers the production of various humoral molecules including AMPs to eventually eliminate invading pathogens (Tassanakajon et al., 2013). It is known that efficient AMPs have various roles in the immune system, including the ability to fight against a broad range of microorganisms, including bacteria, fungi, and viruses through their antimicrobial properties (Brown & Hancock, 2006; Guaní-Guerra, Santos-Mendoza, Lugo-Reyes, & Terán, 2010; Yount, Bayer, Xiong, & Yeaman, 2006). To further investigate the essential role of *MrTRAF6* in regulating AMPs expression through the immune signaling pathway, specific dsRNA was used to suppress the expression of *MrTRAF6* transcript. The expression levels of various immune-related genes, such as crustin, MBL and ALF5, were analyzed in *MrTRAF6*-silenced prawns. The result revealed the effective silencing of *MrTRAF6* by RNAi in *M. rosenbergii*. In case where *MrTRAF6* was knocked-down, the expression of MBL and crustin exhibited significant down-regulation immediately after *MrTRAF6* was statistically decreased. On the contrary, the expression of ALF5 was slightly decreased with no significant change. MBL, crustin, and ALF are proteins involved in Toll signaling pathway in shrimp, contributing to antiviral and antibacterial activities. Thus, silencing *TRAF6* could have effects on the expression of these genes. This result is consistent with previous reports of *TRAF6* silencing in other invertebrates that could inhibited several kinds of AMPs or other immune-related genes such as *Crossastrea gigas* interferon regulatory factor (IRF) 1 and IRF8 in *CgTRAF6*-depleted oysters (Mao et al., 2017), *Sp*ALF1, *Sp*ALF2, *Sp*ALF5, and *Sp*ALF6 in *TRAF6*-silenced mud carb (*S. paramamosain*) (Sun et al., 2017), *Hc*Lysozyme and *Hc*Defensin in gills of *HcTRAF6*-silenced mussel (*H. cumingii*) (Huang, Bai, Shen, Zhao, & Jiale, 2018), *Pc*-Dorsal, *Pc*-ALF, *Pc*Lys, and *Pc*-crustin2 in *Pc*TRAF6-depleted crayfish (*P. clarkii*) (Li et al., 2020).

In addition, to investigate more thoroughly whether suppressing *MrTRAF6* has impact on bacterial resistance, the cumulative mortality experiment was performed in TRAF6-silenced *M. rosenbergii* by challenging with *A. hydrophila*. The result showed

that by knocking down *MrTRAF6*, the accumulative mortality rate of *M. rosenbergii* increased since the early stage after *A. hydrophila* infection. Although this evidence of TRAF6 suppression is limited in crustaceans (only three species; *S. paramamosain*, *F. pennicillatus*, and *P. clarkii* have been reported), the results of those previous studies provided that knocking down of *TRAF6* dramatically decreased the ability to defense against bacterial infection, leading to significant increase in cumulative mortality and decrease in survival rate (Cai et al., 2017; B. Li et al., 2020; Sun et al., 2017). Consistently, in mollusks *H. cumingii*, silence of *HcTRAF6* inhibited the elimination of *A. hydrophila* (Huang, Bai, Shen, Zhao, & Jiale, 2018). Taken together, it can be implied that the silencing of *MrTRAF6* resulted in decreased expression levels of AMPs and increased mortality rates in *M. rosenbergii*.

5.2 Conclusion

In summary, the homolog of *TRAF6* was identified and characterized in giant freshwater prawn (*M. rosenbergii*). *Mr*TRAF6 exhibited conserved characteristics of the TRAF6 family and was clustered with crustacean's TRAF6. Through gene expression analysis result, *MrTRAF6* transcripts were widely expressed in various tissues, with the highest expression in the gill and the lowest in muscle. Furthermore, the expression of *MrTRAF6* was found to be inducible by the Gram-negative bacterium, *A. hydrophila.*

To further investigate the functional role of *MrTRAF6*, a silencing experiment using dsRNA was conducted. The silencing of *MrTRAF6* resulted in a decrease in the expression of MBL and crustin, which subsequently led to an increased cumulative mortality rate in *M. rosenbergii* following *A. hydrophila* infection. These findings strongly indicate that *MrTRAF6* plays a crucial role in the innate immune defense against bacterial infections in prawns.

APPENDIX

1. Primer binding sites

CAGATCAACTGCTTTTAAGCA**ATG**GAAGGCTCGGACGGGAGTTCGATAACCCTGATATCTAG
GCAAGAGGGGTTTGATTACGACTTCGTGCCCCCCTTAGATAGCAAGTATGAGTGTGCCATAT
GTCTCTTAGGCCTCAGATCTCCAATGCAGACAACCTGTGGGCACCGATTTTGTAAAGACTGC
ATCTTCAATTGCCTAAGTGAGAGCAGCAGTCGGTGTCCTGTTGACAATACACCACTGTTGGA
GAGTGACTTGTTTGCTGATTCTTGTGCTGAAAGAGAAATACTACAGCTTAAAGTAAAGTGTC
CAAACCATGCACTTGGTTGTTCAACAGTGGTAGATCTCATGTACATAGAA**CATCACACACAG**
GCATGTTCCTGTCAGCCGGTGATGTGCCCTAATGAGTGTTCAGCAACAGTTCTGCAAAAGGA
ACTTGAACAGCACCTCACATCGCAGTGCATCTTGCGGGTTACCAGGTGTGC**ACTGTGTGACC**
AGCCTTTCACTTTTAATCAAGAGCAGCTCCATCTCTTGAGTTGTTCGCGGGTGACTGTGACG
TGCGAGATGTGTGGAGCTATGATGCCCCGAGGTGAAGTGCCATCCCATACCACAGAATCCTG
TCCTAGAGTCGTAGTTGCCTGTACATTTGCAGAACATGGATGCCATCATAAAATGACAAGAT
CTGACCTTGATCAGCATATGGAACAAGCAATCCAGTACCATCTCCAGCTTCTTTCATCAGCC
AACAAAAAGATGAATGCATTTGTTTCTGACTTAAGCCGAACAGTAGGACTCATTCAGTCTCC
TTATGGAAACTTTAGCCGGCAACCAAGTCTTCGAAGCCAGATGTCAGCAACTTCGCCCATAC
CTGAAAATCATTCAAGCCCATCACAGCATGACAGAAATCTTGAGAAATCTTTTGGTGCTTAT
GGAGGAACTATTAGTCTCAATGATAGATCATCATTAACTCCACAGAGTGATGAATTGGGAAA
TGAAATCAATAAGCTGGAGCTCCAGTTAAACAATCTAAGTGCGAGTGAAACAAAGAGTGGGT
CTAAAATTCCAAACACTATTACTCATCAGGAAATCATTTTACGGGATGTTAGTGAAAAGACA
GTAGACTTAAATCAGAGGATGTTAGAGGAAACTATAAAGTTAAGCAATCTGAGTAAGAGAAT
TGAGGAAGTTGATGCTATGGTAGAAGTTCAGTTAGCAGATGTGAGTGGTAAATTTTGTAATG
GAGAGTATGTCTGGAAAATCAAGCATTTCTCTCATTTGTGTGTAGAGCT**TCAAAATAAACCA**
GGCAGGGTGCTCCACAGTCCACCTTTTTACACATCACAATTTGGATATAAATTCTGTTTACG
TACTAATATCACGTGGAAGTCTAATGAATACTTTTTTTACTTTGTTCATACACTCAATGCAAG
GAGAAAATGATGACTTTTTAGAATGGCCTTTTAGTGGGGAAATAACTCTCTCAATTCTGGAT
TGTGGTCCCACTGCACCAAAAAAACACATTACGGAATCCATGGTAAGCAAGCCAGATCTGCA
AGCATTTCAGCGACCCATGGTATCAAGAAATCCTAAAGGTTTTGGTTACACTGAATTTGTAC
CCTTGGCCAAGTTACTGAAATCTGAAGGGGGAAGTTACATCAACAGTGATGTTCTGTGTATC
CGTGCAATTGTTTCTCCAAAAGCACCAAAATCATCAAGT**TGA**TGTATGAGCAATATGTACAG
TATTATCTTTTTTCTACTCAGTTTTTCTTTCTCTACCTGCATT**GATTTGTATGCTGCCTTG**C
ATCTATGTTTGTTGATATTTGGCTGAATTTAAAAGGAAAGTGCAGTTCAATACATTCCTCT
TTGTGTGATTGCTTCTTTCAATTATATAGCAATTTATACCCTATTTTTATATATGGTAATGG
CACTCTGCTTTATACTTTAATGTTTAAAGTTTATACATTGTTGTGTACAGTATTACAGTGGC
TTCAAAGGGACCATTTAGCTCATTTTTTAATGTTACATATTCTTTAAAATTATATGTATATT
TACAGCGAAAAAAAAAAAAAAAAAAAAAAAAGTACTCTGCGTTGATACCACTGCTTAAGGGC
GAATTC

1 = TRAF6-CDS-F	6 = TRAF6-CDS-R
2 = qTRAF6_F	"ATG" with bold and underline = Start codon
3 = qTRAF6_R	"TGA" with bold and underline = Stop codon
4 = TRAF6-RNAi-F	Sequence with underline = MATH domain
5 = TRAF6-RNAi-R	

2. Primer efficiency

Table A1. Raw data for standard curve analysis.

Tube	Ct 1	Ct 3	Ct 2	Average Ct	Sample Quantity	Log (sample quantity)
A	28.550	28.470	28.63	28.550	1000.00	3.00
B	29.53	29.26	29.73	29.50667	500.00	2.70
C	30.76	30.53	30.81	30.7	250.00	2.40
D	31.55	31.73	31.39	31.55667	125.00	2.10
E	32.67	32.53	32.59	32.59667	62.50	1.80

Slope	-3.369542398
R Squared	0.9981
Efficiency (%)	98.05

$$E = \left(10^{-\frac{1}{slope}}\right) - 1$$

NOTE: %E = E * 100

$$y = -3.3695x + 38.662$$
$$R^2 = 0.9981$$
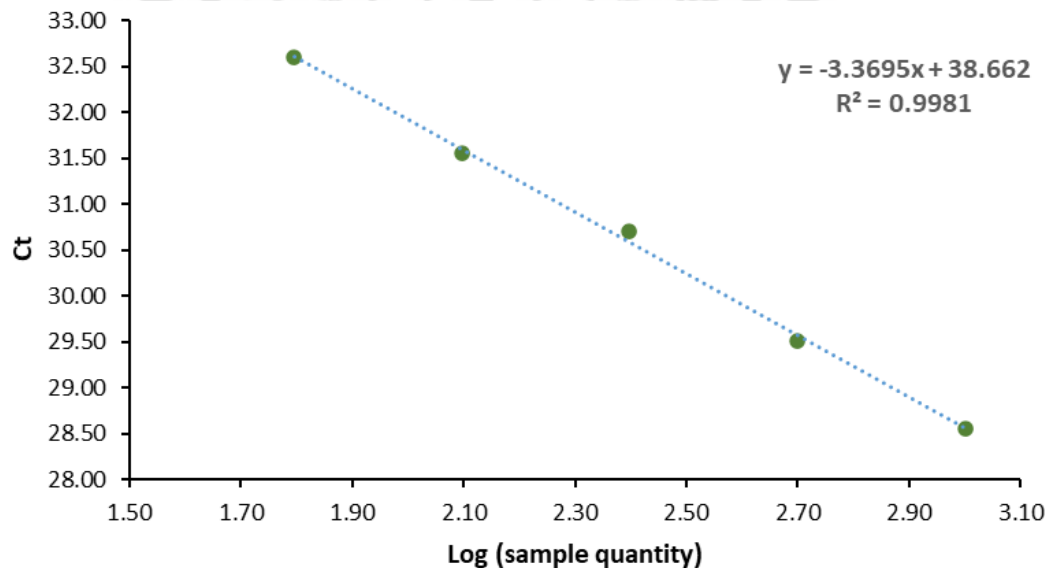
Figure A1 Standard curve of *MrTRAF6* real-time PCR.

3. How to calculate relative mRNA expression level

      1. Perform a qPCR with three replicates and calculate the average Ct of both *MrTRAF6* (gene of interest) and EF1α (internal control gene)

      2. Calculate ΔCt of each shrimp sample (avg Ct of *MrTRAF6* – avg Ct of EF1α)

      3. Calculate average ΔCt of EF1α of three shrimp (used for control)

                Avg. ΔCt of EF1α (control) = 1

*NOTE: For immune challenge or knockdown experiment, the normalized values must be Avg. ΔCt of control group (2X PBS).

      4. Calculate ΔΔCt (Avg. ΔCt − Avg. Ct of control)

      5. Calculate relative expression level using Livak's method $(2^{-\Delta\Delta Ct})$

      6. Calculate the average of relative expression of all three samples
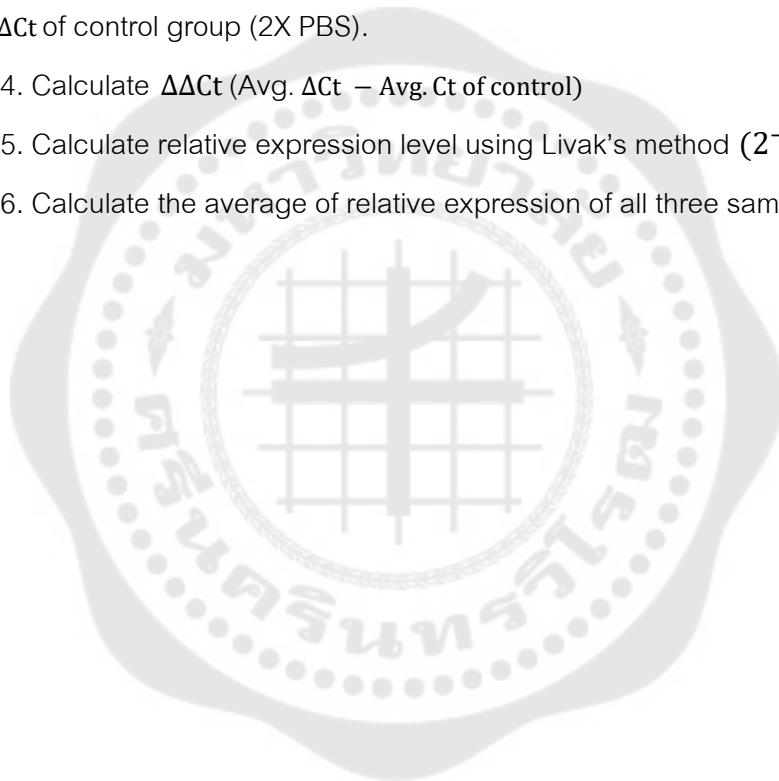
Table A2 Calculation of normal expression level of *MrTRAF6* in gill.

Shrimp 1

Rep	Ct of *MrTRAF6*	Ct of *EF1α*	ΔCt	ΔΔCt	$(2^{-\Delta\Delta Ct})$
1	29.77	23.21	6.56		
2	29.21	22.57	6.64		
3	28.40	23.45	4.95		
Average	29.13	23.08	6.05	5.05	0.030186

Shrimp 2

Rep	Ct of *MrTRAF6*	Ct of *EF1α*	ΔCt	ΔΔCt	$(2^{-\Delta\Delta Ct})$
1	29.87	24.28	5.59		
2	29.01	24.69	4.32		
3	28.88	24.38	4.5		
Average	29.25	24.45	4.80	3.80	0.071628

Shrimp 3

Rep	Ct of *MrTRAF6*	Ct of *EF1α*	ΔCt	ΔΔCt	$(2^{-\Delta\Delta Ct})$
1	30.37	25.22	5.15		
2	30.04	25.63	4.41		
3	29.35	25.40	3.95		
Average	29.92	25.42	4.50	3.503	0.088184

So that, the averaged expression level of *MrTRAF6* in gill must be as follows:

$$R\text{elative mRNA expression} = \frac{0.030186 + 0.071628 + 0.088184}{3}$$

$$= 0.063332$$

REFERENCES

Aguirre-Guzman, G., Sanchez-Martinez, J. G., Campa-Cordova, A. I., Luna-Gonzalez, A., & Ascencio, F. (2009). Penaeid Shrimp Immune System. *The Thai Journal of Veterinary Medicine, 39*(3), 205-215. Retrieved from https://he01.tci-thaijo.org/index.php/tjvm/article/view/35847

Aguirre Guzman, G., Sánchez-Martínez, J., Cordova, A., Luna, A., & Ascencio, F. (2009). Penaeid Shrimp Immune System. *The Thai veterinary medicine, 39*, 205-215.

Arch, R. H., Gedrich, R. W., & Thompson, C. B. (2000). Translocation of TRAF proteins regulates apoptotic threshold of cells. *Biochemical and Biophysical Research Communications, 272*(3), 936-945. doi:10.1006/bbrc.2000.2873

Areschoug, T., & Gordon, S. (2009). Scavenger receptors: role in innate immunity and microbial pathogenesis. *Cell Microbiol, 11*(8), 1160-1169. doi:10.1111/j.1462-5822.2009.01326.x

Belvin, M. P., & Anderson, K. V. (1996). A conserved signaling pathway: the *Drosophila* toll-dorsal pathway. *Annu Rev Cell Dev Biol, 12*, 393-416. doi:10.1146/annurev.cellbio.12.1.393

Bernstein, E., Caudy, A., Hammond, S., & Hannon, G. (2001). Role for a bidentate ribonuclease in the initiation step of RNA interference. *Nature, 409*, 363-366. doi:10.1038/35053110

Brown, K. L., & Hancock, R. E. W. (2006). Cationic host defense (antimicrobial) peptides. *Current Opinion in Immunology, 18*(1), 24-30. doi:10.1016/j.coi.2005.11.004

Budhidarmo, R., Nakatani, Y., & Day, C. L. (2012). RINGs hold the key to ubiquitin transfer. *Trends in Biochemical Sciences, 37*(2), 58-65. doi:10.1016/j.tibs.2011.11.001

CABI. (2019). *Macrobrachium rosenbergii* (giant freshwater prawn). Retrieved from https://www.cabi.org/isc/datasheet/96269#tosummaryOfInvasiveness

Cai, S., Huang, Y., Wang, B., Jian, J., & Xu, Y. (2017). Tumor necrosis factor receptor-associated factor 6 (TRAF6) participates in peroxinectin gene expression in *Fenneropenaeus penicillatus*. *Fish & Shellfish Immunology, 64*, 193-201. doi:10.1016/j.fsi.2017.03.026.

Cao, Z., Xiong, J., Takeuchi, M., Kurama, T., & Goeddel, D. V. (1996). TRAF6 is a signal transducer for interleukin-1. *Nature, 383*(6599), 443-446. doi:10.1038/383443a0

Chai, Y.-M., Zhu, Q., Yu, S.-S., Zhao, X.-F., & Wang, J.-X. (2012). A novel protein with a fibrinogen-like domain involved in the innate immune response of Marsupenaeus japonicus. *Fish & shellfish immunology, 32*(2), 307-315. doi:10.1016/j.fsi.2011.11.020

Chung, J. Y., Park, Y. C., Ye, H., & Wu, H. (2002). All TRAFs are not created equal: common and distinct molecular mechanisms of TRAF-mediated signal transduction. *Journal of Cell Science, 115*(4), 679-688. doi:10.1242/jcs.115.4.679

Deepika, A., Sreedharan, K., Paria, A., Makesh, M., & Rajendran, K. V. (2014). Toll-pathway in tiger shrimp (*Penaeus monodon*) responds to white spot syndrome virus infection: Evidence through molecular characterisation and expression profiles of MyD88, TRAF6 and TLR genes. *Fish & Shellfish Immunology, 41*(2), 441-454. doi:10.1016/j.fsi.2014.09.026

Du, X.-J., Zhao, X.-F., & Wang, J.-X. (2007). Molecular cloning and characterization of a lipopolysaccharide and β-1,3-glucan binding protein from fleshy prawn (Fenneropenaeus chinensis). *Molecular Immunology, 44*(6), 1085-1094. doi:10.1016/j.molimm.2006.07.288

Everett, H., & McFadden, G. (1999). Apoptosis: an innate immune response to virus infection. *Trends in Microbiology, 7*(4), 160-165. doi:10.1016/S0966-842X(99)01487-0

FAO. (2020). *Macrobrachium rosenbergii* (De Man, 1879). Retrieved from http://www.fao.org/fishery/culturedspecies/Macrobrachium_rosenbergii/en

FAO. (2023). Global Production 2023. doi:https://www.fao.org/fishery/en/statistics/global-aquaculture-production/en

Frohman, M. (1994). On beyond classic RACE (rapid amplification of cDNA ends). *PCR methods and applications, 4*, S40-58. doi:10.1101/gr.4.1.S40

Frohman, M. A. (1993). [24] Rapid amplification of complementary DNA ends for generation of full-length complementary DNAs: Thermal race. In R. Wu (Ed.), *Methods in Enzymology* (Vol. 218, pp. 340-356): Academic Press.

Gao, Q., Tang, Q., Xia, Z., Yi, S., Cai, M., Du, H., . . . Yang, G. (2021). Molecular identification and functional analysis of MyD88 in giant freshwater prawn (*Macrobrachium rosenbergii*) and expression changes in response to bacterial challenge. *International Journal of Biological Macromolecules, 178*, 492-503. doi:10.1016/j.ijbiomac.2021.02.177

Guaní-Guerra, E., Santos-Mendoza, T., Lugo-Reyes, S. O., & Terán, L. M. (2010). Antimicrobial peptides: General overview and clinical implications in human health and disease. *Clinical Immunology, 135*(1), 1-11. doi:10.1016/j.clim.2009.12.004

Hamilton, A., Voinnet, O., Chappell, L., & Baulcombe, D. (2002). Two classes of short interfering RNA in RNA silencing. *Embo j, 21*(17), 4671-4679. doi:10.1093/emboj/cdf464

Hannon, G. J. (2002). RNA interference. *Nature, 418*(6894), 244-251. doi:10.1038/418244a

He, C.-B., Wang, Y., Liu, W., Gao, X.-G., Chen, P.-H., Li, Y.-F., & Bao, X.-B. (2013). Cloning, promoter analysis and expression of the tumor necrosis factor receptor-associated factor 6 (TRAF6) in Japanese scallop (*Mizuhopecten yessoensis*). *Molecular biology reports, 40*. doi:10.1007/s11033-013-2573-8

Hoffmann, A., Funkner, A., Neumann, P., Juhnke, S., Walther, M., Schierhorn, A., . . . Stubbs, M. T. (2008). Biophysical Characterization of Refolded *Drosophila* Spatzle, a Cystine Knot Protein, Reveals Distinct Properties of Three Isoforms.

Journal of Biological Chemistry, 283(47), 32598-32609. doi:10.1074/jbc.M801815200

Holthuis, L. B. (1980). SHRIMPS AND PRAWNS OF THE WORLD (An Annotated Catalogue of Species of Interest to Fisheries). *FAO Fisheries Synopsis, 1*(125), 101-107.

Hooper, C., Debnath, P. P., Stentiford, G. D., Bateman, K. S., Salin, K. R., & Bass, D. (2023). Diseases of the giant river prawn Macrobrachium rosenbergii: A review for a growing industry. *Reviews in Aquaculture, 15*(2), 738-758. doi:https://doi.org/10.1111/raq.12754

Hou, F., He, S., Liu, Y., Zhu, X., Sun, C., & Liu, X. (2014). RNAi knock-down of shrimp *Litopenaeus vannamei* Toll gene and immune deficiency gene reveals their difference in regulating antimicrobial peptides transcription. *Developmental & Comparative Immunology, 44*(2), 255-260. doi:10.1016/j.dci.2014.01.004

Huang, D., Bai, Z., Shen, J., Zhao, L., & Jiale, L. J. (2018). Identification of tumor necrosis factor receptor-associated factor 6 in the pearl mussel *Hyriopsis cumingii* and its involvement in innate immunity and pearl sac formation. *Fish & Shellfish Immunology, 80*. doi:10.1016/j.fsi.2018.06.035

Huang, D., Bai, Z., Shen, J., Zhao, L., & Li, J. (2018). Identification of tumor necrosis factor receptor-associated factor 6 in the pearl mussel Hyriopsis cumingii and its involvement in innate immunity and pearl sac formation. *Fish & Shellfish Immunology, 80*, 335-347. doi:10.1016/j.fsi.2018.06.035

Huang, X., Wang, W., & Ren, Q. (2016). Dorsal transcription factor is involved in regulating expression of crustin genes during white spot syndrome virus infection. *Developmental & Comparative Immunology, 63*, 18-26. doi:10.1016/j.dci.2016.05.006

Huang, Y., Chen, Y.-H., Wang, Z., Wang, W., & Ren, Q. (2014). Novel myeloid differentiation factor 88, EsMyD88, exhibits EsTube-binding activity in Chinese mitten crab *Eriocheir sinensis*. *Developmental & Comparative Immunology, 47*(2), 298-308. doi:10.1016/j.dci.2014.08.005

Huang, Y., & Ren, Q. (2020). Research progress in innate immunity of freshwater crustaceans. *Developmental & Comparative Immunology, 104*, 103569. doi:10.1016/j.dci.2019.103569

Jaronczyk, K., Carmichael, J. B., & Hobman, T. C. (2005). Exploring the functions of RNA interference pathway proteins: some functions are more RISCy than others? *The Biochemical journal, 387*(Pt 3), 561-571. doi:10.1042/BJ20041822

Jensen, S., & Thomsen Allan, R. (2012). Sensing of RNA Viruses: a Review of Innate Immune Receptors Involved in Recognizing RNA Virus Invasion. *Journal of Virology, 86*(6), 2900-2910. doi:10.1128/JVI.05738-11

Jensen, S., & Thomsen, A. R. (2012). Sensing of RNA viruses: a review of innate immune receptors involved in recognizing RNA virus invasion. *Journal of virology, 86*(6), 2900-2910. doi:10.1128/JVI.05738-11

Kim, D., & Rossi, J. (2008). RNAi mechanisms and applications. *BioTechniques, 44*(5), 613-616. doi:10.2144/000112792

Kim, H.-Y., & Rikihisa, Y. (2002). Roles of p38 mitogen-activated protein kinase, NF-**K**B, and protein kinase C in proinflammatory cytokine mRNA expression by human peripheral blood leukocytes, monocytes, and neutrophils in response to *Anaplasma Phagocytophila*. *Infection and Immunity, 70*(8), 4132-4141. doi:10.1128/IAI.70.8.4132-4141.2002

Lemaitre, B., & Hoffmann, J. (2007). The Host Defense of Drosophila melanogaster. *Annual Review of Immunology, 25*(1), 697-743. doi:10.1146/annurev.immunol.25.022106.141615

Li, B., Yang, B.-b., Shen, X.-l., Wang, K., Wei, Z., & Du, Z.-q. (2020). Molecular characterization and expression analysis of tumor necrosis factor receptor-associated factor 6 (traf6) like gene involved in antibacterial innate immune of fresh water crayfish, *Procambarus clarkii*. *Fish & Shellfish Immunology, 104*, 517-526. doi:10.1016/j.fsi.2020.06.027

Li, F., & Xiang, J. (2013a). Recent advances in researches on the innate immunity of shrimp in China. *Developmental & Comparative Immunology, 39*(1), 11-26. doi:10.1016/j.dci.2012.03.016

Li, F., & Xiang, J. (2013b). Signaling pathways regulating innate immune responses in shrimp. *Fish & Shellfish Immunology, 34*(4), 973-980. doi:10.1016/j.fsi.2012.08.023

Lin, Y., Mao, F., Zhang, X., Xu, D., He, Z., Li, J., . . . Yu, Z. (2020). TRAF6 suppresses the apoptosis of hemocytes by activating pellino in *Crassostrea hongkongensis*. *Developmental & Comparative Immunology, 103*, 103501. doi:10.1016/j.dci.2019.103501

Liu, S., Zheng, S.-C., Li, Y.-L., Li, J., & Liu, H.-P. (2020). Hemocyte-Mediated Phagocytosis in Crustaceans. *Frontiers in immunology, 11*, 268. doi:10.3389/fimmu.2020.00268

Livak, K. J., & Schmittgen, T. D. (2001). Analysis of Relative Gene Expression Data Using Real-Time Quantitative PCR and the $2^{-\Delta\Delta CT}$ Method. *Methods, 25*(4), 402-408. doi:10.1006/meth.2001.1262

Magnusson, C., & Vaux, D. L. (1999). Signalling by CD95 and TNF receptors: not only life and death. *Immunol Cell Biol, 77*(1), 41-46. doi:10.1046/j.1440-1711.1999.00800.x

Majumdar, R., Rajasekaran, K., & Cary, J. W. (2017). RNA Interference (RNAi) as a Potential Tool for Control of Mycotoxin Contamination in Crop Plants: Concepts and Considerations. *Frontiers in Plant Science, 8*(200). doi:10.3389/fpls.2017.00200

Mali, B., & Frank, U. (2004). Hydroid TNF-receptor-associated factor (TRAF) and its splice variant: a role in development. *Molecular Immunology, 41*(4), 377-384. doi:10.1016/j.molimm.2004.03.008

Mao, F., Li, J., Zhang, Y., Xiang, Z., Zhang, Y., & Yu, Z. (2017). Molecular cloning and functional analysis of tumor necrosis factor receptor-associated factor 6 (TRAF6)

in *Crossastrea gigas*. *Fish & Shellfish Immunology, 68*, 37-45. doi:10.1016/j.fsi.2017.06.049

Megas, C., Hatzivassiliou, E., Yin, Q., Marinopoulou, E., Hadweh, P., Vignali, D., & Mosialos, G. (2010). Mutational analysis of TRAF6 reveals a conserved functional role of the RING dimerization interface and a potentially necessary but insufficient role of RING-dependent TRAF6 polyubiquitination towards NF-**K**B activation. *Cellular signalling, 23*, 772-777. doi:10.1016/j.cellsig.2010.12.004

Mishra, A. K., Sachan, N., Mutsuddi, M., & Mukherjee, A. (2014). TRAF6 is a novel regulator of Notch signaling in *Drosophila melanogaster*. *Cellular signalling, 26*(12), 3016-3026. doi:10.1016/j.cellsig.2014.09.016

Moncrieffe, M. C., Grossmann, J. G., & Gay, N. J. (2008). Assembly of oligomeric death domain complexes during Toll receptor signaling. *The Journal of biological chemistry, 283*(48), 33447-33454. doi:10.1074/jbc.M805427200

Mulinari, S., Häcker, U., & Castillejo-López, C. (2006). Expression and regulation of Spätzle-processing enzyme in *Drosophila*. *FEBS Letters, 580*(22), 5406-5410. doi:10.1016/j.febslet.2006.09.009

New, B. M. (2002). *Farming freshwater prawns: a manual for the culture of the giant river prawn (Macrobrachium rosenbergii)*: Food and Agriculture Organization of the United Nations.

New, M. B., Valenti, W. C., Tidwell, H. J., D'Abramo, L. R., & Kutty, M. N. (2010). *Freshwater Prawns Biology and Farming* (1st ed.). United Kingdom: John Wiley & Sons, Ltd.,.

Pastori, C., Velmeshev, D., & Peschansky, V. (2017). Deep-RACE: Comprehensive Search for Novel ncRNAs Associated to a Specific Locus. In (Vol. 1543, pp. 129-143).

Pearson, A. M., Baksa, K., Rämet, M., Protas, M., McKee, M., Brown, D., & Ezekowitz, R. A. B. (2003). Identification of cytoskeletal regulatory proteins required for efficient phagocytosis in *Drosophila*. *Microbes and Infection, 5*(10), 815-824. doi:10.1016/S1286-4579(03)00157-6

Pillai, D., & Bonami, J.-R. (2012). A review on the diseases of freshwater prawns with special focus on white tail disease of Macrobrachium rosenbergii. *Aquaculture Research, 43*. doi:10.1111/j.1365-2109.2011.03061.x

Qiu, L., Song, L., Yu, Y., Zhao, J., Wang, L., & Zhang, Q. (2009). Identification and expression of TRAF6 (TNF receptor-associated factor 6) gene in Zhikong Scallop *Chlamys farreri*. *Fish & Shellfish Immunology, 26*(3), 359-367. doi:10.1016/j.fsi.2008.10.010

Rothe, M., Wong, S. C., Henzel, W. J., & Goeddel, D. V. (1994). A novel family of putative signal transducers associated with the cytoplasmic domain of the 75 kDa tumor necrosis factor receptor. *Cell, 78*(4), 681-692. doi:10.1016/0092-8674(94)90532-0

Rozi, R., Rahayu, K., & Daruti, D. (2018). Detection and analysis of hemolysin genes in Aeromonas hydrophila isolated from Gouramy (Osphronemus gouramy) by polymerase chain reaction (PCR). *IOP Conference Series: Earth and Environmental Science, 137*, 012001. doi:10.1088/1755-1315/137/1/012001

Schwantes, V., Diana, J., & Yi, Y. (2007). Freshwater prawn farming in Thailand. Retrieved from https://www.aquaculturealliance.org/advocate/freshwater-prawn-farming-thailand/

Scotto-Lavino, E., Du, G., & Frohman, M. A. (2006). 5' end cDNA amplification using classic RACE. *Nat Protoc, 1*(6), 2555-2562. doi:10.1038/nprot.2006.480

Senapin, S., Jaengsanong, C., Phiwsaiya, K., Prasertsri, S., Laisutisan, K., Chuchird, N., . . . Flegel, T. W. (2012). Infections of MrNV (*Macrobrachium rosenbergii* nodavirus) in cultivated whiteleg shrimp *Penaeus vannamei* in Asia. *Aquaculture, 338-341*, 41-46. doi:10.1016/j.aquaculture.2012.01.019

Srisuk, C., Longyant, S., Senapin, S., Sithigorngul, P., & Chaivisuthangkura, P. (2014). Molecular cloning and characterization of a Toll receptor gene from *Macrobrachium rosenbergii*. *Fish & Shellfish Immunology, 36*(2), 552-562. doi:10.1016/j.fsi.2013.12.025

Sritunyalucksana, K., Lee, S. Y., & Söderhäll, K. (2002). A β-1,3-glucan binding protein from the black tiger shrimp, *Penaeus monodon*. *Developmental & Comparative Immunology, 26*(3), 237-245. doi:10.1016/S0145-305X(01)00074-X

Stuart, L. M., & Ezekowitz, R. A. (2008). Phagocytosis and comparative innate immunity: learning on the fly. *Nature Reviews Immunology, 8*(2), 131-141. doi:10.1038/nri2240

Sun, W.-w., Zhang, X.-x., Wan, W.-s., Wang, S.-q., Wen, X.-b., Zheng, H.-p., . . . Li, S.-k. (2017). Tumor necrosis factor receptor-associated factor 6 (TRAF6) participates in anti-lipopolysaccharide factors (ALFs) gene expression in mud crab. *Developmental & Comparative Immunology, 67*, 361-376. doi:10.1016/j.dci.2016.08.015

Tassanakajon, A., Rimphanitchayakit, V., Visetnan, S., Amparyup, P., Somboonwiwat, K., Charoensapsri, W., & Tang, S. (2018). Shrimp humoral responses against pathogens: antimicrobial peptides and melanization. *Developmental & Comparative Immunology, 80*, 81-93. doi:10.1016/j.dci.2017.05.009

Tassanakajon, A., Somboonwiwat, K., Supungul, P., & Tang, S. (2013). Discovery of immune molecules and their crucial functions in shrimp immunity. *Fish & Shellfish Immunology, 34*(4), 954-967. doi:10.1016/j.fsi.2012.09.021

Vaniksampanna, A., Longyant, S., Charoensapsri, W., Sithigorngul, P., & Chaivisuthangkura, P. (2019). Molecular isolation and characterization of a spätzle gene from *Macrobrachium rosenbergii*. *Fish & Shellfish Immunology, 84*, 441-450. doi:10.1016/j.fsi.2018.10.015

Vazquez, L., Alpuche, J., Maldonado, G., Agundis, C., Pereyra-Morales, A., & Zenteno, E. (2009). Review: Immunity mechanisms in crustaceans. *Innate Immunity, 15*(3), 179-188. doi:10.1177/1753425909102876

Wajant, H., Henkler, F., & Scheurich, P. (2001). The TNF-receptor-associated factor family: Scaffold molecules for cytokine receptors, kinases and their regulators. *Cellular signalling, 13*(6), 389-400. doi:10.1016/s0898-6568(01)00160-7

Walsh, M. C., Lee, J., & Choi, Y. (2015). Tumor necrosis factor receptor- associated factor 6 (TRAF6) regulation of development, function, and homeostasis of the immune system. *Immunological Reviews, 266*(1), 72-92. doi:10.1111/imr.12302

Wang, P.-H., Gu, Z.-H., Wan, D.-H., Zhang, M.-Y., Weng, S.-P., Yu, X.-Q., & He, J.-G. (2011). The Shrimp NF-**K**B Pathway Is Activated by White Spot Syndrome Virus (WSSV) 449 to Facilitate the Expression of WSSV069 (ie1), WSSV303 and WSSV371. *PLOS ONE, 6*(9), e24773. doi:10.1371/journal.pone.0024773

Wang, P.-H., Wan, D.-H., Gu, Z.-H., Deng, X.-X., Weng, S.-P., Yu, X.-Q., & He, J.-G. (2011). *Litopenaeus vannamei* tumor necrosis factor receptor-associated factor 6 (TRAF6) responds to *Vibrio alginolyticus* and white spot syndrome virus (WSSV) infection and activates antimicrobial peptide genes. *Developmental & Comparative Immunology, 35*(1), 105-114. doi:10.1016/j.dci.2010.08.013

Wang, X.-W., & Wang, J.-X. (2013). Pattern recognition receptors acting in innate immune system of shrimp against pathogen infections. *Fish & Shellfish Immunology, 34*(4), 981-989. doi:10.1016/j.fsi.2012.08.008

Wang, Z., Chen, Y.-H., Dai, Y.-J., Tan, J.-M., Huang, Y., Lan, J.-F., & Ren, Q. (2015). A novel vertebrates Toll-like receptor counterpart regulating the anti-microbial peptides expression in the freshwater crayfish, *Procambarus clarkii*. *Fish & Shellfish Immunology, 43*(1), 219-229. doi:10.1016/j.fsi.2014.12.038

Wen, R., Li, F., Sun, Z., Li, S., & Xiang, J. (2013). Shrimp MyD88 responsive to bacteria and white spot syndrome virus. *Fish & Shellfish Immunology, 34*(2), 574-581. doi:10.1016/j.fsi.2012.11.034

WoRMS. (2007). *Macrobrachium rosenbergii* (de Man, 1879). Retrieved from http://www.marinespecies.org/aphia.php?p=taxdetails&id=220137

Xu, D., Liu, W., Alvarez, A., & Huang, T. (2014). Cellular immune responses against viral pathogens in shrimp. *Developmental & Comparative Immunology, 47*(2), 287-297. doi:10.1016/j.dci.2014.08.004

Xu, Y., Huang, Y., & Cai, S. (2017). Characterization and function analysis of interleukin-1 receptor-associated kinase-1 (IRAK-1) from *Fenneropenaeus penicillatus*. *Fish & Shellfish Immunology, 61*, 111-119. doi:10.1016/j.fsi.2016.12.030

Yang, K., Zhu, J., Sun, S., Tang, Y., Zhang, B., Diao, L., & Wang, C. (2004). The coiled-coil domain of TRAF6 is essential for its auto-ubiquitination. *Biochemical and Biophysical Research Communications, 324*(1), 432-439. doi:10.1016/j.bbrc.2004.09.070

Ye, H., Arron, J. R., Lamothe, B., Cirilli, M., Kobayashi, T., Shevde, N. K., . . . Wu, H. (2002). Distinct molecular mechanism for initiating TRAF6 signalling. *Nature, 418*(6896), 443-447. doi:10.1038/nature00888

Yount, N. Y., Bayer, A. S., Xiong, Y. Q., & Yeaman, M. R. (2006). Advances in antimicrobial peptide immunobiology. *Peptide Science, 84*(5), 435-458. doi:10.1002/bip.20543

Zhang, S., Li, C.-Z., Yan, H., Qiu, W., Chen, Y.-G., Wang, P.-H., . . . He, J.-G. (2012). Identification and Function of Myeloid Differentiation Factor 88 (MyD88) in *Litopenaeus vannamei*. *PLOS ONE, 7*(10), e47038. doi:10.1371/journal.pone.0047038

Zhou, S.-M., Li, M., Yang, N., Liu, S., Yuan, X.-M., Tao, Z., & Wang, G.-L. (2015). First description and expression analysis of tumor necrosis factor receptor-associated factor 6 (TRAF6) from the swimming crab, *Portunus trituberculatus*. *Fish & Shellfish Immunology, 45*(2), 205-210. doi:10.1016/j.fsi.2015.04.005

REFERENCES

VITA

NAME   CHANITCHA CHOOLERT

DATE OF BIRTH   12 October, 1994

INSTITUTIONS ATTENDED   2013 – 2016   Bachelor of Science – Biology,
Srinakharinwirot University, Bangkok, THAILAND
2011 – 2013   High school certificate, Ratchaborikanukroh
School, Ratchaburi, THAILAND